NSF Grant ATM-0118021
National Science Foundation
and
NOAA/COMET Grant S02-38660
National Oceanic and Atmospheric Administration

GROUND TRUTH AND MODELING VERIFICATION OF THE HAIL QUADRATURE PARAMETER

by Tracy K. Depue and Steven A. Rutledge

Colorado State University

DEPARTMENT OF ATMOSPHERIC SCIENCE

PAPER NO. **746**

GROUTH TRUTH AND MODELING VERIFICATION OF THE HAIL QUADRATURE PARAMETER

by

Tracy K. Depue

and

Steven A. Rutledge

Department of Atmospheric Science

Colorado State University

Fort Collins, CO 80523

Research Supported by

National Science Foundation

under Grant ATM-0118021

and

National Oceanic and Atmospheric Administration

under Grant SO2-38660

Fall 2003

Atmospheric Science Paper No. 746

ABSTRACT OF THESIS

GROUND TRUTH AND MODELING VERIFICATION OF THE HAIL QUADRATURE PARAMETER

The purpose of this study is to determine the usefulness of a new hail detection and size classification algorithm known as the Hail Quadrature Parameter (HQP). The parameter is explored from a theoretical, modeling, and ground truth perspective.

HQP uses scatterer size and intensity information contained in horizontal reflectivity (Z_h) and shape information contained in differential reflectivity (Z_{dr}) (combined in the differential reflectivity hail signal, H_{dr}). It also adds the particle canting and surface irregularity information detectable by the linear depolarization ratio (LDR). The purpose of this study is to determine whether this additional information from LDR assists in hail detection and size classification.

A modeling sensitivity study was performed using the *T*-matrix model to determine how HQP would react to changes in certain hailstone characteristics such as size, water-coat thickness, axis ratio, canting angle, ice density and percent water volume. Of greatest interest was whether small hailstones with thicker water coats would appear the same to the radar as larger hailstones with thinner water coats, causing potential false alarms in HQP. It was found that increasing water-coat thickness did not produce consistently larger HQP values. Rather, the water-coat thickness simply determined at

which diameter hailstones entered the Mie regime and began displaying unpredictable and widely varying values.

A ground-truth verification study was also conducted to determine how well HQP detected the presence and size of hail at the surface. Post-storm surveys were conducted in northern and eastern Colorado. The polarimetric radar parameters of interest were calculated at each survey point and relationships between these relevant parameters and hail size and damage were explored. Through both statistics and raw data plots it was determined that HQP does not perform better than H_{dr} for hail detection or size classification. It was also determined that it is unlikely that LDR adds as much information about hail size as was previously thought.

Tracy Depue
Atmospheric Science Department
Colorado State University
Fort Collins, CO 80523
Fall 2003

ACKNOWLEDGEMENTS

My deepest thanks go to Patrick Kennedy, without whom this project never would have been possible. Working with him was one of the most enjoyable aspects of my graduate school experience. Further thanks go to Dave Brunkow, Dr. Walt Petersen, Dr. Lawrence Carey, Cathy Kessinger, David Barjenbruch, and Fredell Boston for their assistance, technical input, and suggestions. I would also like to thank Margi Cech, Laura Ciasto, and Gustavo Pereira for their support and assistance. This research was supported under National Science Foundation Grant ATM-0118021, NOAA/COMET Grant S02-38660, and an American Meteorological Society/NASA Graduate Fellowship.

TABLE OF CONTENTS

LIST OF TABLES

LIST OF FIGURES

CHAPTER ONE

Introduction

1.1 Motivation

For many years radar meteorologists have been attempting to develop and refine methods of identifying precipitation types. Identification of hail is of particular interest, since hail is an obvious danger to people, livestock, and property. More effective warnings about such severe weather would allow the public to be more prepared and could reduce injuries and preventable property damage.

Another, less well-known motivation for accurate hail identification is not predictive, but involves damage already done. Hail causes over 500 million dollars of property damage a year (David Barjenbruch, NWS, personal communication). Unfortunately, it also provides an opportunity for fraudulent insurance claims when hail damage has been known to have occurred in a given area. Insurance adjusters have expressed interest in a product that would assist them in determining whether insurance claims due to hail damage are legitimate or not.

Several different methods and algorithms exist for the purpose of hail identification and prediction, using both operational WSR-88D Doppler radars and research-oriented polarimetric radars. Current operational algorithms using non-polarized radar have improved over time, but are still not the most effective algorithms available (Zrnić, 1996; Zrnić and Ryzhkov, 1999). Algorithms utilizing polarimetric

radar also exist, and have shown demonstrable skill in identifying hydrometeor types (Aydin *et al.*, 1990; Brandes and Vivekanandan, 1998; Husson and Pointin, 1989). Due to the superior skill of polarimetric radar-based algorithms, the National Weather Service is currently planning to implement polarimetric upgrades to the WSR-88D radars (Doviak *et al.*, 2000). In order to facilitate the change-over, studies need to be conducted to determine how this polarimetric functionality can be used in the most efficient, accurate operational sense. The purpose of this thesis is to consider a currently-used polarimetric hail detection algorithm known as the differential reflectivity hail signal (H_{dr}) and to thoroughly test and analyze a new algorithm, the Hail Quadrature Parameter (HQP), created in 2001.

1.2 CSU-CHILL Radar

Polarimetric radar data used in this study was provided by the Colorado State University – Universities of Chicago and Illinois (CSU-CHILL) radar, located near Greeley, Colorado. The range of the radar is approximately 150 km, covering a large portion of northeastern Colorado. The CSU-CHILL is a well-maintained, well-calibrated, state-of-the-art polarimetric radar. The radar system specifications are listed below.

Table 1.1: CSU-CHILL System Specifications

Antenna	
Shape:	Parabolic
Diameter:	8.5 m
Feed type:	Scalar
Gain:	43 dB (includes waveguide loss)
3 dB Beamwidth:	1.1 deg

Maximum sidelobe:	-27 dB (In worst ϕ plane.)
Inter-channel isolation:	-45 dB (limited by orothomode transducer)
ICPR (two-way):	-34 dB

Transmitters	
Wavelength:	11.01 cm
Peak Power:	800-1000 kW
Final PA Type:	VA-87B/C (Klystron)
PRT Range:	800 - 2500 micro-seconds
Pulse width:	0.3 - 1.0 μs
Available Polarizations:	Horizontal, Vertical, slant 45°/135°, right/left circular

Receivers/Digital Signal Processing	
Noise Figure:	~3.4 dB
Noise Power @SNR=1:	~ -114.0 dBm
Dynamic range:	~96 dB
Bandwidth:	750 KHz typ. with programmable filter
Output Range Resolution:	50, 75, 150 m
Maximum range gates:	Estimated to be > 3000

1.3 Scientific Background

Several different methods of radar-based hail detection have been employed in the past. These fall into five basic categories: 1)those using reflectivity only, 2)those using dual-polarization radars, 3)those using dual-wavelength radars, 4)those combining radar with some other meteorological observation technique, and 5)those using fuzzy logic. Of greatest interest in this thesis are those currently being used operationally by the National Weather Service (using reflectivity), and those using dual-polarized radar.

The other methods deserve mention, however, as they have met with more or less success over time. Dual wavelength observations have been performed since the 1960's, and still continue in a limited way today. The theory behind dual-wavelength radar hail detection is that large scatterers, such as hail, behave differently in 10 cm and 3 cm

wavelength radiation (Rayleigh vs. Mie scattering conditions; Atlas, 1964; Eccles and Atlas, 1973; Carbone *et al.*, 1973). Raindrops are in the Rayleigh regime for both wavelengths, but most hail is in the Mie regime for a 3 cm wavelength radar. The power returns at each wavelength are compared, and the difference can be related to the presence of hail. This method has drawbacks, however, in that the shorter wavelength radar may experience a great deal of attenuation (Tuttle and Rinehart, 1983), and the antenna patterns must be carefully matched at each wavelength (Rinehart and Tuttle, 1982).

One example of combining radar with another observation technique is that used by Auer (1994). In this method, cloud-top temperatures are used, as well as radar reflectivity. Combined reflectivities and cloud-top temperatures were compared with ground truth data, and a linear regression was performed to create a line, much like that used by Aydin *et al.* (1986), above which, precipitation is expected to be rain, and below which, it is expected to be hail. Possible sources of error with this method are rapidly growing and decaying storms, for which satellite data are not available at a useful temporal resolution. This method was tested in New Zealand with a great deal of success, but to this author's knowledge, has not been tested in the multitude of climatological regimes found here in the United States.

Fuzzy logic and Neural Network methodologies are currently being actively developed and tested at such places as the National Center for Atmospheric Research (NCAR), Colorado State University and the National Severe Storms Laboratory (NSSL) in Norman, Oklahoma (Marzban and Witt, 2001). Neural Networks employ new methods of computing, in which a highly parallelized network is given a variety of

learning, testing and validation data. The network is given some number of data sets including input data and output data. The network is trained to give certain outputs when certain inputs are received. After sufficient training and validation has been performed, the network can be given input data and it will produce outputs that are hopefully close to correct. This method has been used to receive meteorological data as input, and then output whether hail is expected, and what size or size category it might be. The fuzzy logic method has also been used in general hydrometeor identification, of which hail is obviously a part.

The National Weather Service has been using reflectivity-based algorithms since the 1970's. Due to the limitations of National Weather Service radars, reflectivity (and with the WSR-88D radar, velocity and spectral width) information is all that is available. Several algorithms have been used through time, and many improvements have been made, as technology has improved and more information can be processed and used in an operational setting. The most current hail-detection algorithm uses storm cell and environmental data to determine the probability of hail (POH), the probability of severe hail (POSH), and the maximum expected hail size (MEHS). A storm cell is defined based on its 3-D reflectivity field. The algorithm uses the maximum reflectivity and height above ground level (AGL) of the centroid of each cell. It then determines from a nearby sounding the height (AGL) of the 0°C and -20°C temperature levels. The POH is based on the vertical distance between the maximum reflectivity value and the freezing level. The greater the distance, the higher the POH. The POSH and MEHS are calculated using the reflectivity and the Hailfall Kinetic Energy (HKE). The HKE is the kinetic energy flux of hailstones, and is based on the height above freezing level of the

maximum reflectivity values. A vertical integration is performed for all areas within a storm that meet reflectivity and height thresholds. The integration is weighted toward areas with highest reflectivity that are also above the -20°C environmental temperature. This integration produces the Severe Hail Index (SHI). The POSH is determined from the SHI and a function of the height of the freezing level. The MEHS is determined from an equation using the SHI. (The entire algorithm is available at http://atmos.pknu.ac.kr/~swimm/wsr88d/pdfs/hail_core_aloft.pdf.) The statistical performance of this algorithm will be compared with the results from this study in Chapter 5.

Several hail-detection methods have been developed using dual-polarimetric radar. Polarimetric radar provides a great deal more information about hydrometeor shape, orientation, and surface roughness than single-parameter radar. Two main types of polarizations exist: linear polarization and circular polarization. Circular polarization has been used to detect hail because it is sensitive to the deformity and random orientation of scatterers. For circularly-polarized radar, the polarization vector rotates continuously through 360° while traveling along the direction of propagation, maintaining a fixed amplitude. When circularly-polarized radiation is transmitted, spherical particles cause backscatter in the orthogonal direction [i.e., right-hand circular (RHC) will be backscattered as left-hand circular (LHC)]. This received orthogonal radiation is the cross-polar signal. Nonspherical, randomly oriented particles cause backscatter in the parallel direction, creating the copolar signal return. The ratio of the copolar signal to the cross-polar signal defines the circular depolarization ratio (CDR). This parameter is useful for detecting the presence of hail because not only is hail

deformed, but it is also randomly oriented. If hail becomes wet either during growth or melting, it can further increase the amount of depolarization, producing a larger CDR. Circularly-polarized radar was used extensively by the Canadians in the 1960s and 1970s (Bringi and Hendry, 1990). The major weakness of this method occurs in heavy rain when differential propagation effects create elliptically-polarized incident radiation, which renders interpretation of CDR difficult.

For linear polarization, both alternating and simultaneous transmission and reception (in the horizontal and vertical) are possible. Most linearly polarized radars alternately transmit horizontal and vertical polarizations in rapid succession. The return signal is usually received simultaneously, but in older radars, it was often received sequentially. Either method of reception allows for the calculation of both copolar and cross-polar terms. Simultaneous reception is possible when two receivers are available – one for the copolar and one for the cross-polar signal. Sequential reception is required when only one receiver is available. The copolar signal is simpler to receive on these systems due to a lack of needing to switch hardware between pulses. The cross-polar signal can also be received through a more difficult process requiring pulse-to-pulse switching over very short time spans to ensure that the measurements are still valid. The proposed upgrades to the WSR-88D National Weather Service radars will utilize a relatively new technique of simultaneous transmission. This method is expected to have practical maintenance and cost advantages over alternating transmission systems. The main drawback to this type of radar, as far as this study is concerned, is that it cannot measure the linear depolarization ratio (LDR, see Section 2.4), since the copolar signal received from each polarization will greatly overwhelm the cross-polar signal. The LDR

can, however, be calculated using separate volume scans (Doviak *et al.*, 2000). Preliminary testing of this simultaneous transmission method has been performed on the CSU-CHILL radar (Doviak *et al.*, 2000), but thorough, operational testing is still necessary. Some of this testing will take place during the Joint Polarization Experiment (JPOLE), currently being conducted by the National Severe Storms Laboratory in Oklahoma (Schuur *et al.*, 2001).

Since dual linear-polarization radar has come to the research forefront, many studies have been done (Doviak and Zrnić, 1993; Straka *et al.*, 2000) to determine the thresholds for various sizes of hail using variables calculated with this type of radar. Each variable relevant to this study and their respective thresholds are discussed in-depth in Chapter 2.

1.4 Objectives

The purpose of this study is to determine whether HQP actually offers a better form of hail detection than previously studied algorithms. This is accomplished in three ways. First, the theoretical basis for the utility of HQP is explored. Second, a modeling sensitivity study is performed to determine how several polarimetric variables (and also HQP, derived from these polarimetric variables) are affected by hail size, axis ratio, canting angle, water coat thickness, density, and water content. Third, a ground-truth study is presented in which observers were contacted and surveyed to determine storm characteristics. The main characteristics of interest were whether hail occurred and what the properties of that hail were, such as size and damaging effects. A statistical analysis was performed using these survey points to determine the effectiveness of both HQP and

H_{dr} in determining the presence of hail, the presence of hail over 19 mm (0.75 in), and structural/vehicular damage. Conclusions are then drawn about the effectiveness of HQP and whether or not it indeed demonstrates an increased ability over both H_{dr} and current National Weather Service algorithms to detect the presence of both hail and warning-class hail. The implications of this study for operational purposes are also discussed. Finally, the need for future work is described which could lead to more knowledge about the effectiveness of HQP, as well as the development of similar hail-detection algorithms.

CHAPTER TWO

Theory

2.1 Polarimetric Radar

As stated in Chapter 1, the radar used in this study is the CSU-CHILL radar. It has both circular and linear polarization capabilities. For most operations, however, including those conducted during this study, the linear polarization was used. The radar used sequential transmission and simultaneous reception via dual receivers, allowing for the calculation of the full spectrum of linear polarization variables. This chapter gives a description of the polarimetric variables relevant to this study, including their utility for identifying hail.

2.2 Reflectivity

Reflectivity is a measure of the transmitted power that is returned to the radar. As seen in equation 2.1, reflectivity is a function of the radar constant (C), the received power (P_r), the range from the radar to the scatterer (r), and the dielectric properties of the scatterer (K):

$$Z = \frac{CP_r r^2}{|K|^2} \tag{2.1}$$

The radar constant contains information specific to the radar, such as pulsewidth, receiver power gain, radar wavelength, transmitter pulse power, peak boresite gain of the antenna,

normalized antenna pattern function, and finite bandwidth loss factor (Bringi and Chandrasekar, 2001). The dielectric constant is 0.93 for pure water and 0.197 for ice.

Two regimes of reflectivity exist based on the size relationship between the wavelength of the radar and the size of the scatterers. Scatterers much smaller than the wavelength of the radar ($D < \lambda/16$ for liquid water and $D < \lambda/6$ for ice; Battan, 1973) are in the Rayleigh regime. In this case, the reflectivity is a function of the number concentration [N(D)], and the diameter of the scatterers.

$$Z = \int_0^\infty N(D) D^6 dD \qquad [\text{mm}^6\ \text{m}^{-3}] \qquad (2.2)$$

From this equation, it is evident that the reflectivity has a very strong dependence on size. This means that a small population of very large hydrometeors can have a tremendous influence on the reflectivity of an entire volume of hydrometeors. The drop size distribution for a chosen population is also important. Scatterers whose sizes are larger than the Rayleigh limit ($D > \lambda/16$) fall into the Mie regime. In the Mie regime, forward scattering plays a larger and larger role, causing a fluctuating, sometimes sinusoidal pattern in backscattered reflectivity (and also causes interference with other polarimetric variables).

Since reflectivity values occur over such a large range (due to the variation in received power from many different types and concentrations of scatterers), reflectivity is represented on a logarithmic scale, using equation 2.3 below:

$$dBZ = 10 \log_{10} Z \qquad [\text{dBZ}] \qquad (2.3)$$

This equation can yield values from around -30 to over 75 dBZ. The smallest values are due to clear-air scatterers or nonprecipitating clouds. The largest values are due to intense convection, including either very heavy rain, or very large, wet hail.

Since reflectivity is dependent (in part) on dielectric constant, reflectivity values are higher for water compared to similar-sized ice. The dielectric for high-density ice is about 20% that of liquid water, and for low-density ice is about 5% that of liquid water. This might lead one to think that reflectivity for hail would be less than that for rain. Hail can, however, be significantly larger than pure liquid hydrometeors, and in addition, with a large enough water coating (during either melting or wet growth), an ice hydrometeor may approximate the backscattering cross section of a pure water hydrometeor (Battan, 1973). This allows hail to achieve a much higher reflectivity, in general, than pure rain.

Reflectivity has been used for many decades as a method of hydrometeor identification. According to Mason (1971), a reflectivity greater than 55 dBZ indicates the presence of hail. Several other methods using reflectivity (see Section 1.3), have also been used, both experimentally and operationally. Reflectivity has its weaknesses, though, especially due to the fact that on occasion, rain can produce reflectivities high enough to be mistaken for hail. This creates unnecessary hail warnings, as well as interference with rain rate algorithms.

2.3 Differential Reflectivity

Since polarimetric radar has the ability to both transmit and receive in the horizontal and vertical, a horizontal reflectivity (Z_h) and vertical reflectivity (Z_v) can be calculated. Z_h (Z_v) is a measure of the power transmitted in the horizontal (vertical), that is received back in the horizontal (vertical). A parameter very useful for hydrometeor identification is differential reflectivity (Z_{dr}) (Seliga and Bringi, 1976). Z_{dr} is the ratio of the horizontal reflectivity to the vertical reflectivity:

$$Z_{dr} = 10\log_{10}\left(\frac{\bar{Z}_h}{\bar{Z}_v}\right) \qquad \text{[dB]} \qquad (2.4)$$

This is basically a measure of the reflectivity-weighted mean axis ratio found over all hydrometeors in a given radar volume. Since different hydrometeor types exhibit different shape characteristics, they will also exhibit different Z_{dr} values. Oblate particles will have a larger Z_h than Z_v, creating a positive Z_{dr}. Spherical objects (or those that appear spherical due to particle motion such as tumbling) will backscatter the same amount of radiation in both the horizontal and vertical, creating a Z_{dr} near zero. And, finally, prolate particles will reflect more in the vertical than in the horizontal, creating a negative Z_{dr}. Large raindrops tend to flatten and become more oblate (Pruppacher and Beard, 1970). This causes volumes consisting of rain to have a positive Z_{dr} signature. Hail, however, tends to be more spherical. And when hailstones become large enough to have axis ratios that differ significantly from one, they have a tendency to tumble (see section 3.3.1), creating a spherical appearance relative to the radar. It has also been shown that some large hail may fall in a prolate manner (Knight and Knight, 1970b). This combination of factors gives hail a near-zero or negative Z_{dr} signature. Since Z_{dr} is so sensitive to both axis ratios and canting angle (see Sections 3.3.1 and 3.3.2), and both of these subjects are still largely under debate, it is difficult to assign specific values of Z_{dr} to hail. In general, however, hail may be found at Z_{dr} values between -2.0 and 0.5 (Straka *et al.*, 2000). Z_{dr} is also subject to Mie effects (especially at wavelengths shorter than S-band), causing dramatic interference patterns as each polarization reflectivity moves through it's own sinusoidal pattern, either constructively or destructively interfering with the other.

2.4 Linear Depolarization Ratio

The linear depolarization ratio (LDR) is the ratio of the cross-polar power (transmit horizontal, receive vertical) to the co-polar power (transmit and receive horizontal):

$$LDR = 10\log_{10}\left(\frac{Z_{vh}}{Z_{hh}}\right) \qquad \text{[dB]} \qquad (2.5)$$

If polarized radiation is incident on an object that is either irregularly shaped or canted with respect to the plane of polarization, some of the radiation will shift to the orthogonal polarization (become depolarized). If the scattering object is either spherical or axially-symmetric, with one of its axes aligned along the plane of polarization, there is no depolarization. In depolarizing situations, the cross-polar signal is 2 to 3 orders of magnitude smaller than the co-polar signal. This makes LDR highly susceptible to being contaminated or overwhelmed by background noise. LDR is sensitive to shape and canting angle. This makes it a good method for determining if hail is present, since hail is usually not smooth nor perfectly spherical, and it can exhibit large canting angles and tumbling, causing an increase in LDR. LDR is very sensitive to the dielectric of the scatterers, so if hail becomes wet, the LDR can increase dramatically. LDR is also subject to Mie effects, causing a similar sinusoidal pattern to that seen with reflectivities, once scatterers enter the Mie regime.

Since LDR is not directly related to size, it is difficult to assign values of LDR that might indicate hail. In general, LDR values of > -25 dB seem to indicate that hail may be present (Straka *et al.*, 2000). Since LDR is sensitive to characteristics that are related to size, however, LDR can be expected to increase to some extent with size, due to these indirect relations. According to Knight (1986), hail axis ratios are loosely

dependent on size, and according to Barge and Isaac (1973), hail becomes more deformed with larger size. Also, List (1986) states that larger hail tends to be more irregular in shape. Each of these factors could lead to an increase in LDR. The high sensitivity to wetting begs the question of whether small wet hail can cause elevated LDR values, creating false indications of large hail. This question is addressed in Chapter 3.

2.5 Differential Reflectivity Hail Signal

The differential reflectivity hail signal (H_{dr}) was proposed by Aydin *et al.* (1986). It is based on both reflectivity and Z_{dr}.

$$H_{dr} = Z_h - f(Z_{dr}) \qquad \text{[dB]} \qquad (2.6)$$

where

$$f(Z_{dr}) = \begin{cases} 27 & Z_{dr} \le 0 \text{ dB} \\ 19Z_{dr} + 27 & 0 < Z_{dr} \le 1.74 \text{ dB} \\ 60 & Z_{dr} > 1.74 \text{ dB} \end{cases} \qquad (2.7)$$

H_{dr} was created in an effort to combine the intensity/size information contained within reflectivity with the shape information offered by Z_{dr}. This parameter was created by using disdrometer measurements in both Illinois and Colorado, which provided information about drop size distribution. Backscattering cross sections for size categories contained in these distributions were calculated using Waterman's (1969) *T*-matrix formulation. Z_h and Z_{dr} values were then calculated using these modeled backscattering cross sections. The Z_h, Z_{dr} pairs were then plotted, and a best fit line was applied to the data to define an upper bound to the H_{dr} values at which rain would be expected. All points falling above this line would then be classified as hail. Different values of raindrop oscillations and drop size distributions were considered in defining this line

(Aydin *et al.*, 1986). Since H_{dr} is based on both reflectivity and Z_{dr}, it is sensitive to the same issues (canting angle, size, dielectric, Mie effects, etc.) affecting each of its components.

According to Aydin *et al.* (1986, 1990), hail should be present when H_{dr} is greater than zero. In these studies, large hail exhibited H_{dr} values upwards of 30 dB. Several H_{dr} thresholds were tested in this study, and the results are presented in Chapter 4.

2.6 Hail Quadrature Parameter

The Hail Quadrature Parameter (HQP) was first proposed by Kennedy *et al.* (2001). It is based on both H_{dr} and LDR. HQP is defined using Figure 2.1.

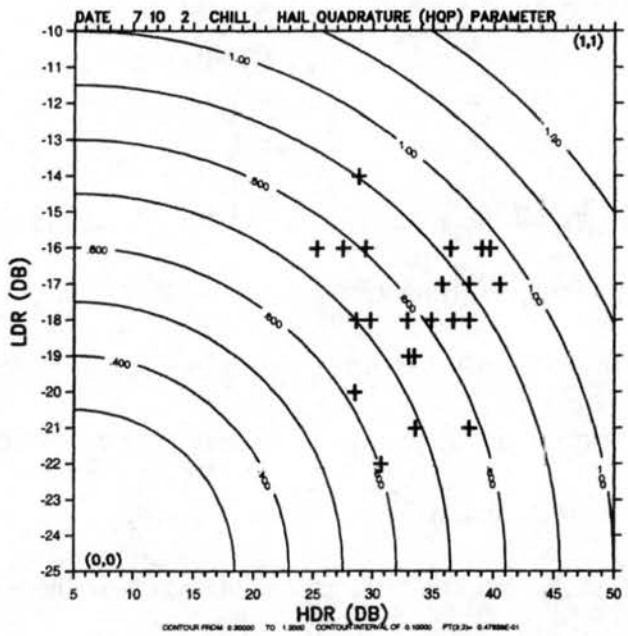

Figure 2.1. Calculation method for HQP.

First, values of both LDR and H_{dr} indicative of hail were chosen (LDR from -25 to -10, and H_{dr} from 5 to 50). These values were placed on perpendicular axes, and then normalized, so a point residing at the end of either axis would have a value of one, and

the greatest value possible, lying at the end of a 45° line through the plot, would be $\sqrt{2}$. LDR/H_{dr} pairs are plotted on this graph, and a vector is drawn from the origin to each point. The magnitude of this vector is the value of HQP. The actual equation for this calculation (2.8) is given below.

$$HQP = \sqrt{\left(\frac{H_{dr} - 5}{45}\right)^2 + \left(\frac{LDR + 25}{15}\right)^2} \qquad (2.8)$$

The purpose of HQP is to augment the already effective hail-detection capability of H_{dr}. Since LDR can also indicate hail, the premise is that information can be found in LDR (based on axis ratio, canting angle, and surface irregularities), that may create a more effective hail-detection algorithm compared to H_{dr} alone.

Since HQP is comprised of H_{dr} and LDR, it is subject to the same weaknesses as each of the individual variables. One of the biggest drawbacks is the susceptibility of LDR to noise. As mentioned in Section 2.4, the depolarized return signal is much smaller than the polarized return signal, making LDR prone to contamination from any of a number of noise sources. This noisy interference usually causes an increase in LDR values, and therefore, an increase in HQP values as well. Occasionally, individual scans must be perused to determine whether such noise effects as anomalous propagation, second-trip echoes or clutter have contaminated the data. Another weakness of HQP is its sensitivity to Mie effects which will be discussed in detail in Section 3.6.5.

No specific values have been determined yet for either identifying the presence or size of hail. When HQP was first studied, a value of 0.3 was proposed to indicate hail, 0.7 to indicate large hail, and 0.9 to indicate very large or extremely damaging hail. These numbers were based on a very preliminary set of data, so one aspect of this study

will be to determine what HQP threshold values are the best to use for both hail detection and size. In addition, it will be determined whether actual size correlations can be drawn, or whether a more categorical approach should be taken.

CHAPTER THREE

Modeling

3.1 Sensitivity Study

Although HQP appears promising based on theory and preliminary observational testing, a detailed sensitivity study is needed to fully evaluate HQP's utility as a reliable hail indicator. In this chapter we report on detailed modeling studies. In Chapter Four we will discuss observational confirmation for HQP and the presence of hail. The primary modeling question needing to be answered revolves around LDR's sensitivity to Mie resonance and dielectric effects influenced by melting or water coating associated with wet growth. Prior to this study, it was unknown whether the water coating around a hailstone (or water contained within a hailstone) could increase the LDR value sufficiently to reduce the usefulness of HQP. Is was also unknown how melting might interact with other changes in hailstone characteristics such as oblateness and orientation during fall. So, a sensitivity study was performed on several hailstone features to determine how each polarimetric variable of interest (see Chapter 2) would react to changes in these characteristics and whether these reactions would have an adverse effect on HQP. The characteristics considered were hail size, axis ratio, canting angle, water-coat thickness, density, and percent water volume. All of these aspects are discussed in detail in Section 3.3 below.

3.2 *T*-matrix Model

For the modeling section of this study, the *T*-matrix modeling method was used. Details on this model can be found in Vivekanandan *et al.* (1991) and Barber and Yeh (1975). In this method, a transition (*T*) matrix is calculated for each hail size, shape and dielectric constant. The size and shape are inputs to the calculation, and the dielectric constant is calculated based on ice density, water-coat thickness, and/or percent water volume, also assigned as inputs. Using the above information, the 2 x 2 scattering matrix is calculated. For details about the equations used, see Waterman (1969) or Barber and Yeh (1975). These equations are specifically suitable for use in the Mie regime. Since most of the hail investigated in this study is in the Mie regime for ice (larger than ~2.0 cm) this makes the *T*-matrix method particularly useful. This method is also very efficient because a *T* matrix only needs to be calculated once for each type of hail being investigated regardless of orientation or radar elevation angle. Two separate coordinate systems are used: a particle-oriented coordinate system which makes use of particle symmetry, and a laboratory coordinate system which accounts for radar elevation angle and canting angle of the particle. In 1979, Wang developed a comparatively simple method for relating the particle coordinate system to the laboratory coordinate system. Once the 2 x 2 scattering *T* matrix is calculated, then the standard Stokes parameters (I, Q, U, V; See Appendix A for definitions) are used, the radar elevation angle and particle orientation are taken into account using Wang's method, and the entire scattering field is completely characterized. The results of this go into the 4 x 4 Mueller matrix. From the elements of the Mueller matrix, the desired polarimetric variables are calculated (see Vivekanandan *et al.*, 1991 for detailed equations).

3.3 Limitations of the *T*-matrix model

Several inherent problems exist with the *T*-matrix model, however, as far as being able to imitate reality. First, the *T*-matrix method models smooth spheroids which may be either dry or have a water coating around the entire surface of the particle. If a water coating is chosen, however, it is always assumed to be a uniformly distributed coating. Rasmussen *et al.* (1984) found that more often than not, hailstones often contain a water torus slightly downwind of the equator of the stone where water preferentially collects until shedding begins. The *T*-matrix model offers no way to simulate this torus, possibly causing the calculation of different values for the polarimetric variables than would be observed by the actual radar. Second, as mentioned above, the stones modeled are smooth. There is no way to model the typically rough, lobed outer surface of a hailstone using the *T*-matrix approach. And, of course, no method exists for modeling spikes or other extreme surface features. The remaining problems arise with the shape of the hailstones. It has been found in several studies (Knight and Knight, 1970b; Thwaites *et al.*, 1977; Browning and Beimers, 1967) that hailstones are triaxial. Several examples are given in which the semi-major axis of the stones is, to varying degrees, smaller than the major axis. The *T*-matrix model only allows the user to define the length of the major axis and the axis ratio, which then determines the size of the minor axis. It is not possible, however, to define a specific semi-major axis of a different length than the major axis. Finally, only spheroidal stones can be modeled. Matson and Huggins (1980), found in their study that around 16% of the stones they collected were better described as conical than as spheroidal. No way exists to simulate any type of conical stones with the *T*-matrix model.

3.4 Physical Characteristics of Hailstones

In order to determine what values should be used for the variables, an extensive literature survey was conducted to find reasonable values based on laboratory, modeling, or field experiments. The main difficulty encountered during this effort was that conflicting ideas have been put forth concerning several of these descriptors.

3.4.1 Canting angle distribution

Several studies have been done to determine the falling motion of hailstones using laboratory, modeling, and field experiments. List (1959) conducted a laboratory experiment in which he dropped model hailstones into a fluid. This experiment led List to conclude that hail fell with the short axis always vertical in such a way as to maximize drag as the stone fell. List *et al.* (1973) used a wind tunnel study to revise this theory and determined that 3 types of motion are possible. 1) Steady fall with the minor axis vertical, as originally proposed, 2) a neutral, constant amplitude oscillation, and 3) continuous rotation or tumbling. In the Rasmussen *et al.* (1984) wind tunnel study, hail stones were prevented from tumbling because they were attached to small strings to keep them from impacting the walls of the tunnel. In addition a water torus developed near the equator of the stone, which appeared to stabilize the stone. Based largely on the results of Rasmussen *et al.* (1984), Rasmussen and Heymsfield (1987a,b) created a model of hail-melting parameters and cited several studies in which hailstones were observed not to tumble, due largely to the presence of a water torus near the stone's equator. None of these studies, however, accounted for destabilizing factors likely encountered in clouds, such as turbulence, wind shear and collisions. Field experiments conducted by Matson

and Huggins (1980), Browning *et al.* (1968) and Knight and Knight (1970b) led to compelling evidence that stones do experience orientation changes of some magnitude in the vast majority of cases. Matson and Huggins (1980) did a field experiment in which falling hailstones were photographed during a series of storms in southeast Wyoming, southwest Nebraska and northeast Colorado. They found that about one third of the stones were tumbling, but a tumbling rate could be determined for only 38 of those stones. The median tumbling rate for these stones was about 40 Hz. They noted that almost all stones photographed were undergoing some type of orientation change as they fell. Browning *et al.* (1968), who collected freshly fallen hailstones, determined that the growth layers completely surrounding most stones suggest that random tumbling probably begins once a hailstone core is about 0.8 cm in diameter. They believe that displacement of water occurred at times during the growth of the stones, and due to asymmetries observed in some stones, they proposed that the rotation rate was small at the time of this displacement. Due to asymmetrical cavities found in the edges of some stones, they also believed that at times during melting, a stone may orient itself so that the same edge continuously faces the air flow. Knight and Knight (1970b) studied the internal structure and symmetry of many collected hailstones. They also hired a skydiver to drop hailstone models and videotape their fall characteristics. From these investigations, they determined that hail generally tumbles as it falls. They decided, however, that the existence and properties of this tumbling are highly sensitive to the characteristics of the hailstones, such as density and surface roughness. Due to the many unknowns surrounding the tumbling nature of hailstones, four canting angle standard deviations were chosen: 25 degrees, 50 degrees, 75 degrees, and random tumbling.

3.4.2 Axis ratio

The axis ratio in this study is defined at the length of the minor axis divided by the length of the major axis. Several field experiments have been done in which hail was collected and analyzed to determine its axis ratio. Matson and Huggins (1980), discussed above, collected 621 individual hailstones with a major axis median value of 10.9 mm. The median value of axis ratios for their sample population was 0.77, with axis ratios ranging from 0.50 to 1.00. The value of 0.75 to 0.79 was determined by Barge and Isaac (1973) after analyzing 101 stones in Alberta, Canada. Nancy Knight (1986) determined a range of axis ratios according to size for hailstones collected in northeast Colorado. Axis ratios ranged from approximately 0.70 for the largest stones to 0.85 for the smallest. Rasmussen and Heymsfield (1987b) determined axis ratios for several hail sizes at various levels of melting using their microphysical model. They found axis ratios ranging from 0.98 before melting began to 0.55 for small stones near the ground. One issue regarding axis ratio that was studied extensively by Rasmussen and Heymsfield related to the water torus found near the equator of stones. They speculate that axis ratios for falling hailstones may be smaller than the hail collection studies indicate, due to the loss of the torus by hailstones once they impact the surface. In addition, the axis ratios very close to one found in Rasmussen and Heymsfield's study are artificially induced by the fact that the model was initialized with spherical stones. This does not take into account the possibility of irregularly or oblately shaped stones being created during the growth phase before the stones begin falling and melting. Due to the large range of axis ratios found, and the potential effect of the melting-induced water torus, three axis ratios were chosen for our modeling study: 0.95, 0.75 and 0.60.

3.4.3 Water coating

Several parameterizations have been proposed involving the melting of hail and how it progresses. Two of these theories that represent opposite ends of the spectrum are Chong and Chen (1974) and Rasmussen and Heymsfield (1987). Chong and Chen theorize that most meltwater is shed from hailstones. Rasmussen and Heymsfield postulate that a certain amount of meltwater is retained as long as stable flow conditions are met. In Rasmussen and Heymsfield's study, stones were initialized at 5 km, and allowed to melt as they approached the surface. In this study, it was found that, as expected, the stones had very little water coating immediately after initialization, but the coating increased as they neared the ground. As expected, the amount of melting and shedding is strongly dependent on temperature, relative humidity, and liquid water content. In Rasmussen and Heymsfield's study, water thicknesses at 2 km MSL (after falling 3 km) ranged from 0.8 cm to 0.48 cm (complete melting of the 0.5 cm hailstone). This study represents, in essence, a maximum amount of water retained. It is possible for far less liquid water to be present on the stone, based on the parameterization used, the potential effects of tumbling, and the amount of time spent at temperatures exceeding 0° C. As a result, water-thickness values of 0.02 cm, 0.05 cm, and 0.10 cm were used, as well as a completely dry hailstone. A water thickness of 0.10 cm was the largest used, due to the problematic nature of the water torus. It is unlikely that a thickness greater than that would be present around the entire perimeter of the stone, although, according to Rasmussen and Heymsfield, larger thicknesses were found, especially on the smallest stones.

3.4.4 Ice Density

Two values of ice density were chosen in this study: 0.91 g cm^{-3}, and 0.45 g cm^{-3}. The 0.91 g cm^{-3} value is representative of solid ice, and 0.45 g cm^{-3} is representative of a graupel-like particle. These values were also chosen because they were used by Rasmussen and Heymsfield, and their model could be used to determine other realistic values (such as water coating and axis ratio) for hailstones of these densities. A full range of hail sizes, water coatings, axis ratios and canting angles were studied for the dense hail. Only smaller hail sizes were explored for ice with a density of 0.45 g cm^{-3}, since it is unlikely for very large graupel particles to form with no interspersed rings of higher-density ice. In addition, no water coating was included on the porous ice since, once melting begins, the water soaks into the ice lattice and the hail becomes spongy, as discussed below.

3.4.5 Percent water volume

During the storm surveys, several reports were received about hail that appeared very soft and "splattered" when the hail particles hit the ground. As a result, it was desirable to simulate spongy hail (which occurs when water infiltrates the ice matrix of the hailstone) in the model. Spongy hail was simulated by defining a specific percent of water, by volume, to be mixed homogeneously with the dense ice. The percent water volume was arbitrarily chosen to be 40%. This allowed for the composition to be slightly more ice than liquid water. Only a water-coat thickness of 0.02 cm was explored fully for spongy hail. Thicker water coats were used only on a sample of hail sizes and axis

ratios. The values were compared to the values calculated for the 0.02 cm water coat and found to be very similar.

3.4.6 Hailstone size

A wide range of hailstone sizes was used to represent the sizes reported in the hail surveys conducted during this investigation. Sizes used in the model ranged from 0.5 cm to 7.0 cm. Intervals of 0.5 cm were used to ensure adequate resolution for observing Mie resonance effects.

3.4.7 Hailstone size distribution

For the majority of this study, a single size distribution was used. The distribution was exponential and was based on the mean values found by Cheng and English (1983) for N_0 and D_0. The D_0 value was adjusted, however, to give reasonable reflectivity values (>~55 dBZ) for the widest range of sizes. The N_0 value used was 8.0 m^{-3} cm^{-3} and the D_0 value used was 2.0 m^{-3} cm^{-3}. If D_0 was decreased or increased much, either the reflectivity for the smaller hail sizes became unrealistically large or the reflectivity for the large hail sizes was too small.

3.5 Methodology

Table 3.1 describes the matrix of options chosen in various modeling runs. Letters are used next to each value to indicate whether these values were used for (d)ense hail, (s)pongy hail, and/or (p)orous hail. The ($s^{.02}$) is used to show that the 0.02 cm water

coating was done over the full range of hailstone characteristics, but the other water coatings, marked with the (s) symbol, were only run for a subset of these.

Table 3.1 Combinations of hailstone characteristics modeled using the *T*-matrix model.

Axis Ratio	Hail Size (cm)	Canting Angle Dist. (°)	Water Coating (cm)
0.95 $ds^{.02}sp$	0.5 $ds^{.02}sp$	25 $ds^{.02}sp$	Dry dp
0.75 $ds^{.02}sp$	1.0 $ds^{.02}sp$	50 $ds^{.02}sp$	0.02 $ds^{.02}$
0.60 $ds^{.02}$	1.5 $ds^{.02}sp$	75 $ds^{.02}sp$	0.05 ds
	2.0 $ds^{.02}sp$	Random $ds^{.02}sp$	0.10 ds
	2.5 $ds^{.02}sp$		
	3.0 $ds^{.02}sp$		
	3.5 $ds^{.02}sp$		
	4.0 $ds^{.02}$		
	4.5 $ds^{.02}$		
	5.0 $ds^{.02}$		
	5.5 $ds^{.02}$		
	6.0 $ds^{.02}$		
	6.5 $ds^{.02}$		
	7.0 $ds^{.02}$		

The above combinations of ice density, percent water volume, water-coat thickness, axis ratio, canting angle standard deviation and hail size were all simulated using the *T*-matrix model, employing the hail size distribution above. The elevation angle chosen was 4.3 degrees. Tests were run to determine whether the elevation angle changed the results and it did not, so 4.3 degrees, corresponding to 3 km AGL, was chosen arbitrarily as the value to be used. The main objective of these tests was to determine what characteristics of hail would affect HQP. The first concern was whether melting would have an effect such that small, wet hailstones would have HQP values similar to large, dry hailstones. The second concern, due to the large size of hailstones

being investigated, was whether Mie resonance effects would cause enough interference to be an issue.

3.6 Results

3.6.1 Reflectivity

Since reflectivity is insensitive to both the axis ratio and canting angle distribution, all results shown use an axis ratio of 0.95 and employ a random canting angle distribution. The results are representative of all axis ratios and canting angle distributions. Figure 3.1 shows the results of the dense hail reflectivities with increasing water-coat thicknesses. A trend can clearly be seen in the sinusoidal pattern of each line: the stones enter Mie scattering regimes progressively at smaller sizes, with local minima occurring at 5.5 cm for the dry stone, 4.0 cm for the 0.02 cm-coated stone, 3.0 cm for the 0.05 cm-coated stone, and 2.0 cm and 6.0 cm for the 0.10 cm-coated stone. As a result of this out-of-phase sinusoidal behavior, stones with thicker water coats reach minima while thinner-coated stones are near their maxima.

Below 2.0 cm, the hail is in the Rayleigh regime for ice and the reflectivity behaves as expected: reflectivity increases with water-coat thickness and size. At 2.0 cm, however, the 0.10 cm-coated hailstone enters the Mie regime. By 3.0 cm, the 0.10 cm-coated hailstone has the highest reflectivity, but the 0.05 cm-coated stone has the lowest reflectivity, having decreased from its 2.0 cm value. By 4.0 cm, the 0.05 cm-coated stone has increased to the second-largest reflectivity, with the 0.02 cm-coated stone having the lowest reflectivity. At 5.0 cm, the reflectivities are back to being well ordered, increasing with water-coat thickness. After 5.0 cm, however, the reflectivity of the 0.10 cm-coated

stone plunges, until it has the lowest reflectivity at 6.0 cm. From 6.0 cm to 7.0 cm, the reflectivity of the 0.10 cm-coated stone increases, while the others decrease, so by 7.0 cm, the reflectivities are very much like they were at 0.5 cm. From these patterns, it is apparent that only at specific hailstone sizes do the reflectivities behave as expected, with reflectivity increasing with water-coat thickness and hailstone size. So, once the stones enter the Mie regime, the reflectivity at any given size is affected more by the Mie resonance effects than directly by the thickness of the water coat.

Figure 3.2 shows the reflectivity of spongy hail with various water coatings. It is apparent that the reflectivity is not affected by the water coating for spongy hail. The reflectivity is affected more by the water contained within the hail than by the addition of water to the surface of the hailstones. The spongy hail enters the Mie regime at a slightly smaller size than the 0.10 cm-coated dense hail, as would be expected due to the increased water content. Figure 3.3 shows the reflectivity of the porous (0.45 g cm^{-3}) hail compared to that of the dense hail. Neither of these have water coats. The reflectivity of the dense hail is consistently approximately 7 dB higher than that of the porous hail. At the sizes investigated, no Mie effects were found for the porous ice.

Figure 3.4 shows the reflectivity of dense hail with a 0.02 cm water coating compared to that of spongy hail with the same water coat. Once again, Mie effects appear beyond about 1.5 cm for the spongy hail, so that from 0.5 cm to 5.0 cm, the spongy hail has greater reflectivity than the solid hail. From 5.0 cm on, however, the dense hail has a greater reflectivity. This emphasizes the point that greater water content alone does not ensure larger reflectivity.

3.6.2 Differential Reflectivity (Z_{dr})

The differential reflectivity (Z_{dr}) is obviously very sensitive to axis ratio, as well as canting angle standard deviation, since it is a measure of scatterer "flatness" which is exaggerated with smaller axis ratios and smaller standard deviations of canting angle. Z_{dr} for a random canting angle distribution is zero by definition, so graphs of random canting angle distribution are not included. In Figure 3.5, it can be seen that Z_{dr} is very close to zero for the most spherical hailstones and the largest canting angle standard deviations. The same out-of-phase quasi-sinusoidal shape seen in the reflectivity is apparent, however, and is especially exaggerated in the 25° canting angle standard deviations. Values of Z_{dr} are strongly positive as soon as the stones enter the Mie regime and quickly fall off to very negative numbers, likely due to Mie effects in both the horizontal and vertical polarizations. It is possible that the horizontal return is enhanced while the vertical return is diminished, or vice-versa, causing artificially large positive or negative Z_{dr} values. So, once again, it is apparent that for particular hail sizes, water coating does not affect Z_{dr} in a predictable way. Figure 3.6 shows that for spongy hail, Z_{dr} is mostly insensitive to water-coat thickness. Figure 3.7 shows that for the sizes investigated, Z_{dr} is very similar for both dense and porous ice. Figure 3.8 shows that the Z_{dr} for spongy hail is consistently either larger than or very close to the value for dense ice, except in the region where the 0.02 cm-coated dense hail experiences its local maximum. (The same trend appears for the other water-coat thicknesses as well). The spread between the Z_{dr} values for the dense and spongy hail is determined by the axis ratio and canting angle, but the basic pattern is the same in each sub-figure.

3.6.3 Linear Depolarization Ratio (LDR)

The linear depolarization ratio (LDR) is highly sensitive to axis ratio, but less sensitive to canting angle distribution, especially at larger axis ratios. For simplicity, graphs are shown for all axis ratios at only a random canting angle distribution. Figure 3.9 shows hail with the same water coats as in Figure 3.1. LDR is subject to Mie resonance effects at the same respective hail sizes for each water-coat thickness as was demonstrated for reflectivity. As a result LDR (like reflectivity) does not behave in any expected manner once the Mie regime is entered. So, for many of the hail sizes a thicker water coat does not unequivocally lead to a larger LDR. One trend apparent from all three sub-figures, however, is that LDR generally increases with hail size. For all water coats and axis ratios, the LDR at 7.0 cm is greater than that for 0.5 cm. Relatively large LDR values can be found, however, at all hail sizes larger than about 2.0 cm. Only large LDR values are found for the largest hail, but similarly large LDR values are also found for much smaller hail. This will be an important issue when overall performance of HQP is discussed in Chapter 5. Figure 3.10, like Figure 3.3, shows that LDR is not affected much by the water coat present on the surface of the spongy hail. Figure 3.11 shows that, as with reflectivity, LDR is about 7 dB greater for dense hail than for porous graupel-like hail. Figure 3.12 shows that, for axis ratios of 0.95 and 0.75, the spongy hail maintains a higher LDR than dense hail for a majority of hail sizes. For the 0.60 axis ratio, however, the spongy LDR is larger only for hail sizes through 4.0 cm. Once again, Mie resonance has a larger effect than simple water content.

3.6.4 Differential Reflectivity Hail Signal (H_{dr})

Since H_{dr} is based on Z_{dr} and Z_h, it is also affected by mechanisms that affect Z_h or Z_{dr}, such as axis ratio and canting angle. Since Z_{dr} is zero for a random canting angle distribution, the patterns are very similar to those for reflectivity alone, so they are not included in the figures. Figure 3.13 shows that when Z_{dr} is near zero (large axis ratios and large canting angles) H_{dr} is affected mostly by Z_h and it takes on the same basic trends as the reflectivity plots. As the stones flatten and are less canted, however, Z_{dr} plays a larger role and H_{dr} magnifies the Mie effects from both Z_h and Z_{dr}. In general, strong minima are seen where Z_{dr} experiences its most drastic maxima. Likewise, strong minima in Z_{dr} create H_{dr} maxima. Figure 3.14 shows that H_{dr} does not change much with water coating for spongy hail. Figure 3.15 shows roughly the same difference between dense and porous ice as is seen in the reflectivity plots. Figure 3.16 shows that spongy hail has either a very similar or larger H_{dr} through 5.0 cm at which point the value for spongy hail decreases below that for dense hail. The spread between spongy and dense hail values is determined mainly by the strength of the local H_{dr} minima for the respective types of hail.

3.6.5 Hail Quadrature Parameter (HQP)

Finally the initial questions can be answered: 1) Will hail either containing or coated by larger amounts of water create a larger HQP value than dry hail, possibly causing false alarms involving wet hail or under-prediction of the severity of dry hail? And 2) will Mie resonance effects interfere with the ability to relate HQP to hail size?

Due to the criteria for HQP discussed in Section 2.6, HQP was not calculated for several hail sizes because either LDR, H_{dr} or both fell outside of the acceptable range of values used to calculate HQP. In Figure 3.17, the 0.95 axis ratio plots are not included because no HQP was calculated. In all other figures, when HQP was not calculated, that point has simply been omitted.

Three features are immediately apparent from Figure 3.17. First the HQP value is generally greater for the largest hail sizes than for the smallest. Although, as with LDR, large HQP values can be found at all sizes above 2.0 cm. Second, for a given hail size, HQP for completely dry hail is almost always lowest. Third, HQP is larger for more oblate stones.

In Figure 3.17(f and g), it can be seen that hail with thicker water coats rapidly increases to higher HQP values at smaller sizes (essentially the sizes at which each water coat enters the Mie regime). Because of this, an HQP of 0.8 in Figure 3.17f, for instance, could indicate the presence of 2.5 cm, 3.5 cm, or roughly 5.0 to 6.0 cm hail, at progressively thinner water coats. For stones with this axis ratio and these canting angle standard deviations, a smaller, wetter stone could easily be interpreted incorrectly as a larger, more damaging stone.

This dramatic increase in HQP as the Mie regime is entered is most apparent in the most oblate hailstones. For nearly spherical hailstones, LDR is too small for an HQP to be calculated, regardless of the thickness of the water coat. In between however, for the stones with a 0.75 axis ratio, HQP increases when the stones enter the Mie regime, but the values do not stay elevated as they do with the more oblate stones. As a result, an HQP of 0.8 in Figure 17c, for instance, could indicate the presence of 2.5 cm, 3.75 cm,

5.5 cm. or 6.25 cm hail, all with a 0.10 cm water coat. (Similar repetitive patterns occur for the other water-coat thicknesses). So, it is not that small, wet hail can be misinterpreted in these cases only as larger, drier hail, but that small, wet hail can have the same HQP value as large, wet hail as well. This can lead to both an over-prediction of the size and damage capacity of small hail, as well as the under-prediction of such characteristics for large hail, water-coat thickness notwithstanding.

Figure 3.18 shows that HQP is slightly more sensitive to the water coating on the spongy hail than are the previously discussed radar parameters. No HQP values were calculated for the 0.95 axis ratio due to LDR and H_{dr} being out of bounds. No HQP was calculated for the porous ice at either of the axis ratios studied, so the dense/porous comparison graph is omitted. Figure 3.19 shows that spongy hail experiences a sharp peak in HQP around 2.0 cm, that then drops off, with a second, smaller peak around 5.5 cm or 6.0 cm. This leads to the spongy hail having a much larger HQP than the dry hail in the vicinity of the first peak. After the initial drop in value for the spongy hail, however, the HQP of the dense hail tends to remain larger than that of the spongy hail for most of the mid- and large sizes.

This leads to several conclusions about the theoretical usefulness of HQP. The first, obvious conclusion is that at certain times, HQP will definitely fail. Hailstones very close to spherical will not return a large enough LDR for an HQP value to even be calculated. As a result, extremely large, dense, very damaging hail could be completely undetected via HQP if it were nearly perfectly spherical. This weakness is mitigated, however, by the fact that, as discussed in Section 3.3.2 above, spherical hail is very seldom seen in nature – usually less than 10% of the time (Matson and Huggins, 1980;

Macklin, 1963; Knight, 1986). In addition, H_{dr} should perform well in cases of spherical hail. HQP will in fact fail in any case where either H_{dr} or LDR are too low due to sphericity and/or tumbling features, for an HQP value to be calculated. This is especially likely to happen for more oblate stones that are not canted much, both increasing the Z_{dr} and decreasing the LDR. Once again, nature provides an occasional solution for this in that it is thought that large amounts of canting and tumbling are believed to be more the rule than the exception. So, the likelihood of very oblate, non-canted hail is quite low. In addition, dry stones may not have a large enough LDR due to their small indices of refraction for an HQP value to be calculated. Unfortunately, the actual amount of water retained on a stone as it falls is relatively poorly studied. The treatment by Rasmussen *et al.* (1984) and Rasmussen and Heymsfield (1987b) of water-coat thicknesses would seem to indicate that perfectly dry hail is very rare, but their study did not account for any tumbling characteristics and how that might affect shedding or retention of meltwater. As discussed above, it is unknown how the prevalent water torus would affect any of the radar parameters determined in the *T*-matrix model.

HQP is most likely to be inaccurate at moderate axis ratios with large canting angles. These are the cases in which HQP values decrease at larger sizes causing potential under-prediction of the severity of the hail. The spongy hail behaves in much the same way, with a decrease in HQP at larger sizes. Between these effects and those caused by the more rapid entry into the Mie regime experienced by the wetter hailstones, it is obviously impossible to confidently assign a hail size to a specific HQP value. The solution for this, which will be explored further in Chapter 4, is to create a more categorical definition for HQP. For instance, the National Weather Service defines

warning category hail to be hail 1.9 cm (0.75 in) or larger. So, it would be convenient and useful if a value of HQP could be determined above which hail would be considered "warning class" or "potentially damaging." According to the model, this could be done with a certain margin of error. Since hail observed with the CHILL radar is within the Rayleigh regime for ice scatterers through 2.0 cm, it is possible to determine the value of HQP most likely to be observed for 2.0 cm and larger hail. For instance, the majority of the larger hail (especially if completely dry hail is excluded) has HQP values larger than 0.6. In general, hail with HQP values below this would be considered non-damaging, while hail with values larger than this would be considered potentially damaging. Obviously, false alarms are likely to occur, and some damaging hail will definitely not have HQP values large enough to merit "warning class" status. But, this is likely the most practical way to make use of HQP. This will be discussed in Chapter 4.

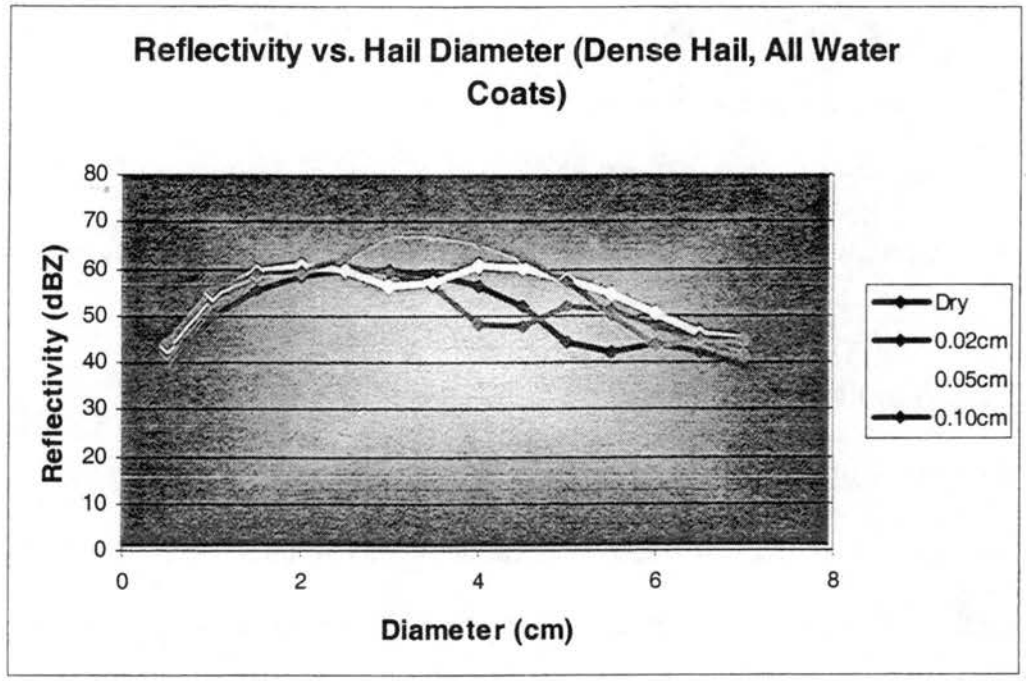

Figure. 3.1: Reflectivity vs. hail diameter for an ice density of 0.91 g cm^{-3}, and all water-coat thicknesses. Axis ratio of 0.95 and random canting angle distribution shown, but representative of all axis ratios and canting angles.

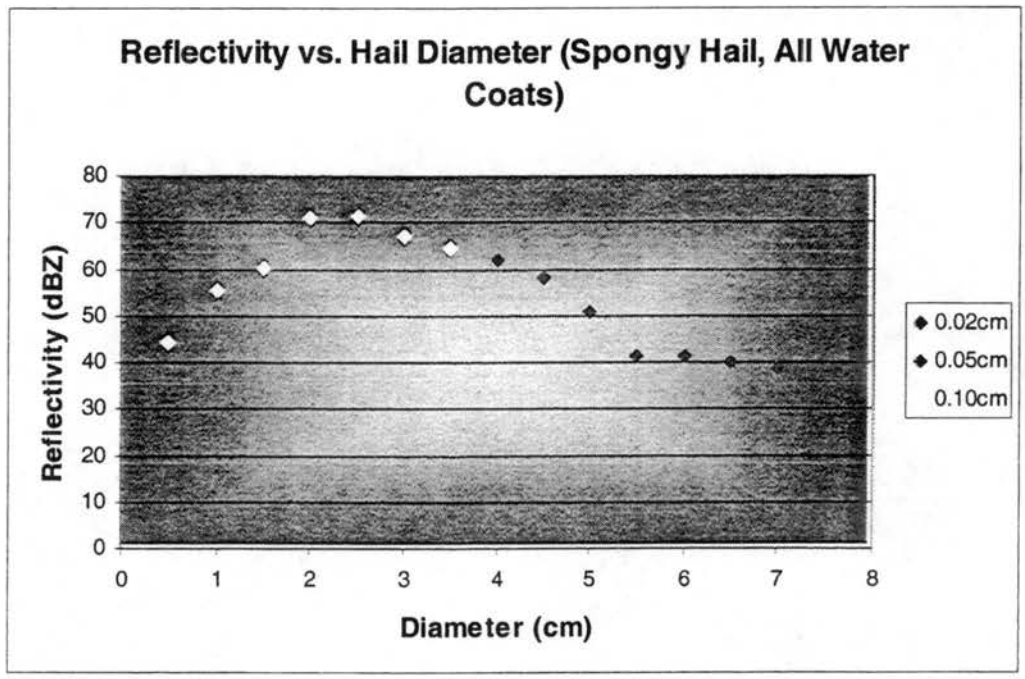

Figure. 3.2: Reflectivity vs. hail diameter for 40% water volume. Axis ratio of 0.95 and random canting angle distribution shown, but representative of all axis ratios and canting angles. Water-coat thicknesses of 0.05 cm and 0.10 cm only explored at smaller sizes.

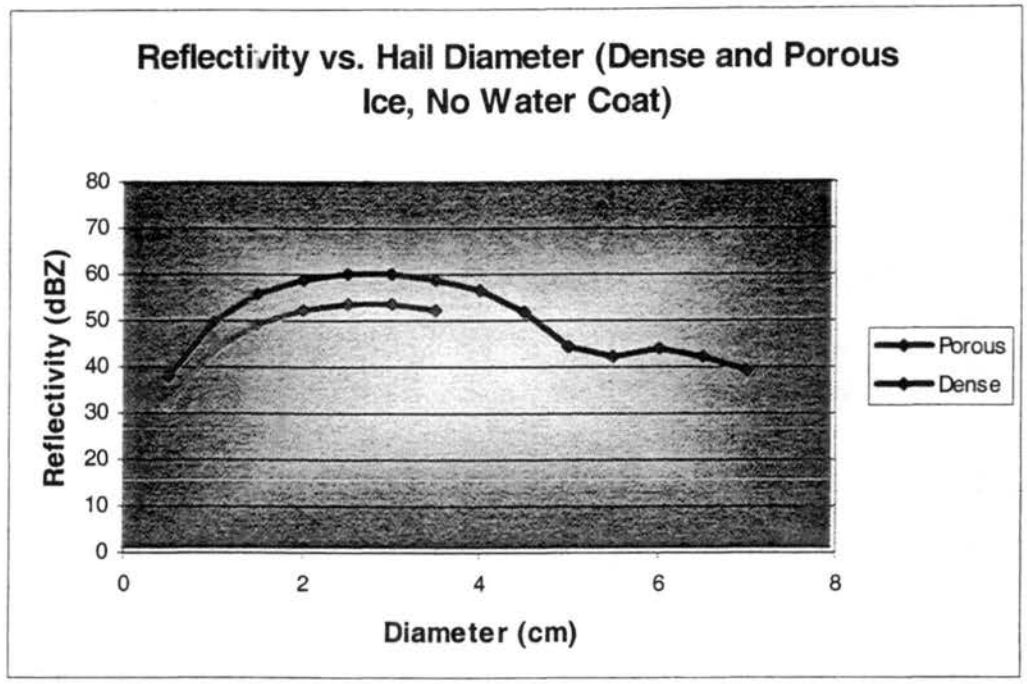

Figure. 3.3: Reflectivity vs. hail diameter for ice densities of 0.91 g cm^{-3} and 0.45 g cm^{-3}. Axis ratio of 0.95 and random canting angle distribution shown, but representative of all axis ratios and canting angles. 0.45 g cm^{-3} density only explored at smaller sizes.

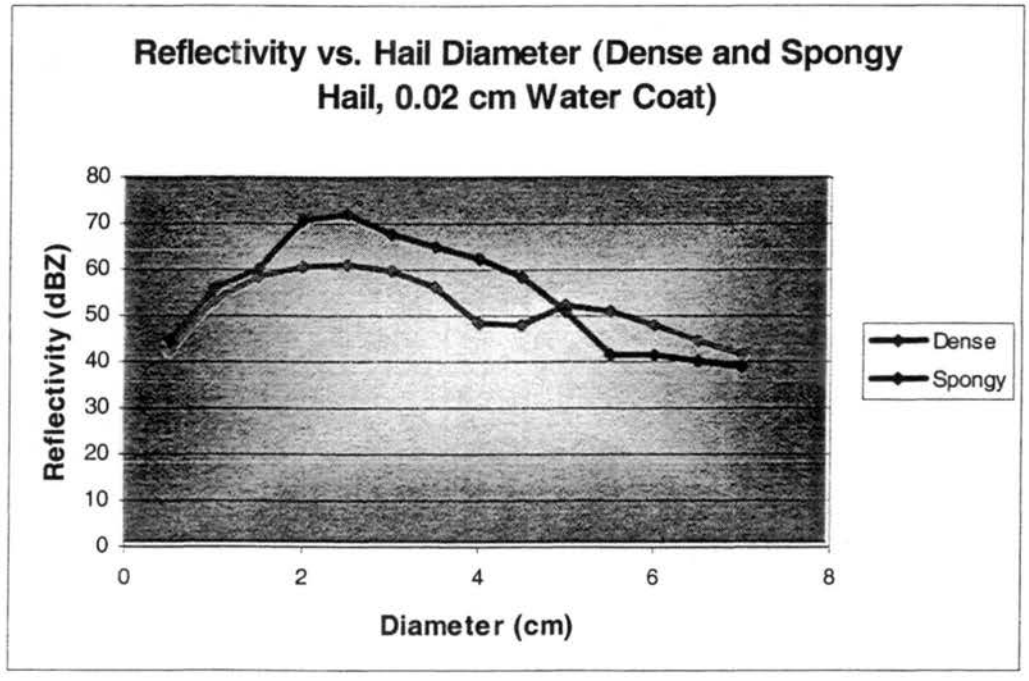

Figure. 3.4: Reflectivity vs. hail diameter for ice densities of 0.91 g cm^{-3} and 40% water volume. Axis ratio of 0.95 and random canting angle distribution shown, but representative of all axis ratios and canting angles.

a)

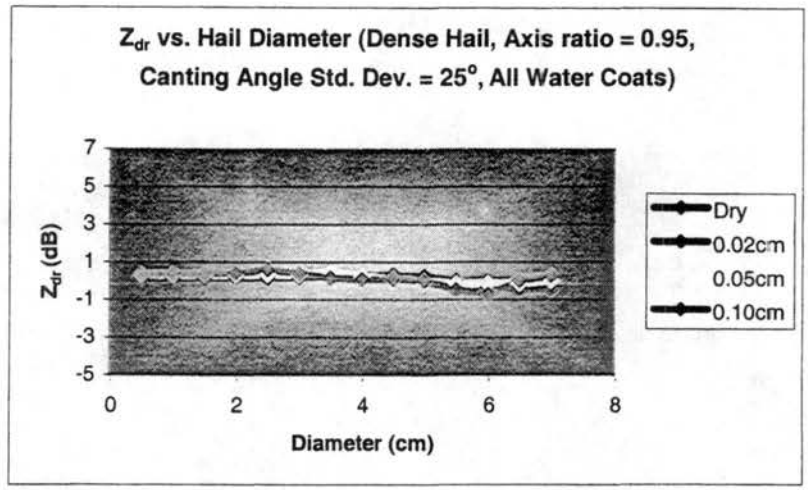

b)

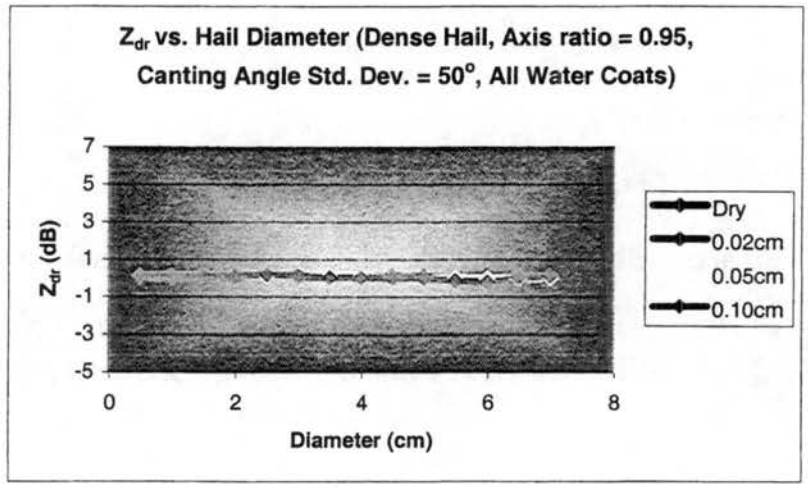

c)

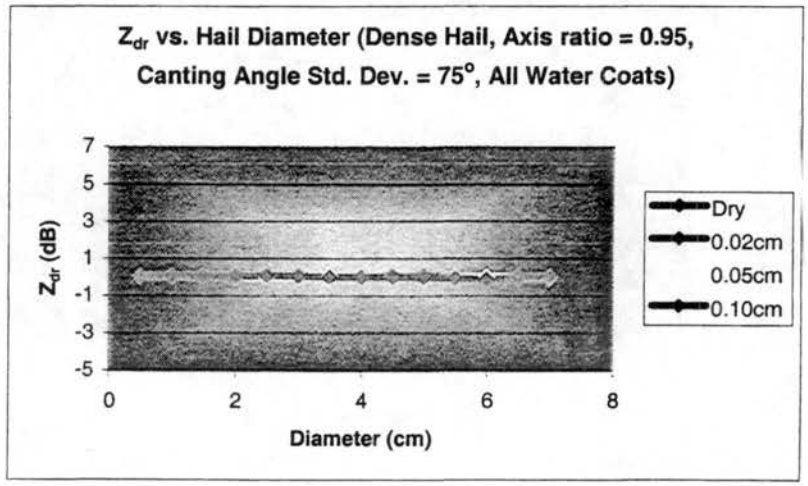

Figure. 3.5: Z_{dr} vs. hail diameter for ice densitiy of 0.91 g cm^{-3} and all water-coat thicknesses. Axis ratio of 0.95 and canting angle standard deviation of a) 25°, b) 50°, and c) 75°.

d)

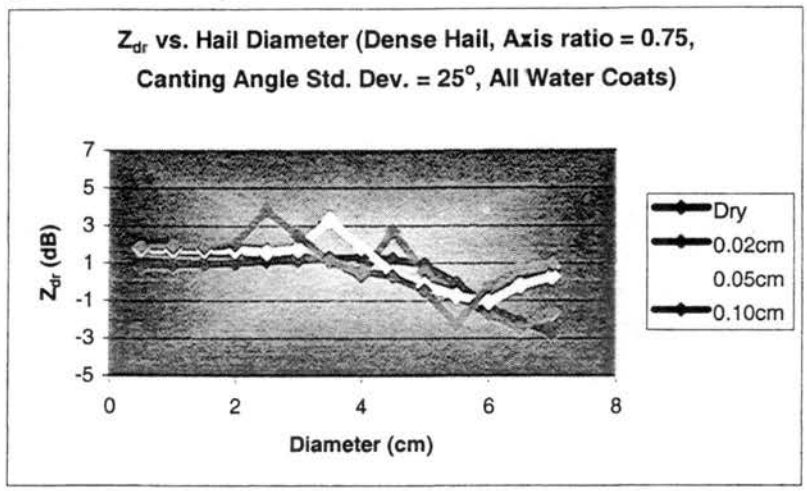

e)

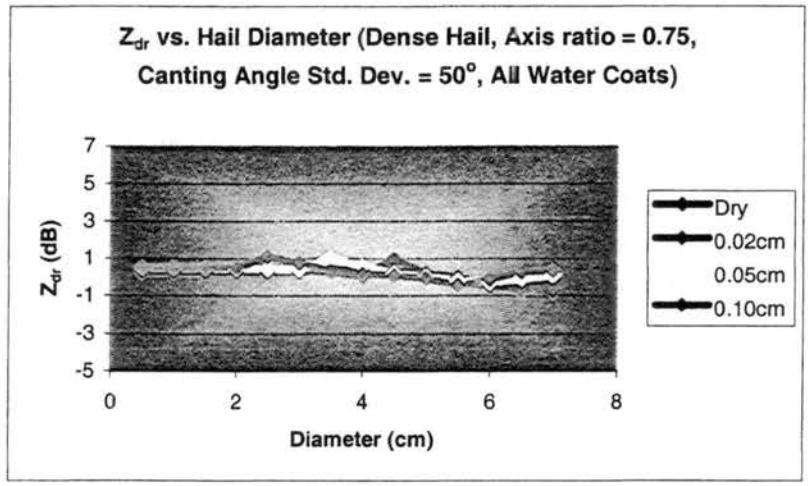

f)

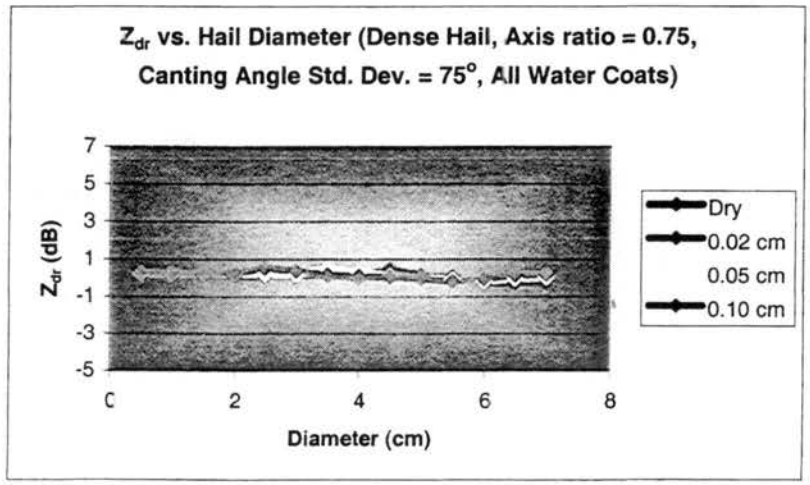

Figure. 3.5 (Cont.): Z_{dr} vs. hail diameter for ice densitiy of 0.91 g cm^{-3} and all water-coat thicknesses. Axis ratio of 0.75 and canting angle standard deviation of d) 25°, e) 50°, and f) 75°.

g)

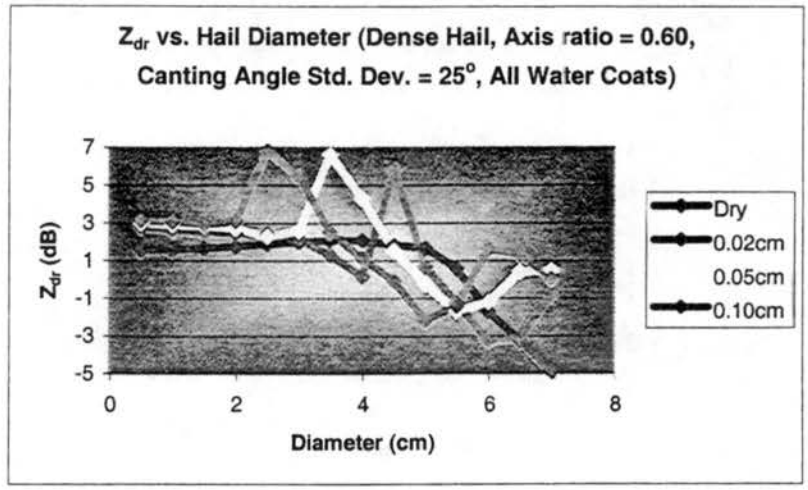

h)

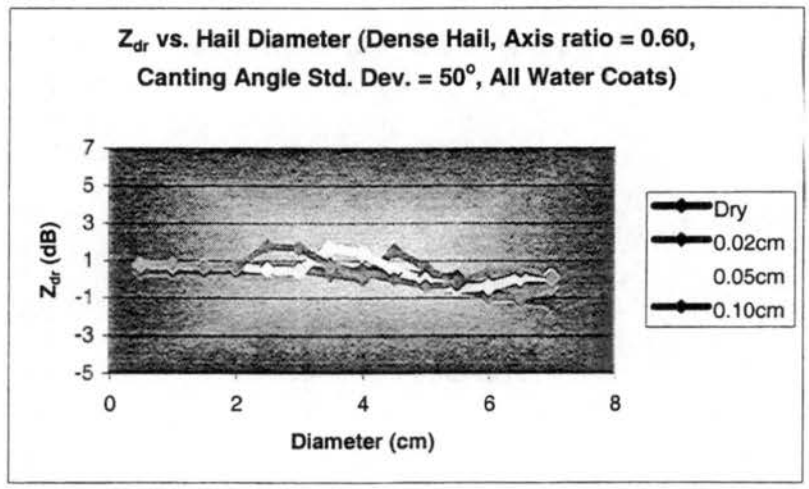

i)

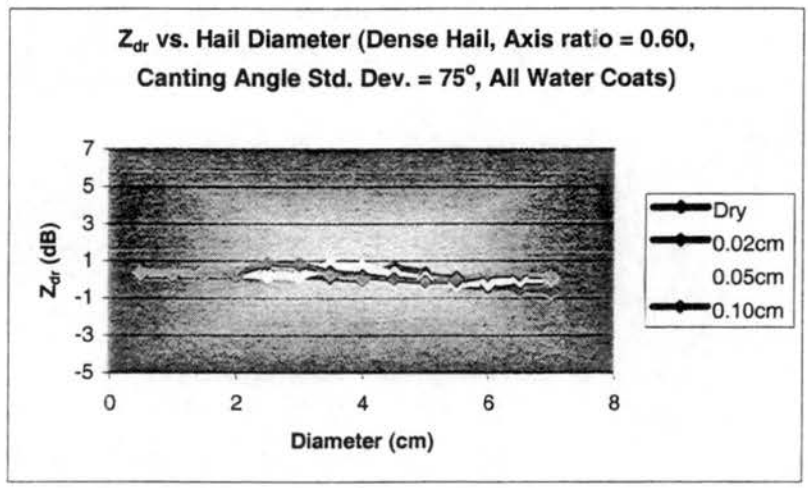

Figure. 3.5 (Cont.): Z_{dr} vs. hail diameter for ice densitiy of 0.91 g cm^{-3} and all water-coat thicknesses. Axis ratio of 0.60 and canting angle standard deviation of g) 25°, h) 50°, and i) 75°.

a)

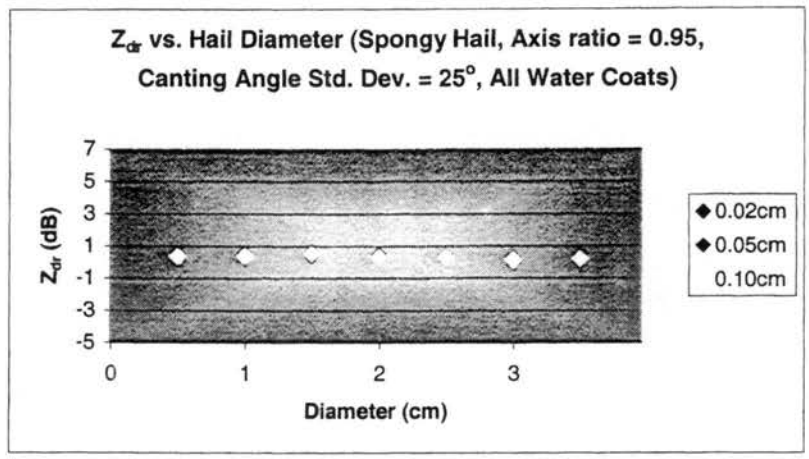

b)

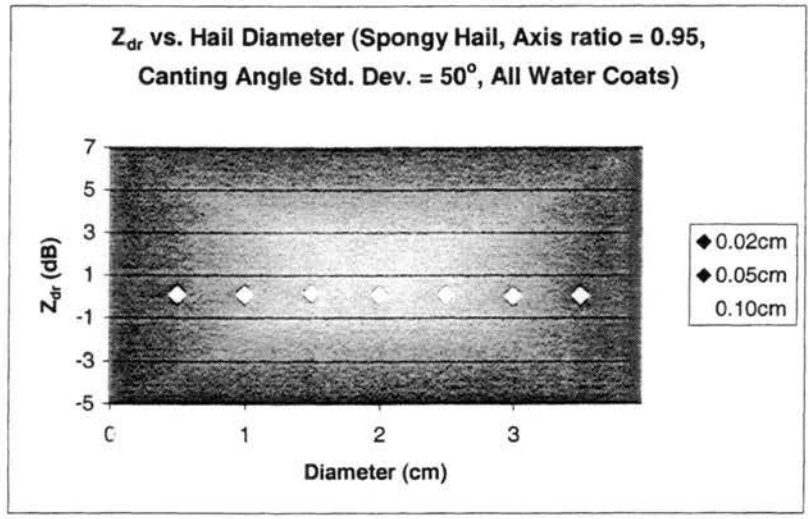

c)

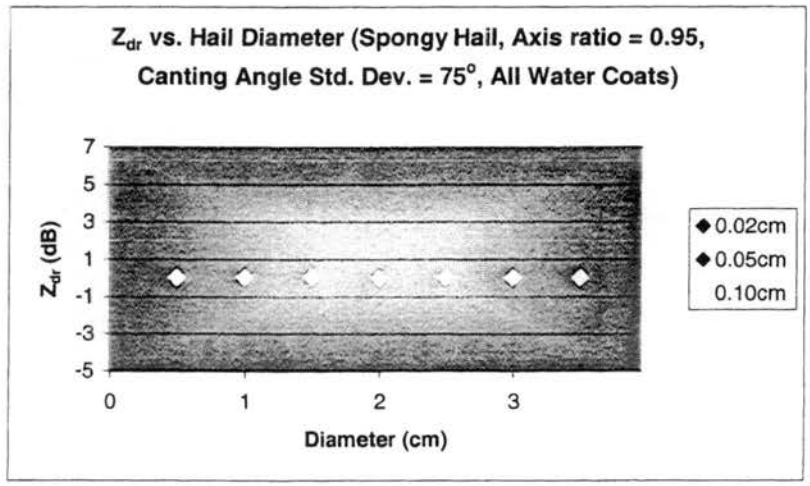

Figure 3.6: Z_{dr} vs. hail diameter for 40% water volume and all non-zero water-coat thicknesses. Axis ratio of 0.95 and canting angle standard deviation of a) 25°, b) 50°, and c) 75°.

d)

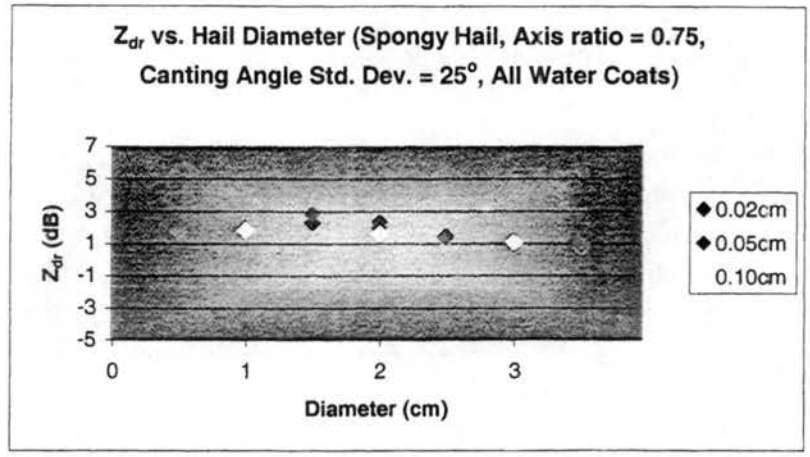

e)

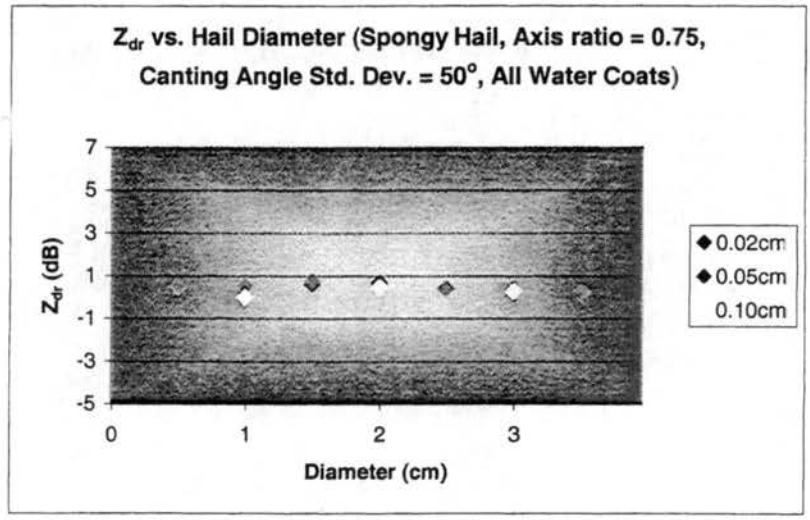

f)

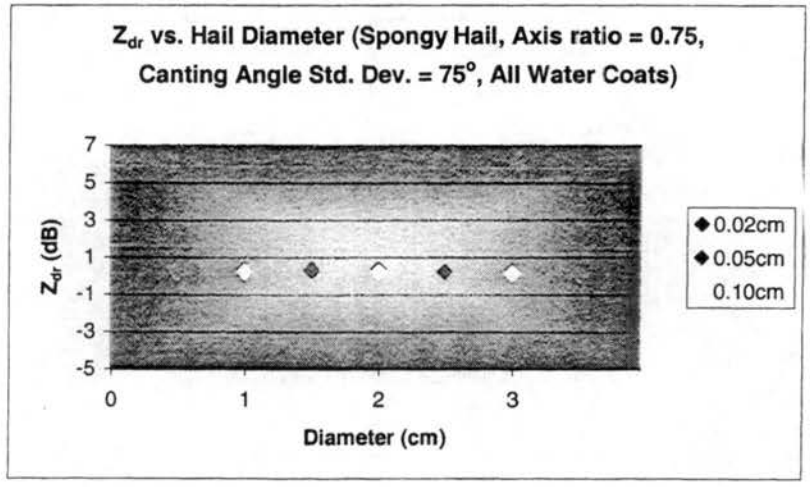

Figure 3.6 (Cont.): Z_{dr} vs. hail diameter for 40% water volume and all non-zero water-coat thicknesses. Axis ratio of 0.75 and canting angle standard deviation of d) 25°, e) 50°, and f) 75°.

a)

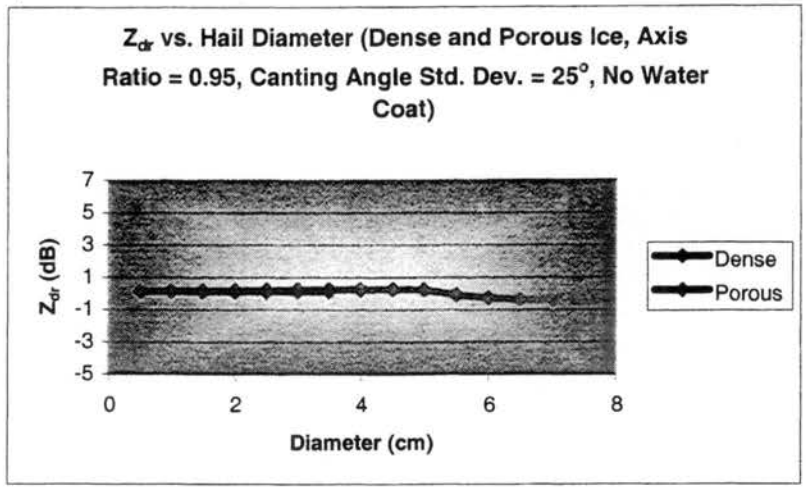

b)

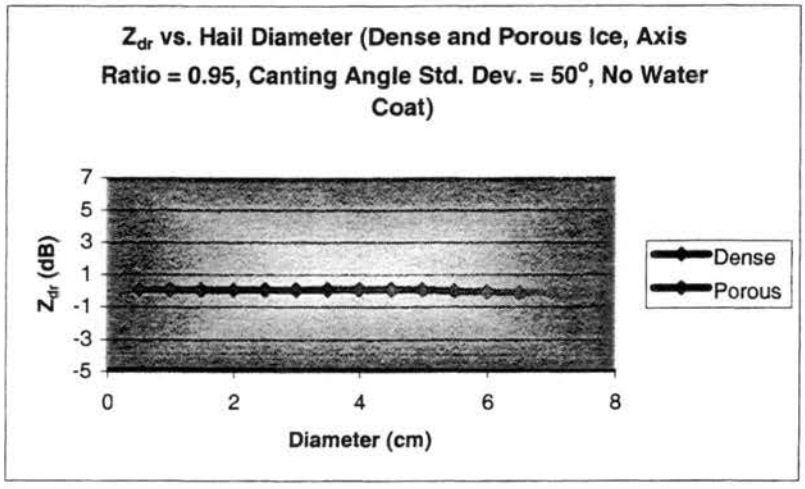

c)

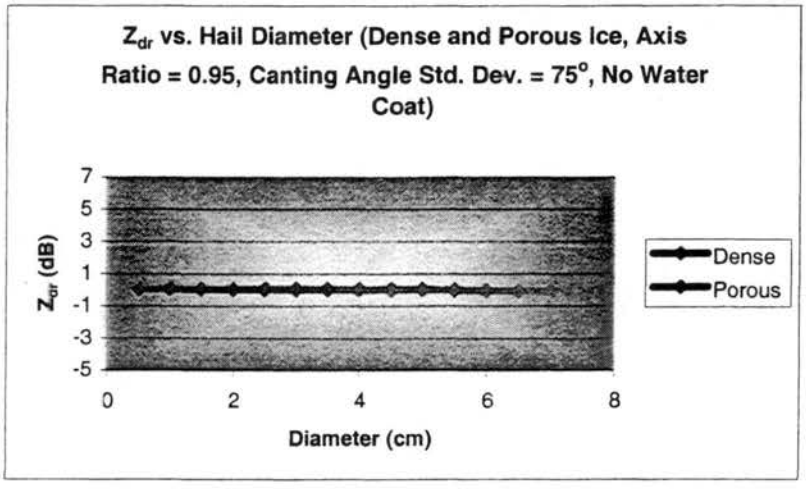

Figure 3.7: Z_{dr} vs. hail diameter for ice densities of 0.91 g cm^{-3} and 0.45 g cm^{-3}. 0.45 g cm^{-3} density only explored at smaller sizes. Axis ratio of 0.95 and canting angle standard deviation of a) 25°, b) 50°, and c) 75°.

d)

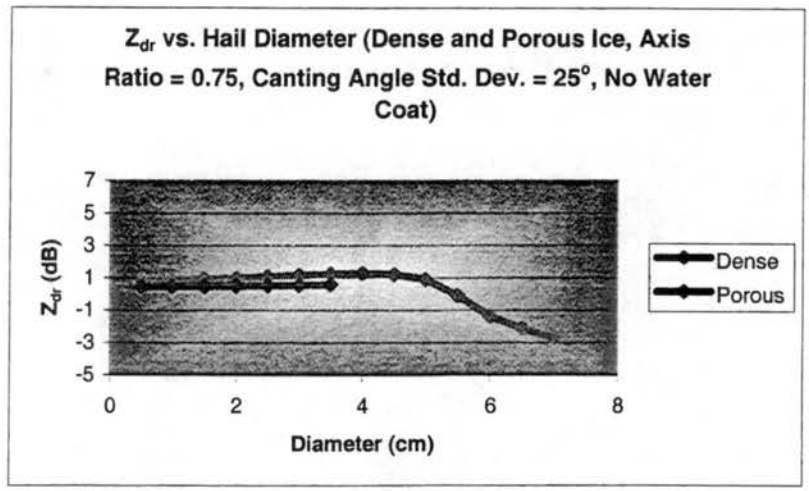

e)

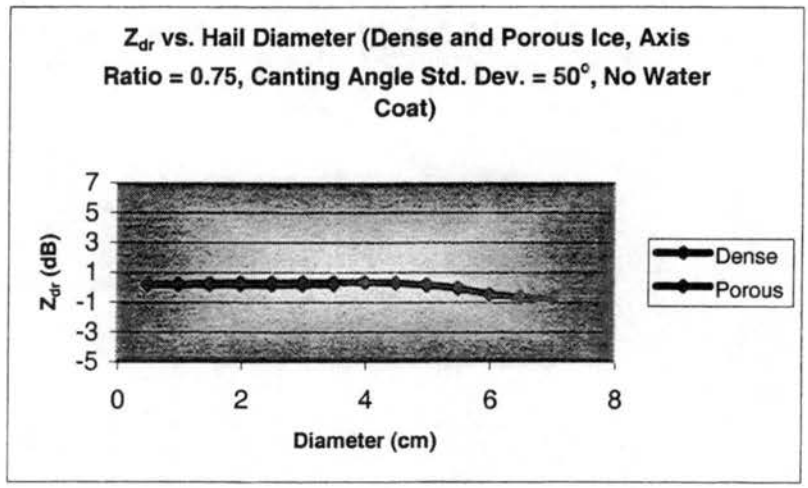

f)

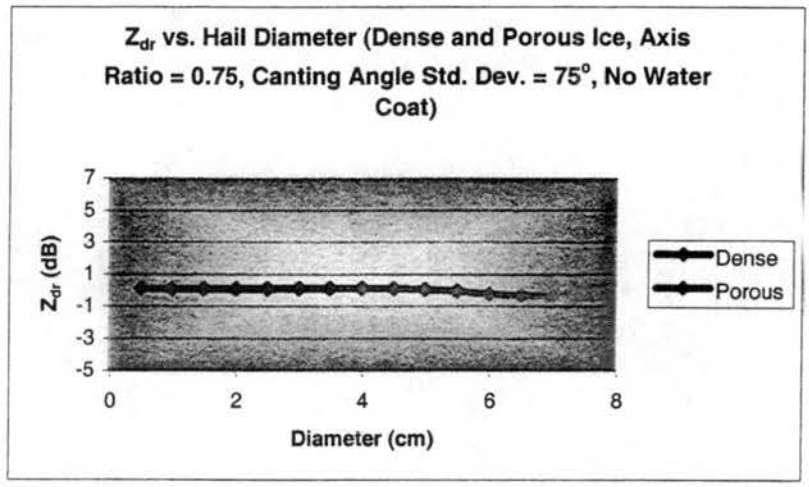

Figure 3.7 (Cont.): Z_{dr} vs. hail diameter for ice densities of 0.91 g cm^{-3} and 0.45 g cm^{-3}. 0.45 g cm^{-3} density only explored at smaller sizes. Axis ratio of 0.75 and canting angle standard deviation of d) 25°, e) 50°, and f) 75°.

a)

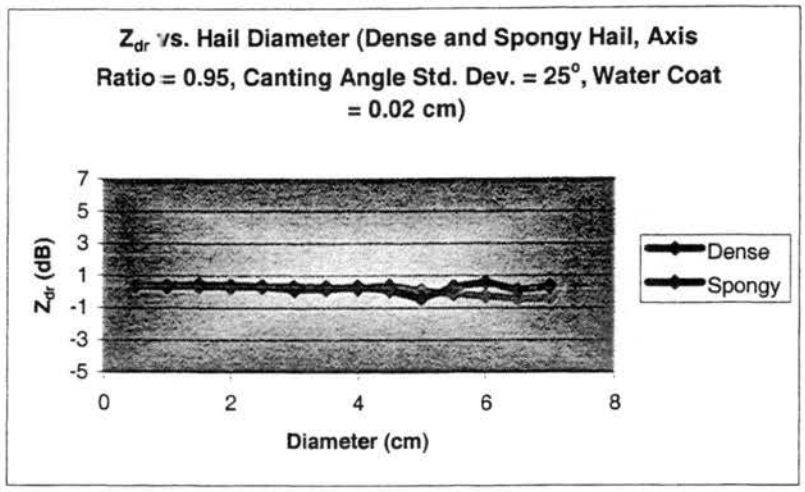

b)

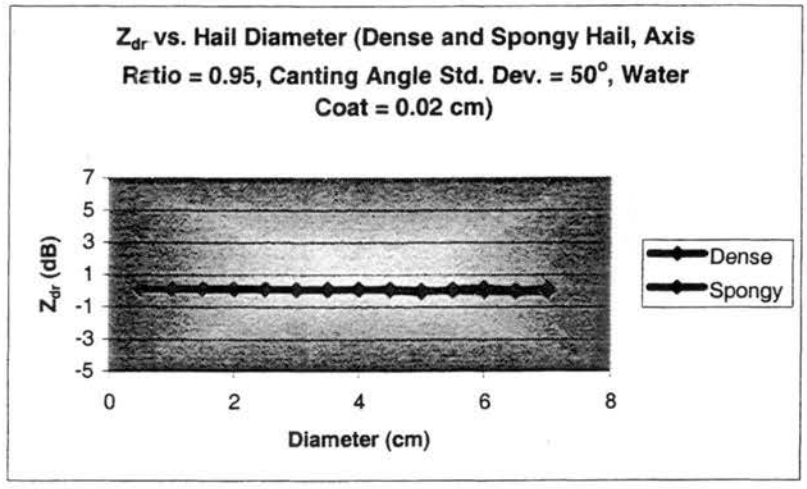

c)

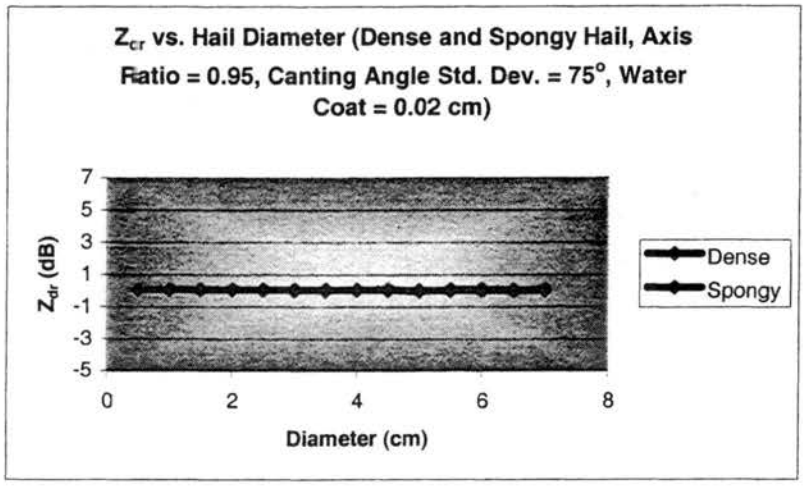

Figure 3.8: Z_{dr} vs. hail diameter for ice densities of 0.91 g cm^{-3} and 40% water volume. Axis ratio of 0.95 and canting angle standard deviation of a) 25°, b) 50°, and c) 75°.

d)

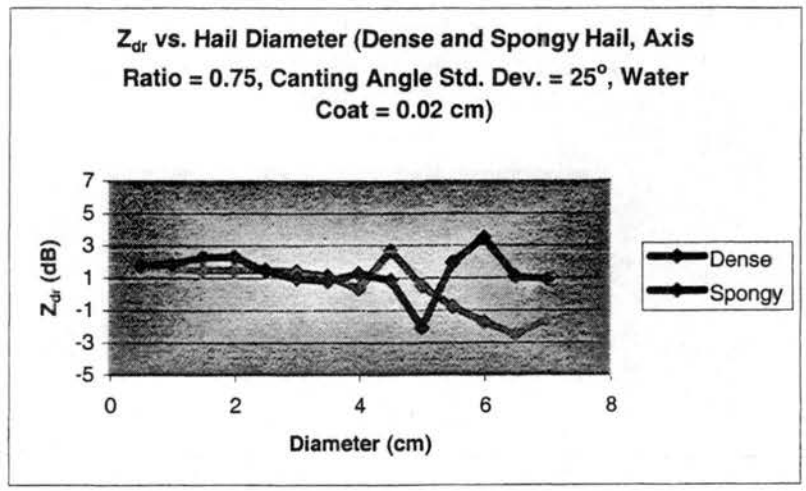

e)

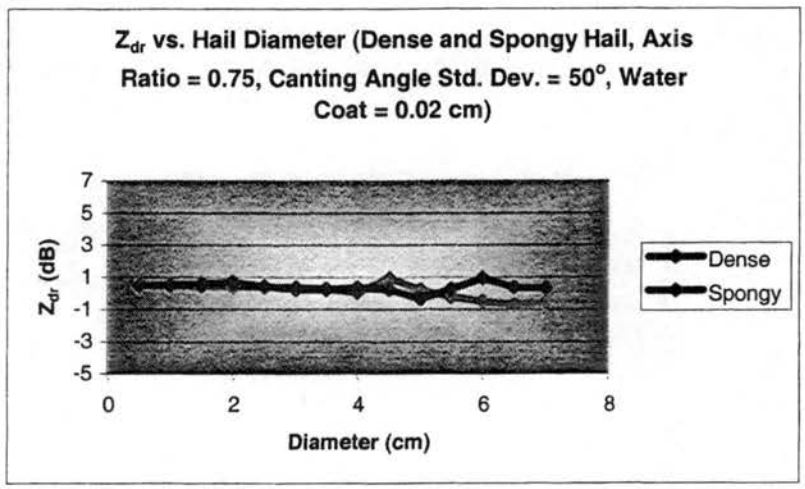

f)

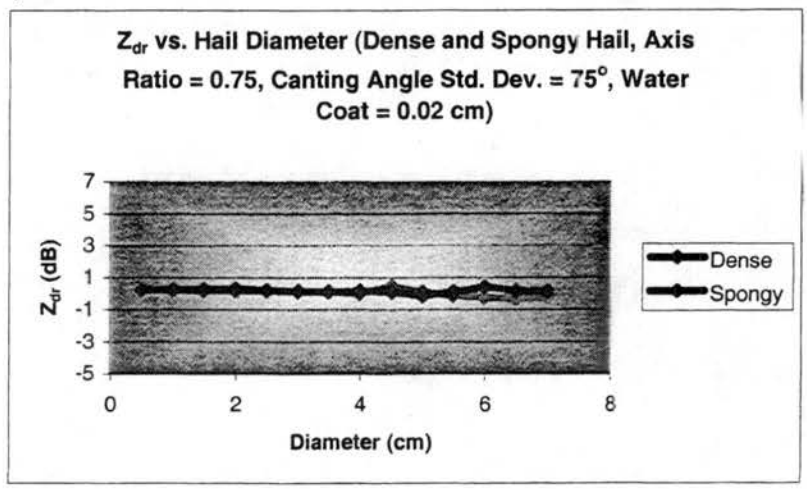

Figure 3.8 (Cont.): Z_{dr} vs. hail diameter for ice densities of 0.91 g cm^{-3} and 40% water volume. Axis ratio of 0.75 and canting angle standard deviation of d) 25°, e) 50°, and f) 75°.

a)

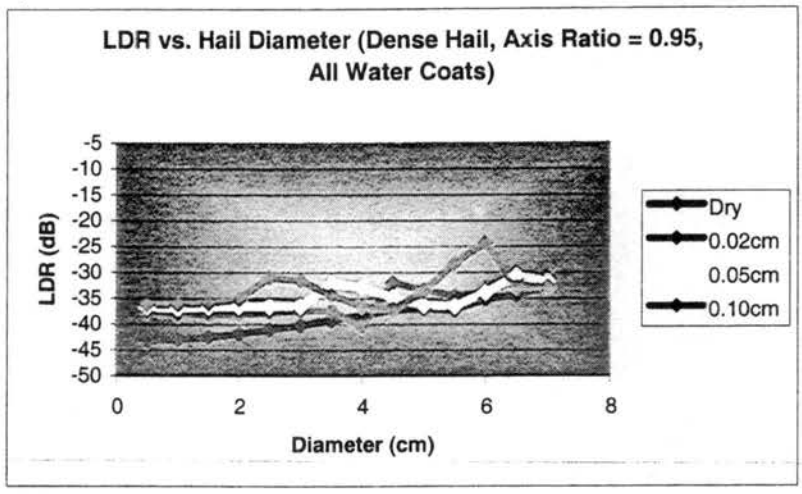

b)

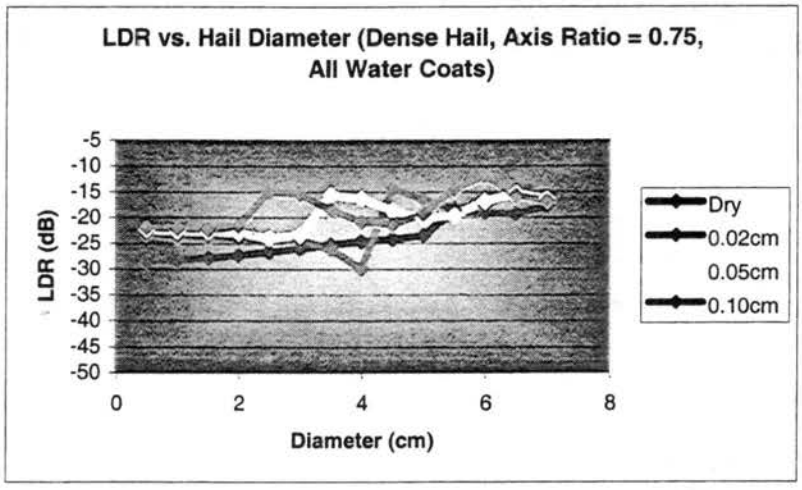

c)

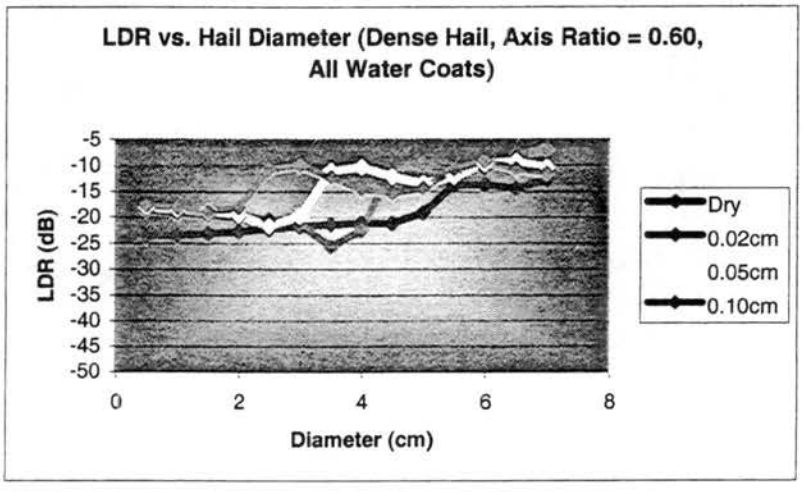

Figure 3.9: LDR vs. hail diameter for an ice density of 0.91 g cm^{-3}, and all water-coat thicknesses. Random canting angle distribution shown, but representative of all canting angles. Axis ratio of a) 0.95, b) 0.75, and c) 0.60.

a)

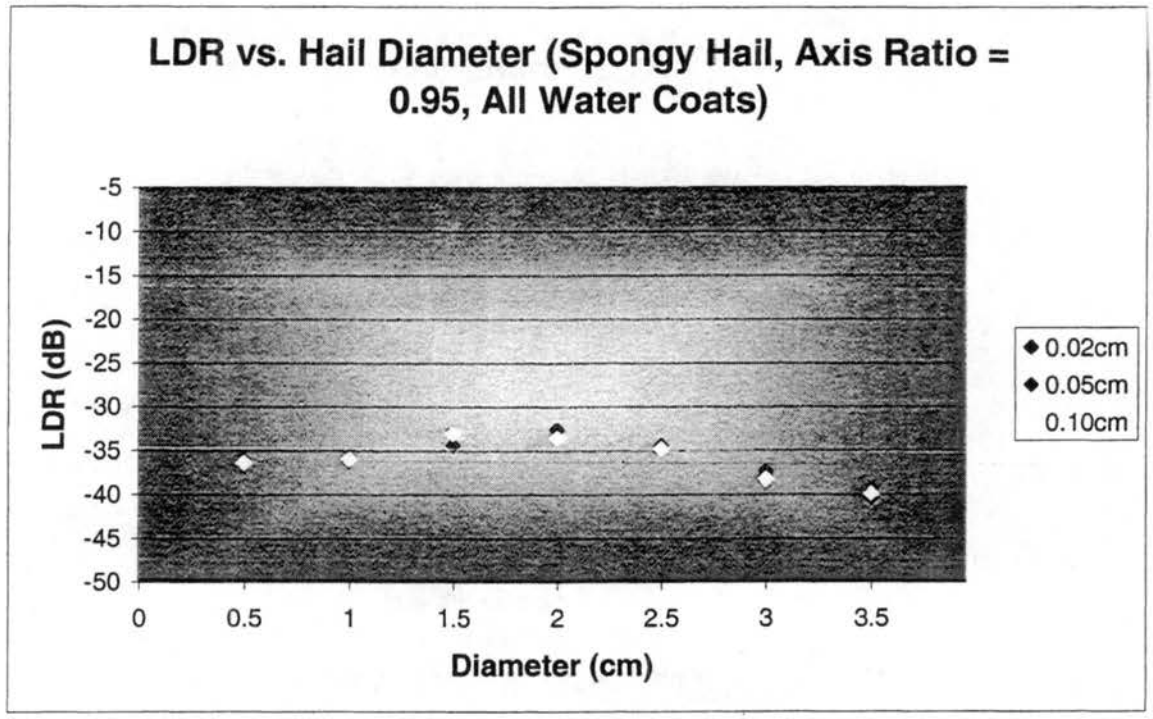

b)

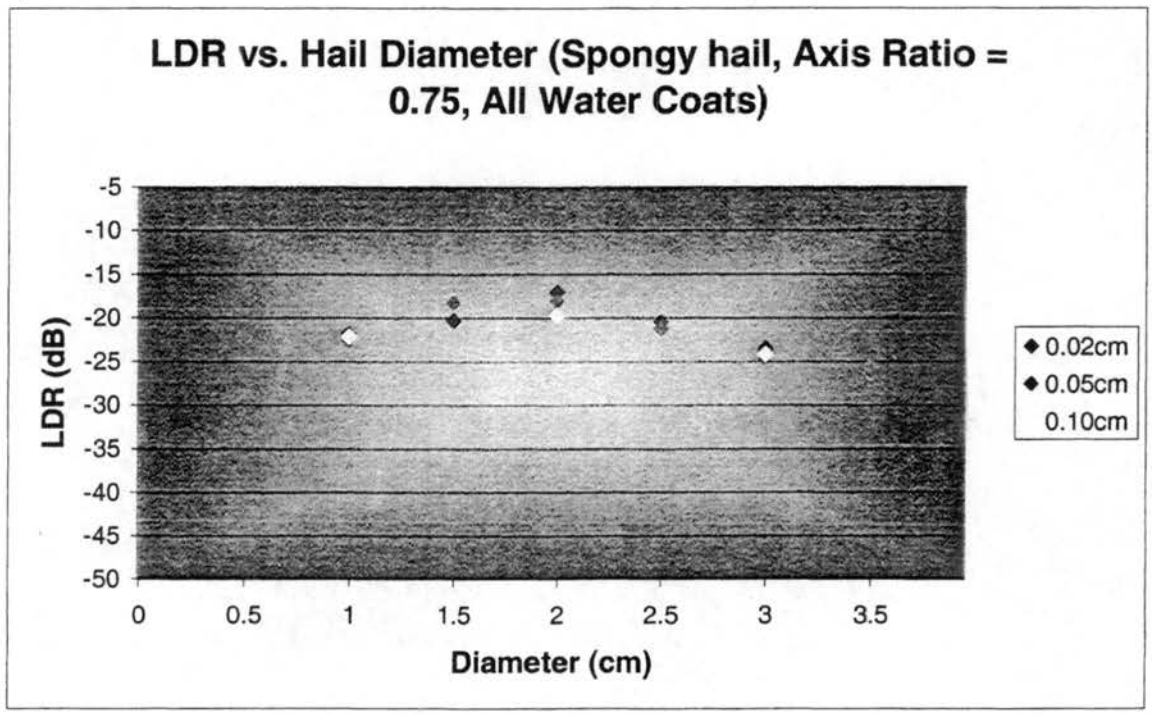

Figure 3.10: LDR vs. hail diameter for 40% water volume and all non-zero water-coat thicknesses. Random canting angle distribution shown, but representative of all canting angles. Axis ratio of a) 0.95, and b) 0.75.

a)

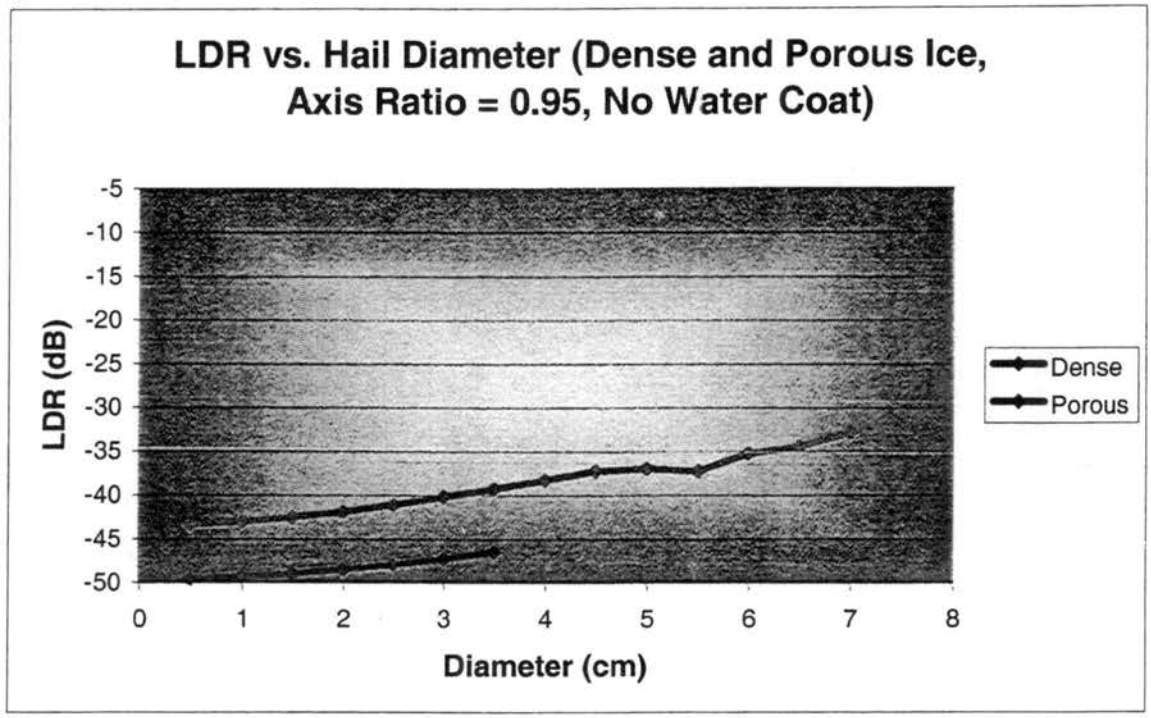

b)

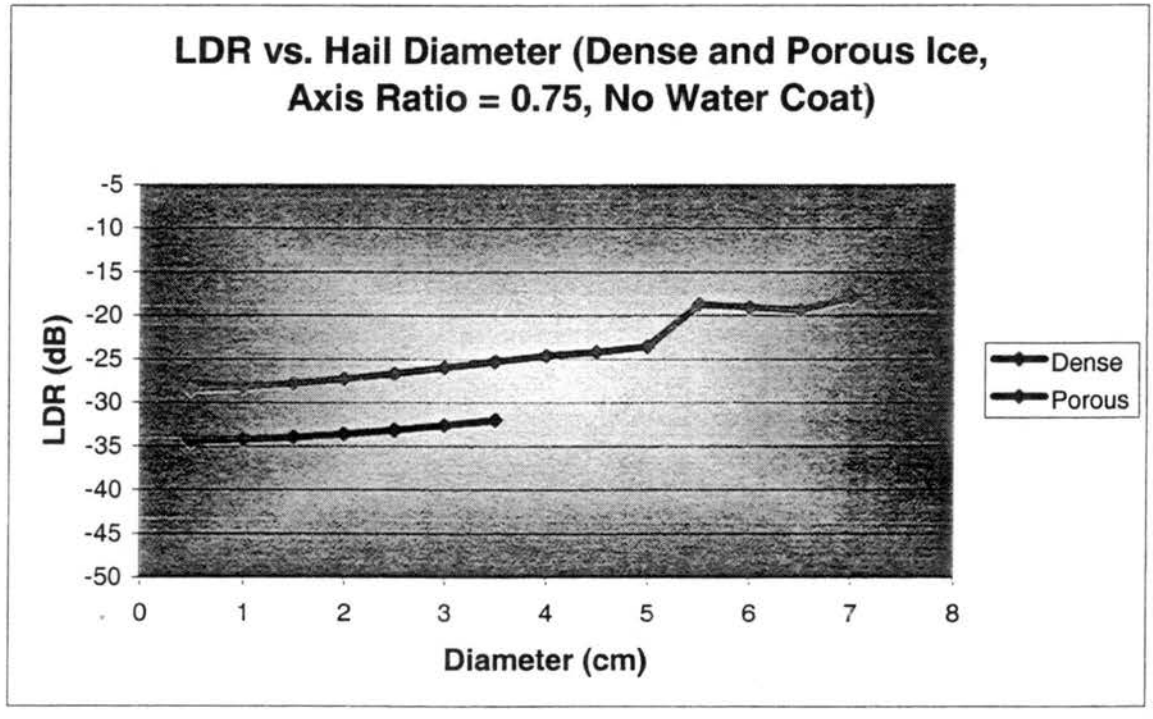

Figure 3.11: LDR vs. hail diameter for ice densities of 0.91 g cm^{-3} and 0.45 g cm^{-3}. 0.45 g cm^{-3} density only explored at smaller sizes. Random canting angle distribution shown, but representative of all canting angles. Axis ratio of a) 0.95, and b) 0.75.

a)

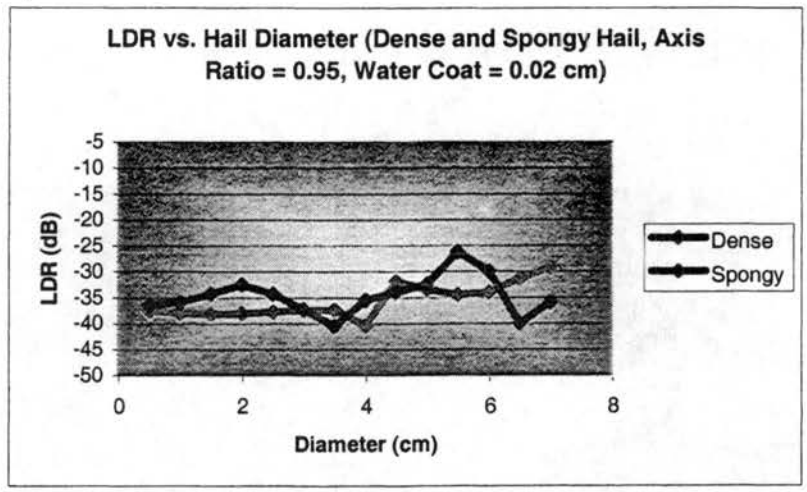

b)

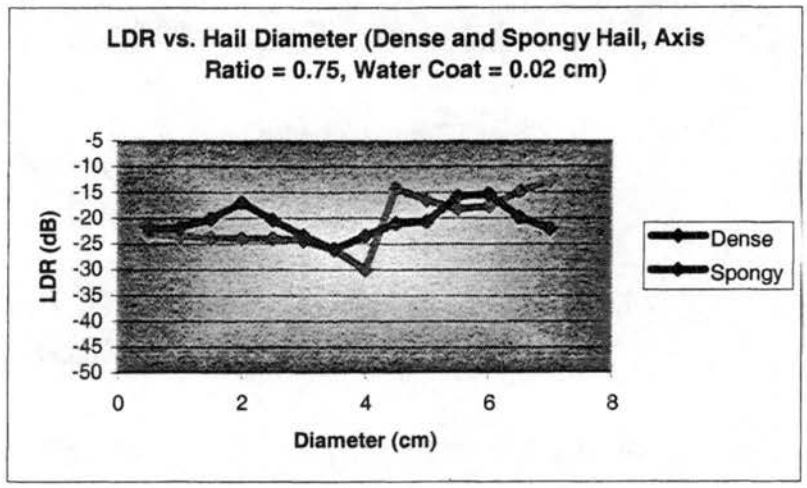

c)

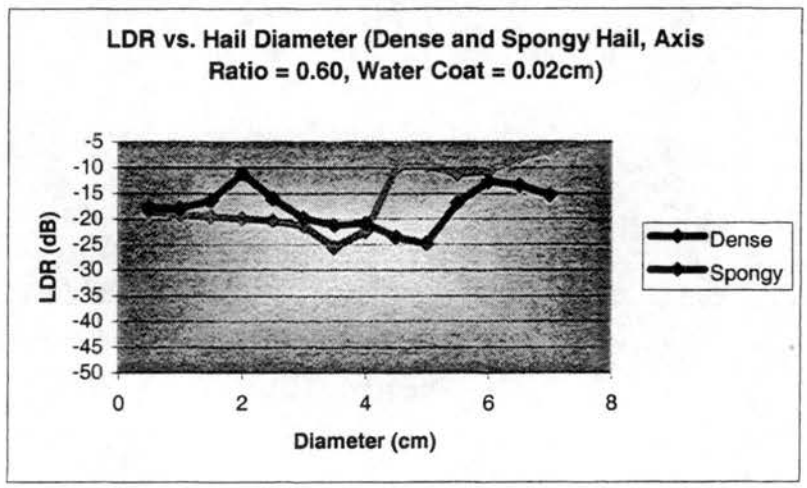

Figure 3.12: LDR vs. hail diameter for ice densities of 0.91 g cm^{-3} and 40% water volume. Random canting angle distribution shown, but representative of all canting angles. Axis ratio of a) 0.95, b) 0.75, and c) 0.60.

a)

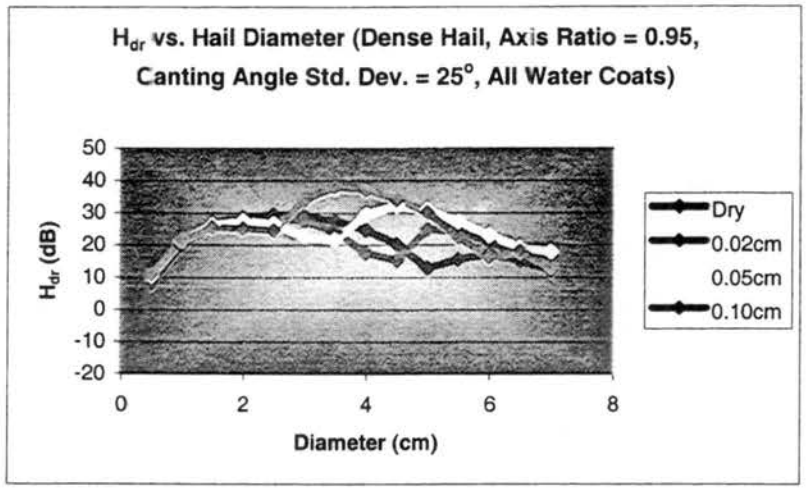

b)

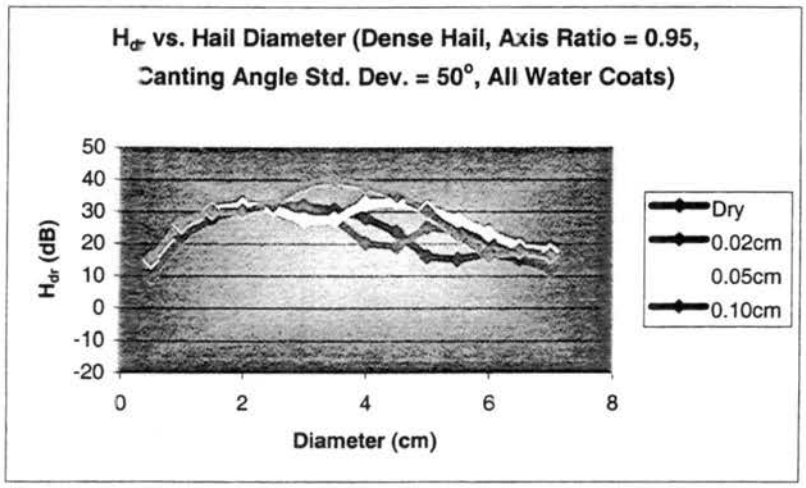

c)

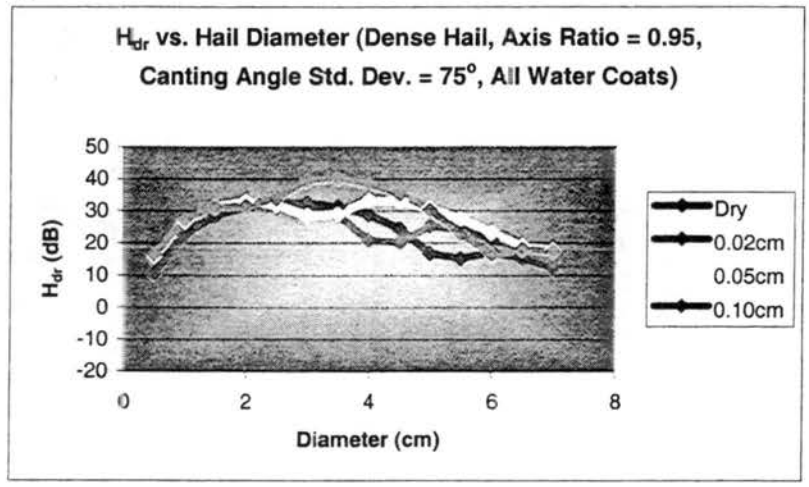

Figure 3.13: H_{dr} vs. hail diameter for ice density of 0.91 g cm^{-3} and all water-coat thicknesses. Axis ratio of 0.95 and canting angle standard deviation of a) 25°, b) 50°, and c) 75°.

d)

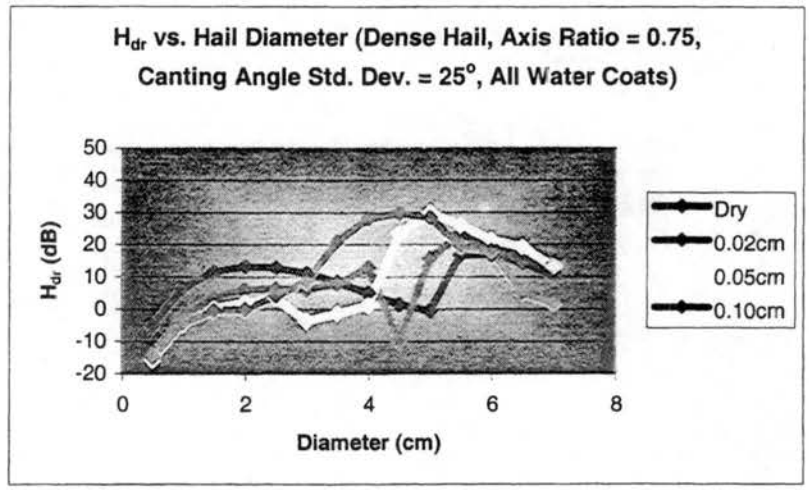

e)

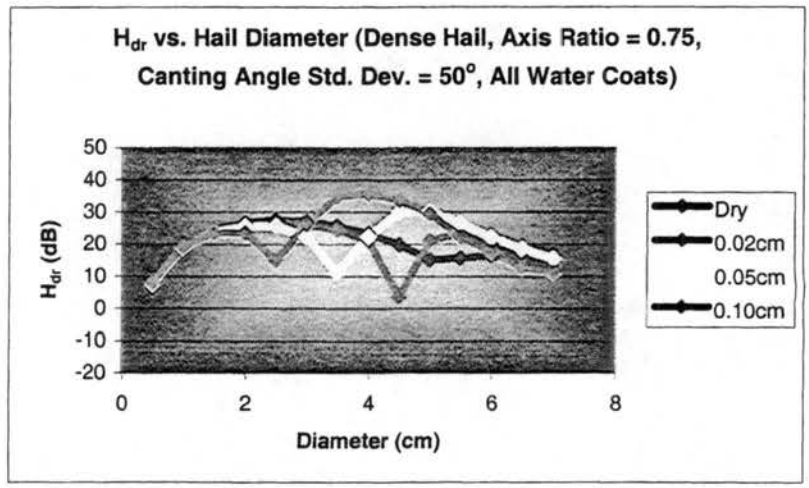

f)

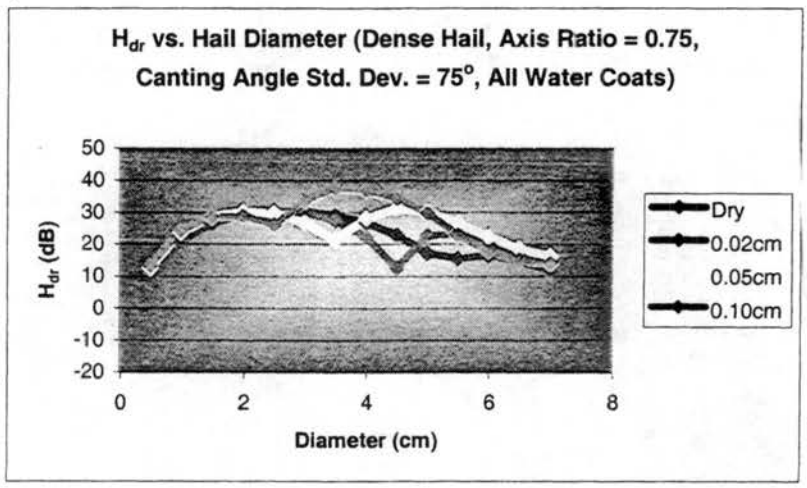

Figure 3.13 (Cont.): H_{dr} vs. hail diameter for ice densitiy of 0.91 g cm^{-3} and all water-coat thicknesses. Axis ratio of 0.75 and canting angle standard deviation of d) 25°, e) 50°, and f) 75°.

g)

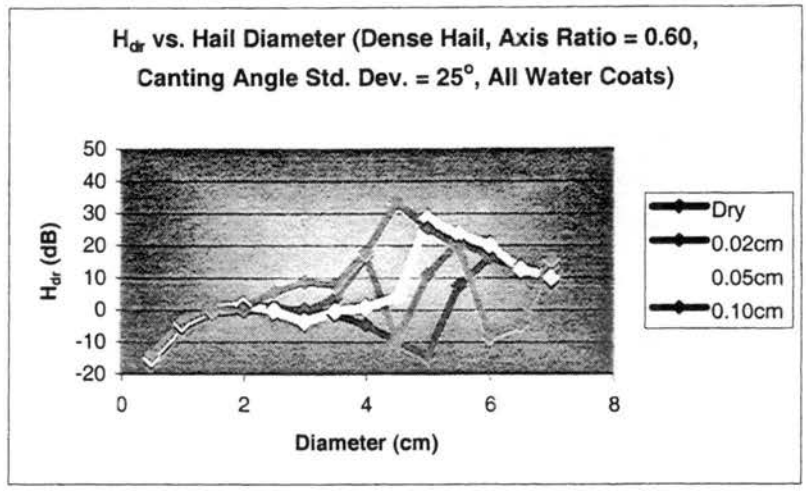

h)

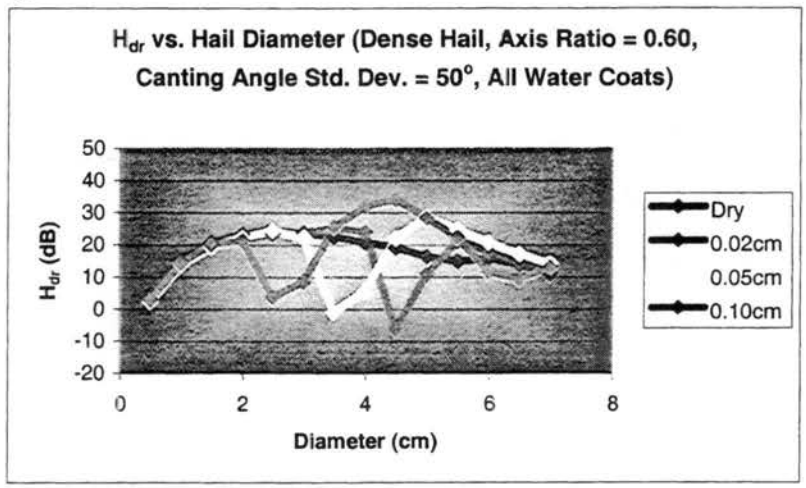

i)

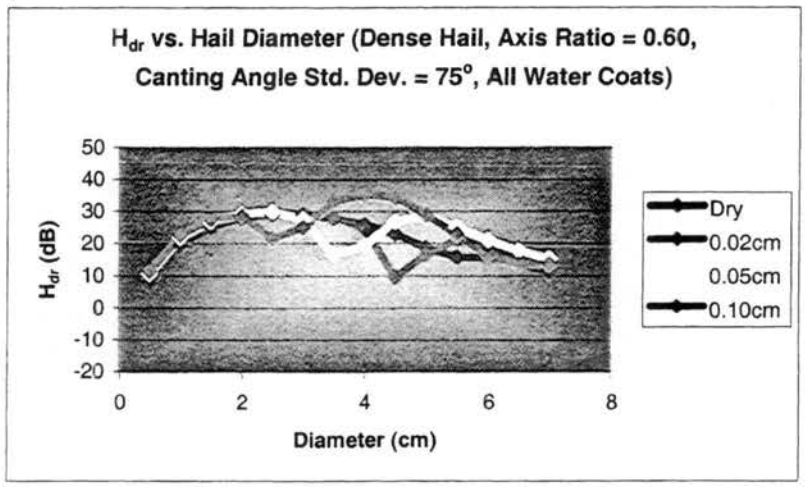

Figure 3.13 (Cont.): H_{dr} vs. hail diameter for ice densitiy of 0.91 g cm^{-3} and all water-coat thicknesses. Axis ratio of 0.60 and canting angle standard deviation of g) 25°, h) 50°, and i) 75°.

a)

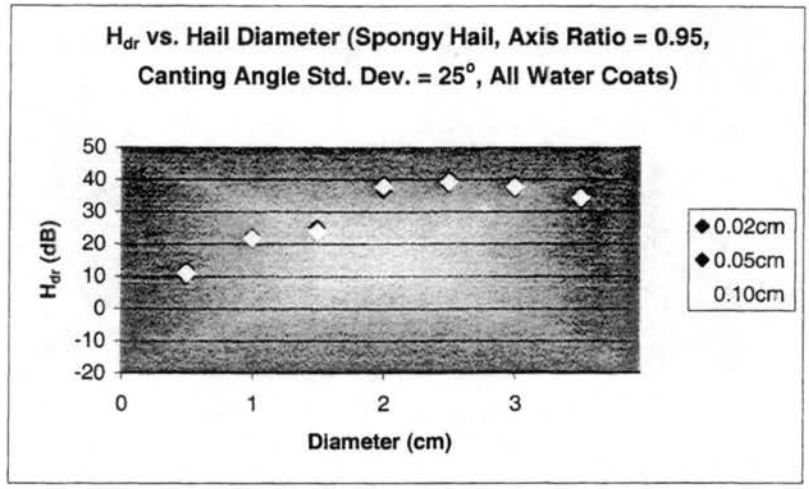

b)

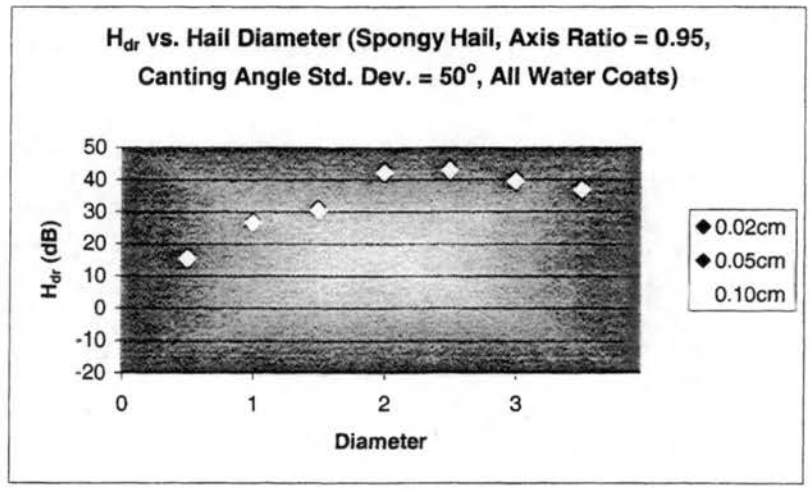

c)

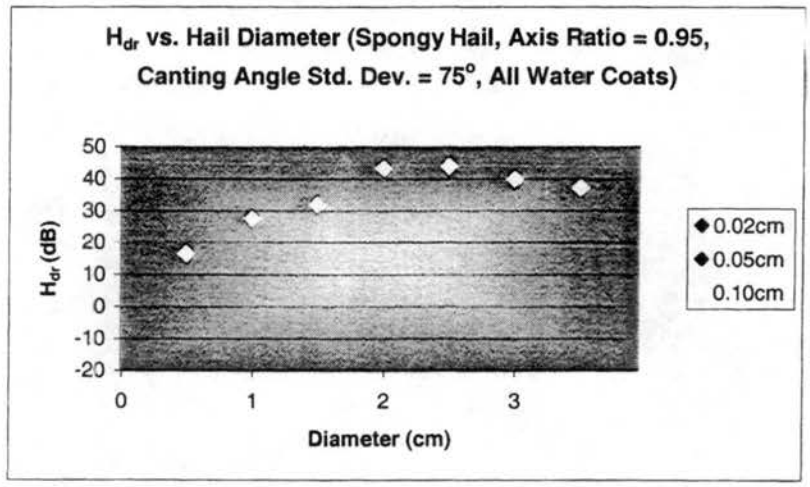

Figure 3.14: H_{dr} vs. hail diameter for 40% water volume and all non-zero water-coat thicknesses. Axis ratio of 0.95 and canting angle standard deviation of a) 25°, b) 50°, and c) 75°.

d)

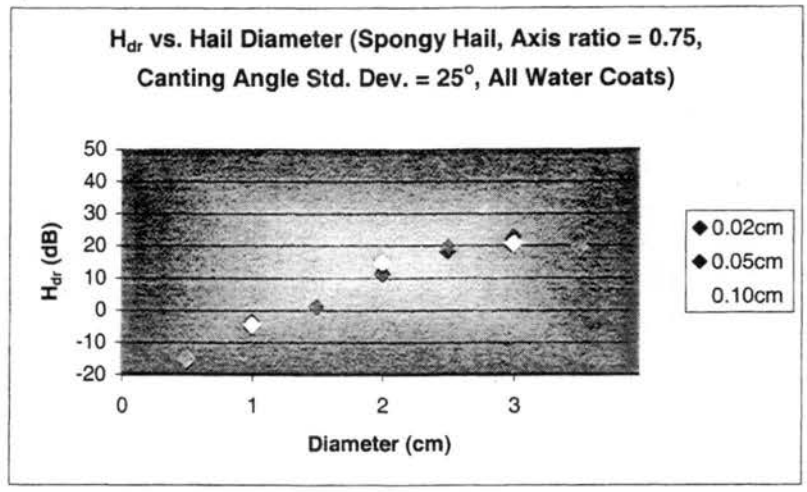

e)

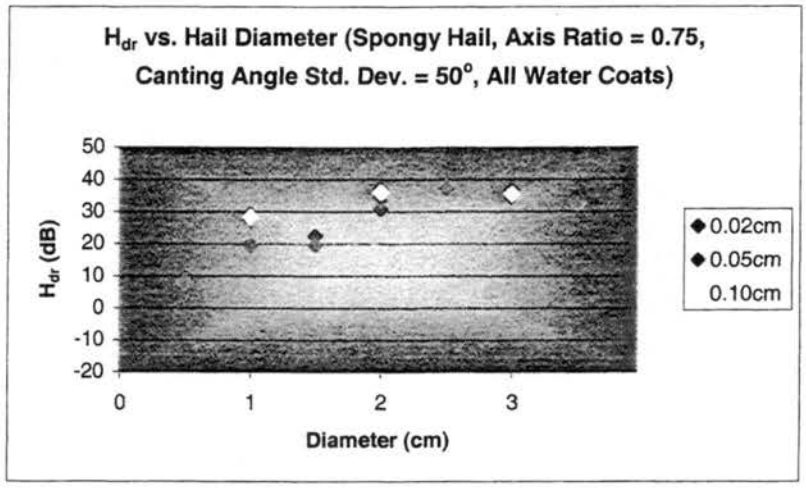

f)

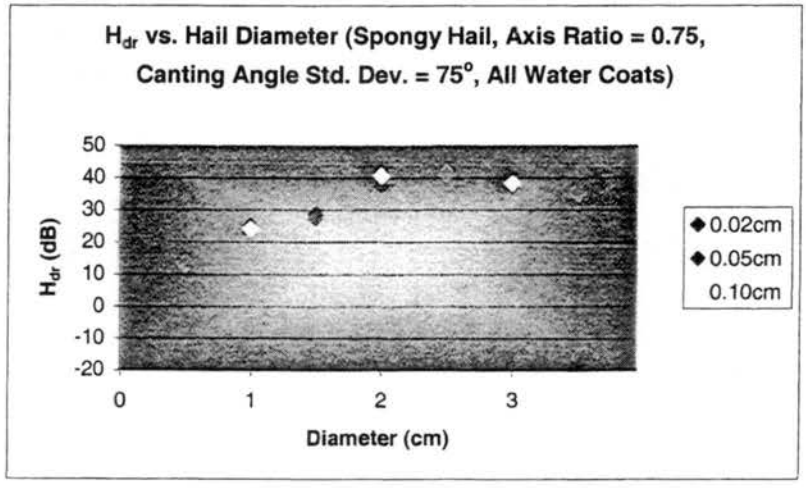

Figure 3.14 (Cont.): H_{dr} vs. hail diameter for 40% water volume and all non-zero water-coat thicknesses. Axis ratio of 0.75 and canting angle standard deviation of d) 25°, e) 50°, and f) 75°.

a)

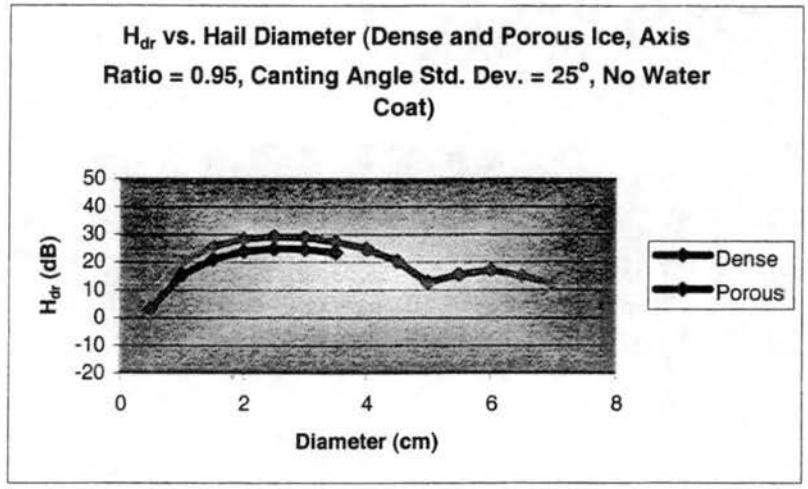

b)

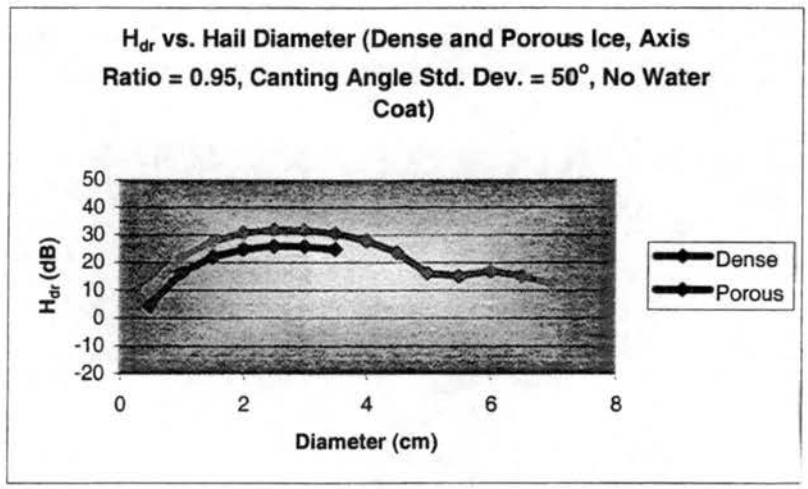

c)

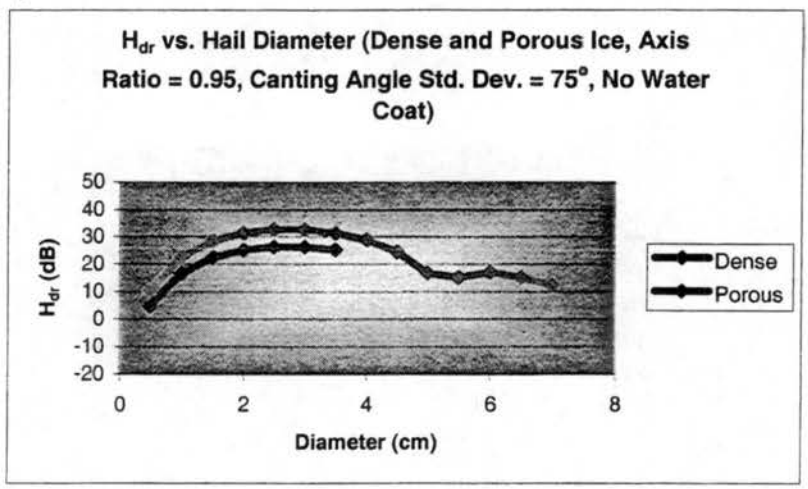

Figure 3.15: H_{dr} vs. hail diameter for ice densities of 0.91 g cm^{-3} and 0.45 g cm^{-3}. 0.45 g cm^{-3} density only explored at smaller sizes. Axis ratio of 0.95 and canting angle standard deviation of a) 25°, b) 50°, and c) 75°.

d)

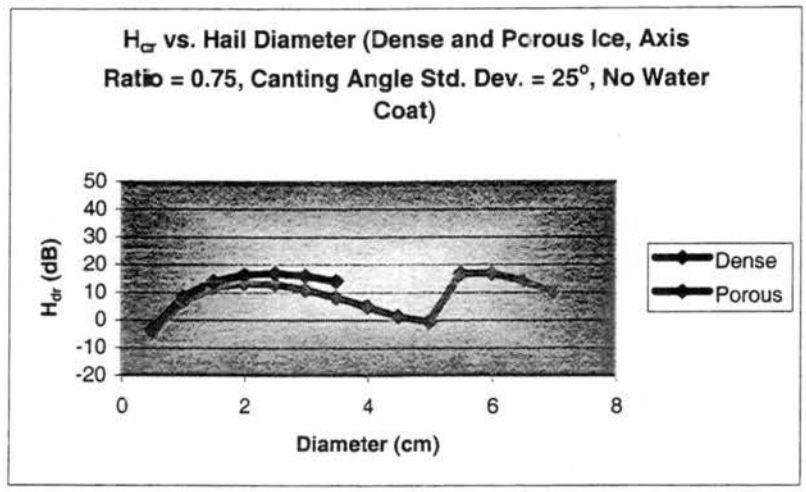

e)

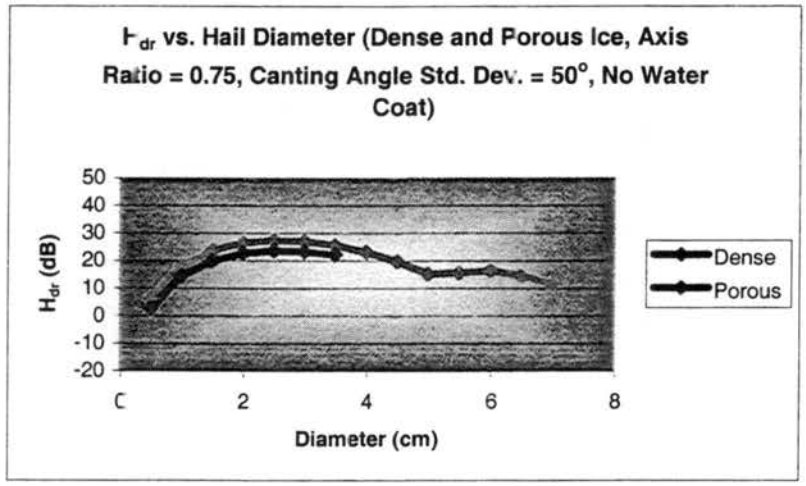

f)

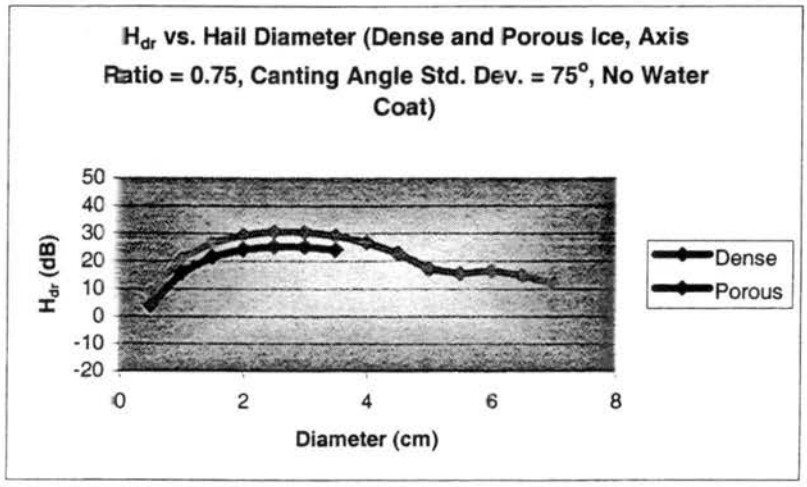

Figure 3.15 (Cont.): H_{dr} vs. hail diameter for ice densities of 0.91 g cm^{-3} and 0.45 g cm^{-3}. 0.45 g cm^{-3} density only explored at smaller sizes. Axis ratio of 0.75 and canting angle standard deviation of d) 25°, e) 50°, and f) 75°.

a)

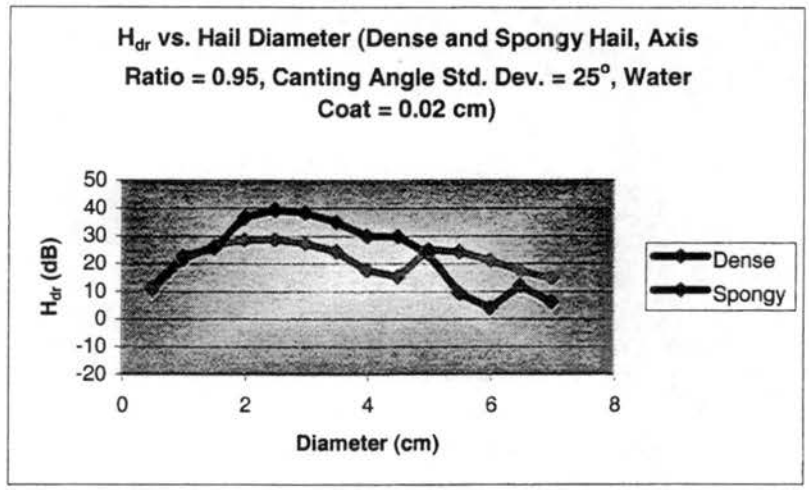

b)

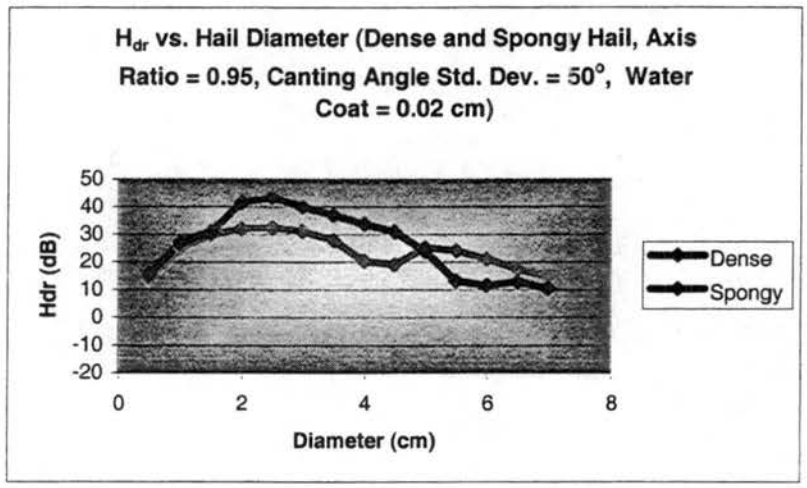

c)

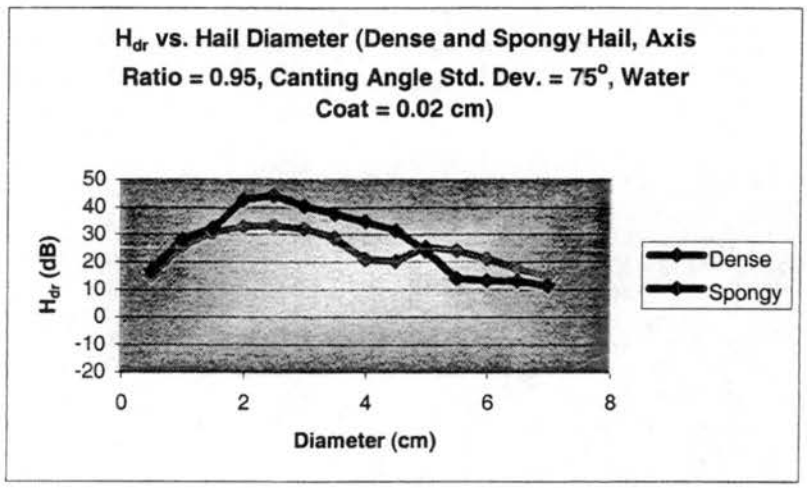

Figure 3.16: H_{dr} vs. hail diameter for ice densities of 0.91 g cm^{-3} and 40% water volume. Axis ratio of 0.95 and canting angle standard deviation of a) 25°, b) 50°, and c) 75°.

d)

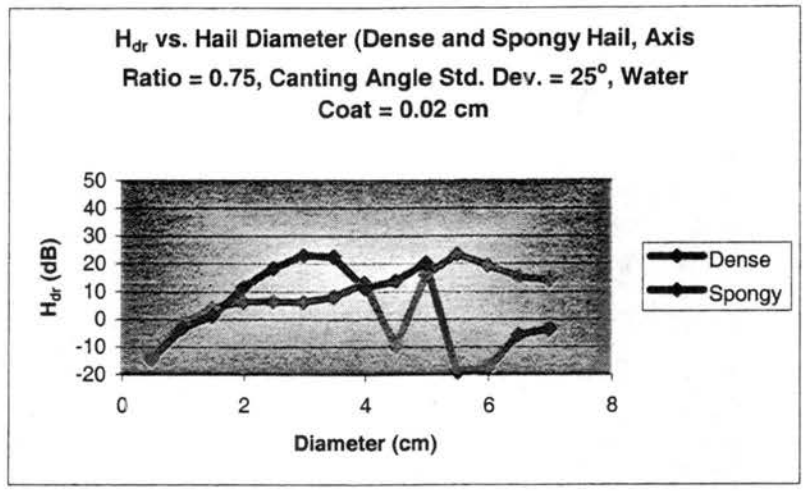

e)

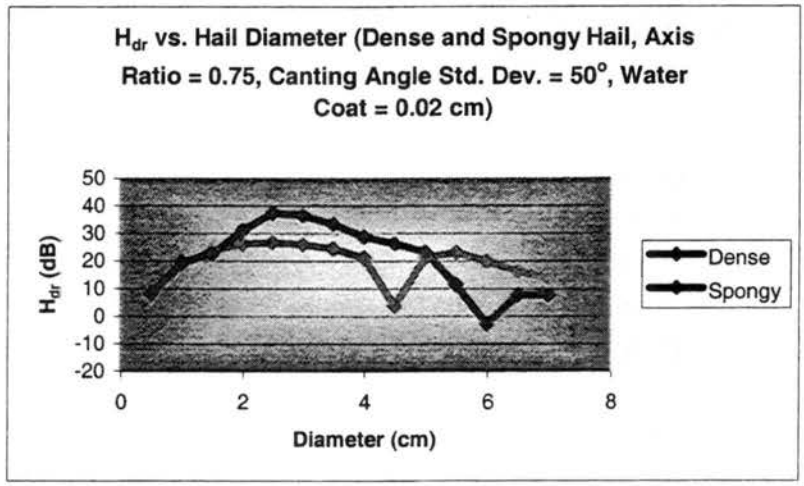

f)

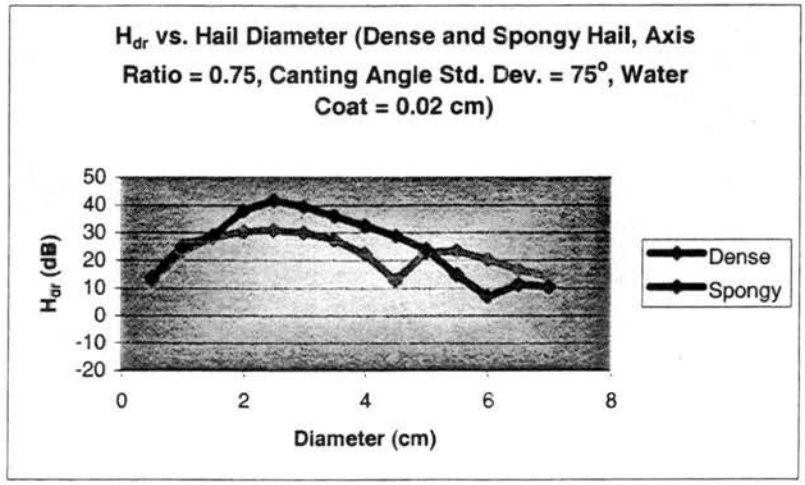

Figure 3.16 (Cont.): H_{dr} vs. hail diameter for ice densities of 0.91 g cm^{-3} and 40% water volume. Axis ratio of 0.75 and canting angle standard deviation of d) 25°, e) 50°, and f) 75°.

a)

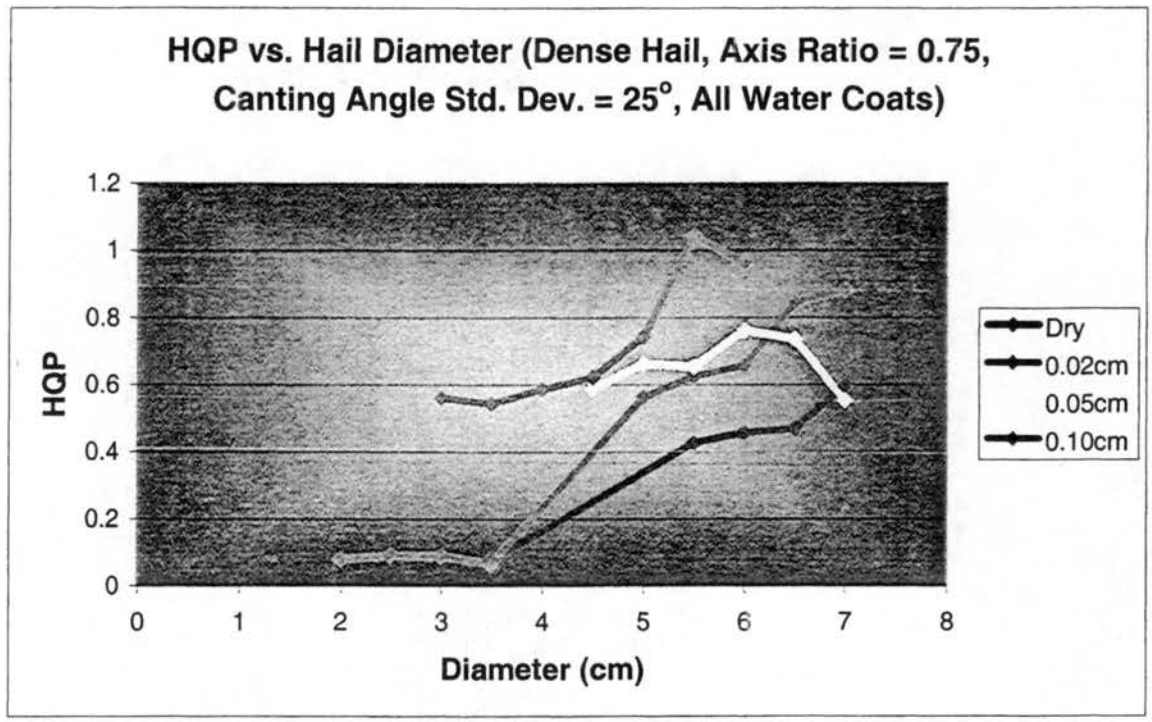

b)

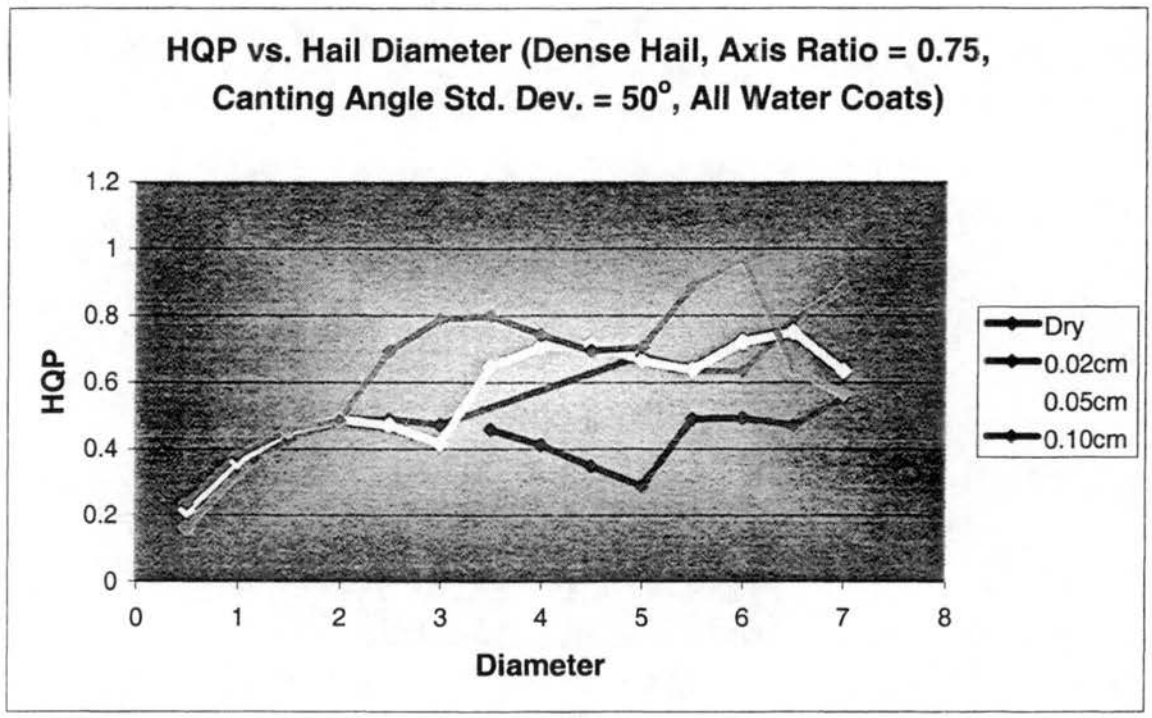

Figure 3.17: HQP vs. hail diameter for ice densitiy of 0.91 g cm^{-3} and all water-coat thicknesses. Axis ratio of 0.75 and canting angle standard deviation of a) 25°, b) 50°.

c)

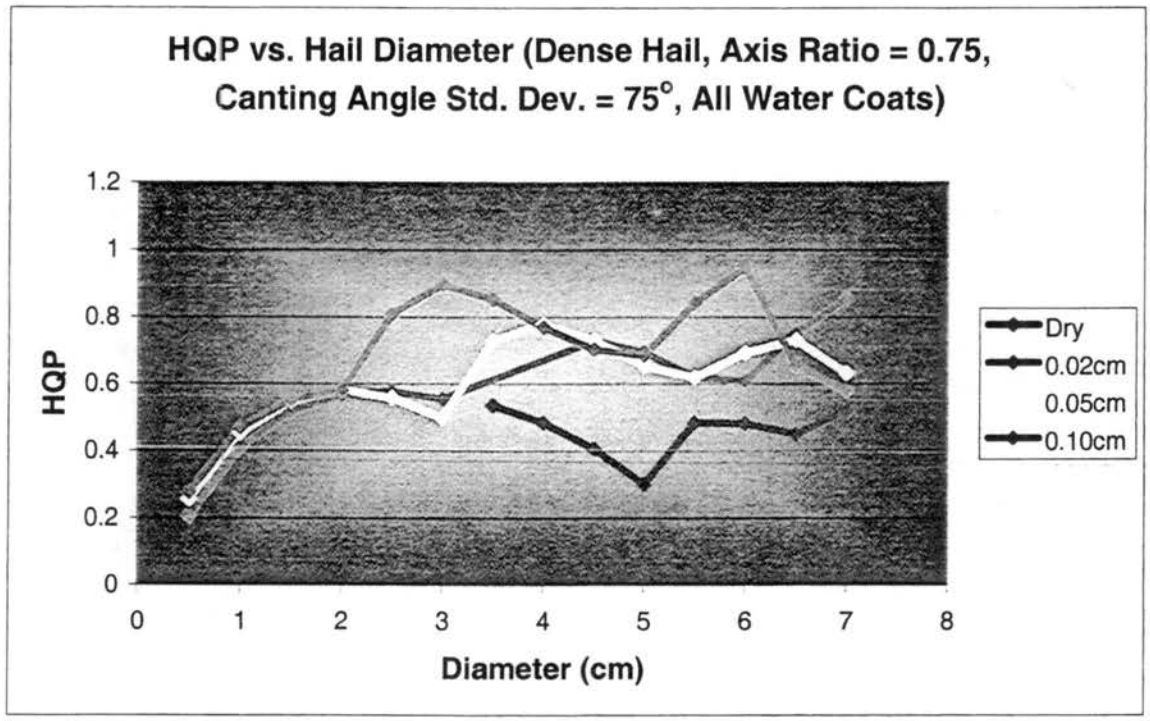

d)

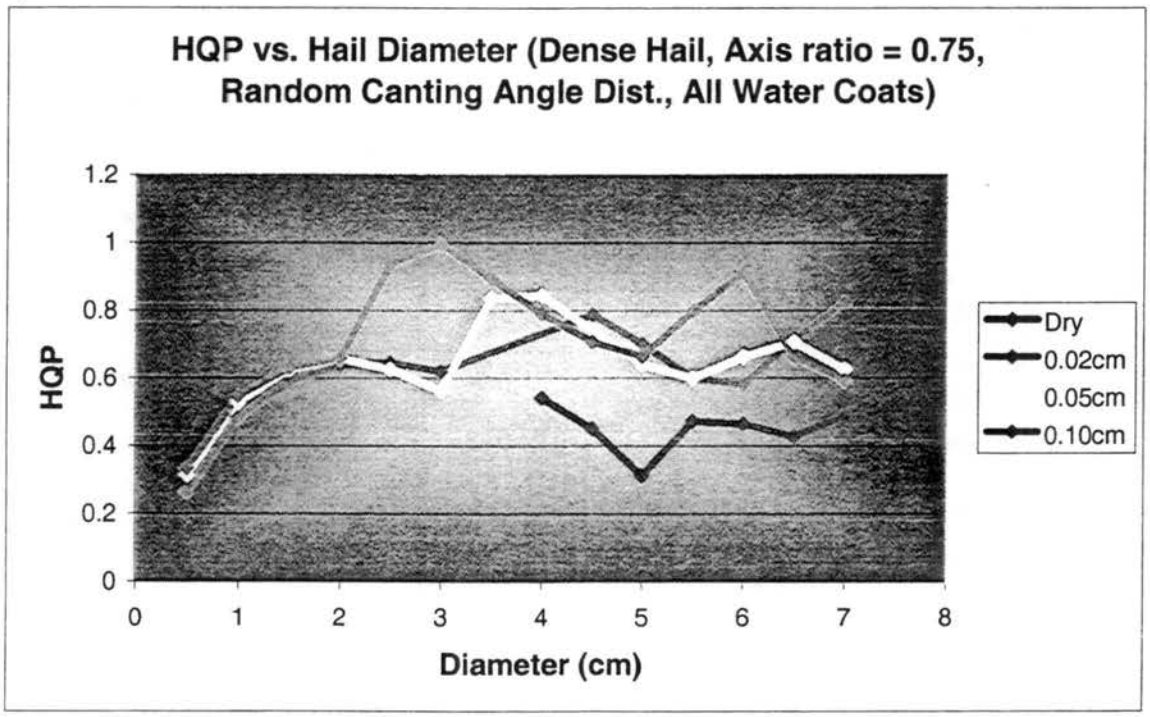

Figure 3.17 (Cont.): HQP vs. hail diameter for ice densitiy of 0.91 g cm^{-3} and all water-coat thicknesses. Axis ratio of 0.75 and canting angle standard deviation of c) 75°, d) random distribution.

e)

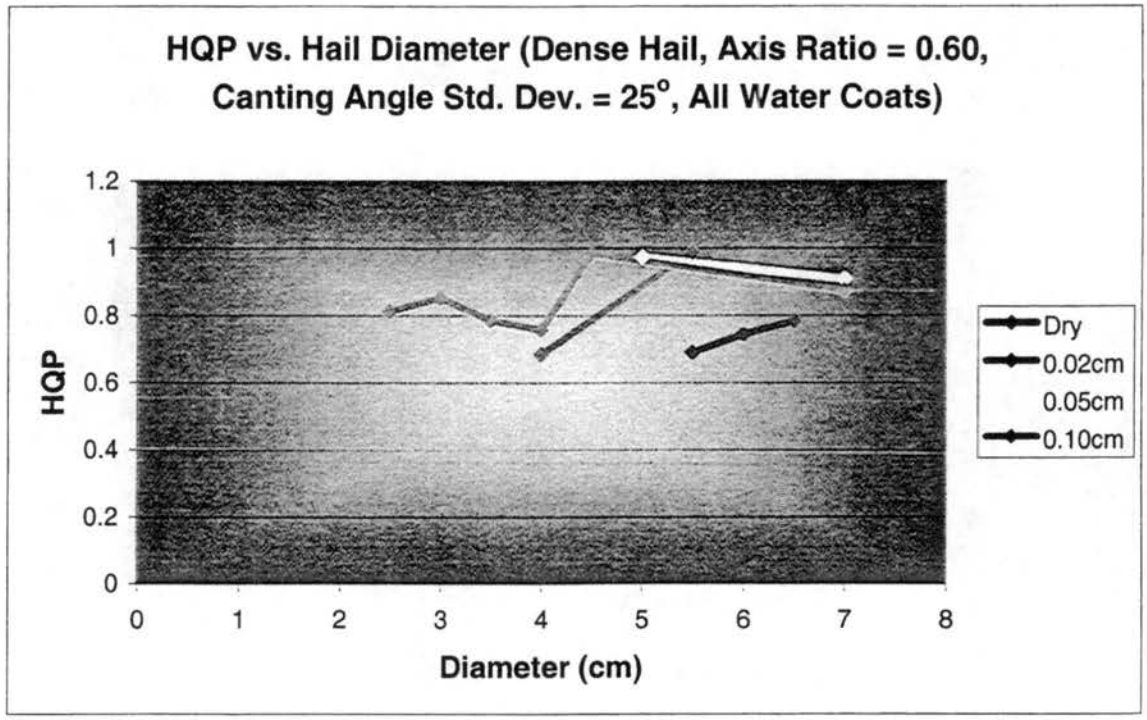

f)

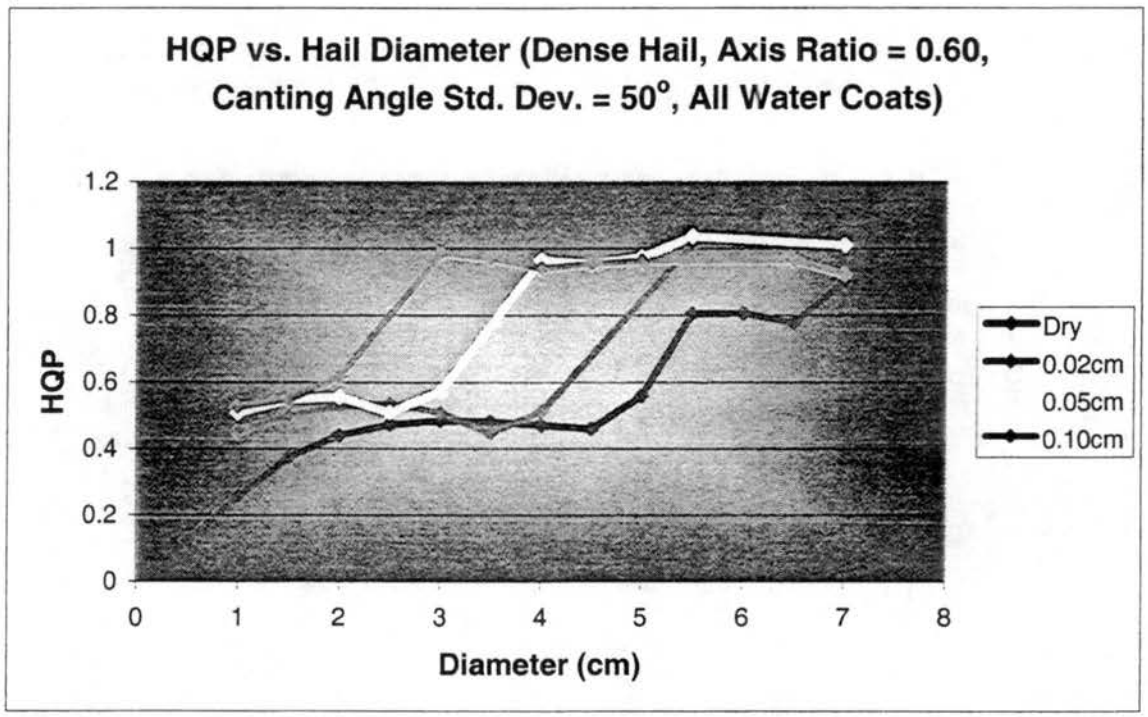

Figure 3.17 (Cont.): HQP vs. hail diameter for ice densitiy of 0.91 g cm^{-3} and all water-coat thicknesses. Axis ratio of 0.60 and canting angle standard deviation of e) 25°, f) 50°.

g)

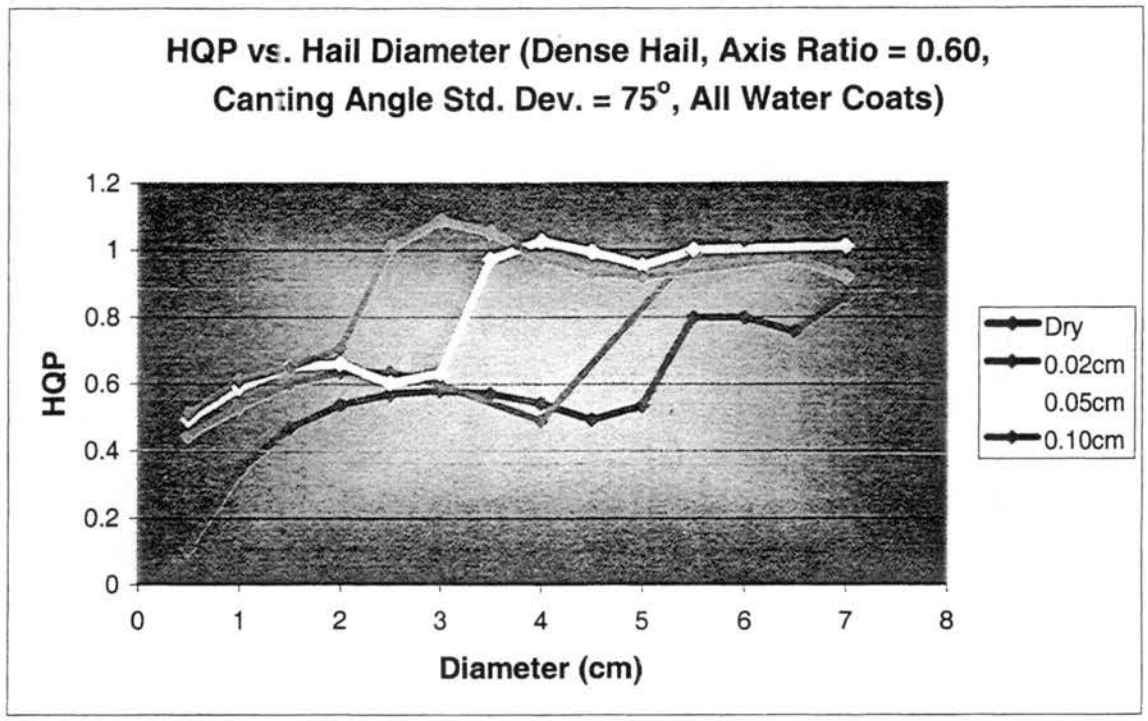

h)

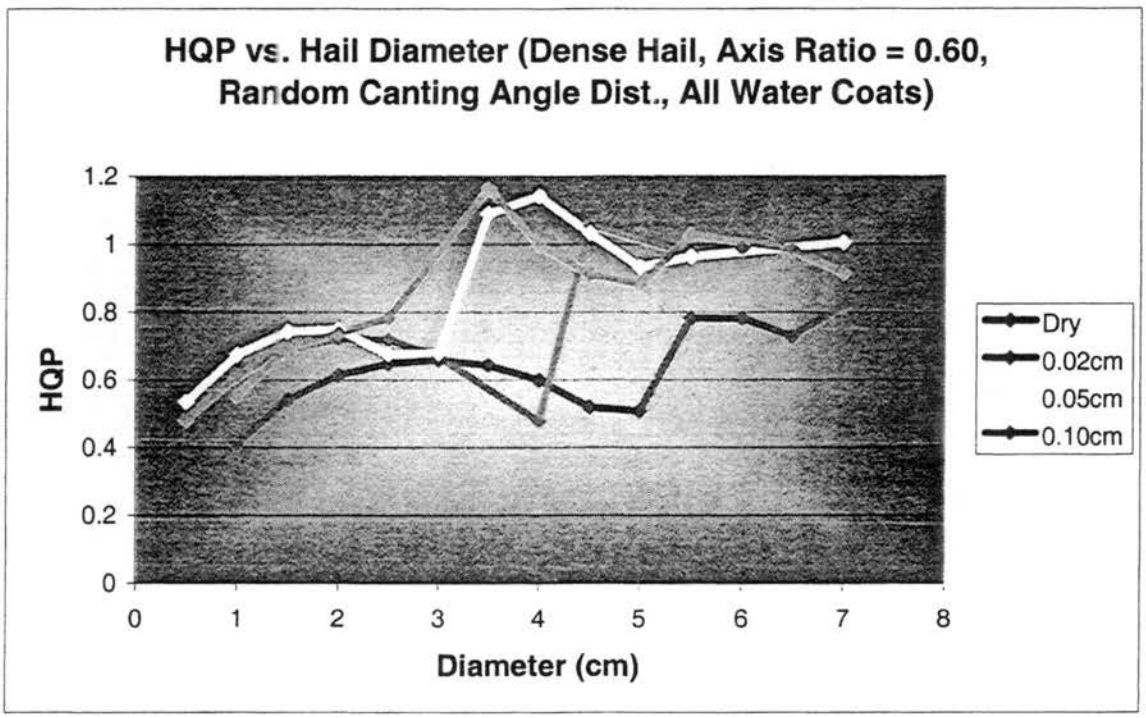

Figure 3.17 (Cont.): HQP vs. hail diameter for ice densitiy of 0.91 g cm^{-3} and all water-coat thicknesses. Axis ratio of 0.60 and canting angle standard deviation of g) 75°, h) random distribution.

a)

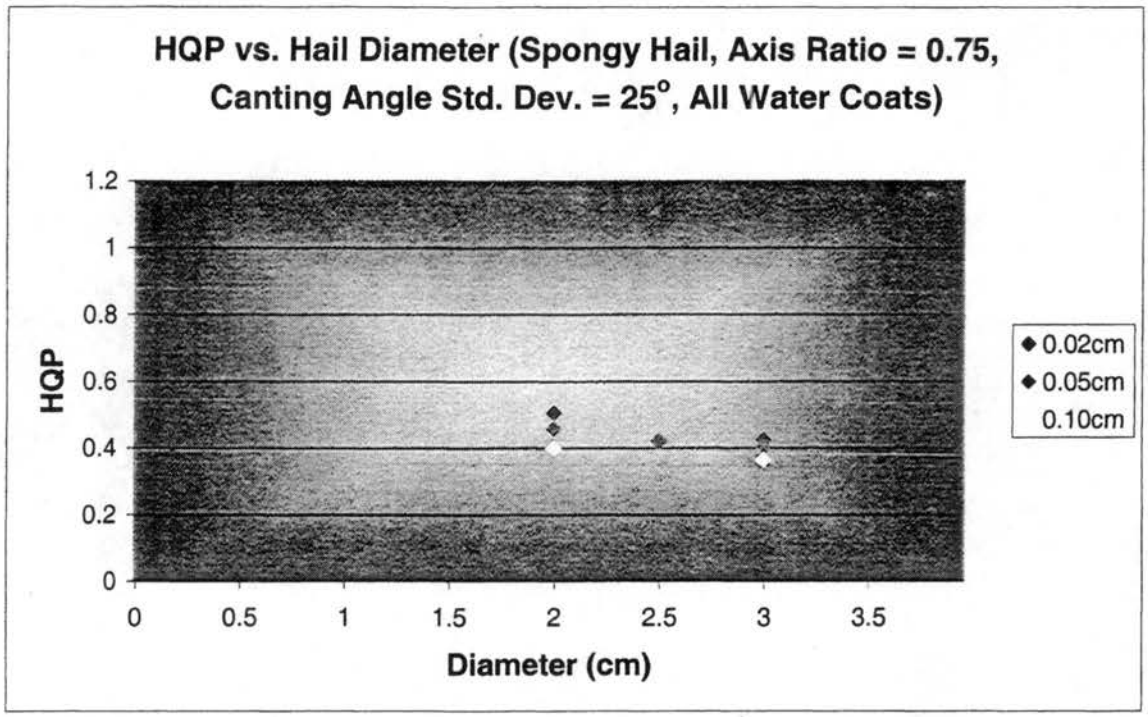

b)

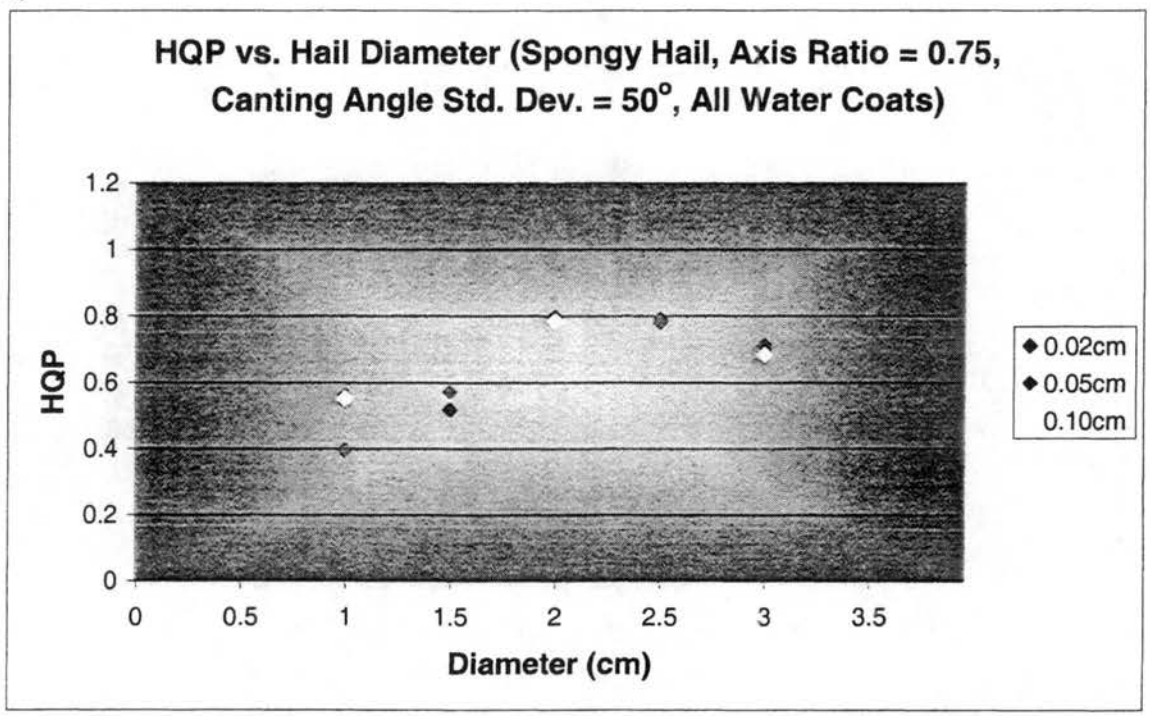

Figure 3.18: HQP vs. hail diameter for 40% water volume and all non-zero water-coat thicknesses. Axis ratio of 0.75 and canting angle standard deviation of a) 25°, b) 50°, c) 75°, and d) random distribution.

c)

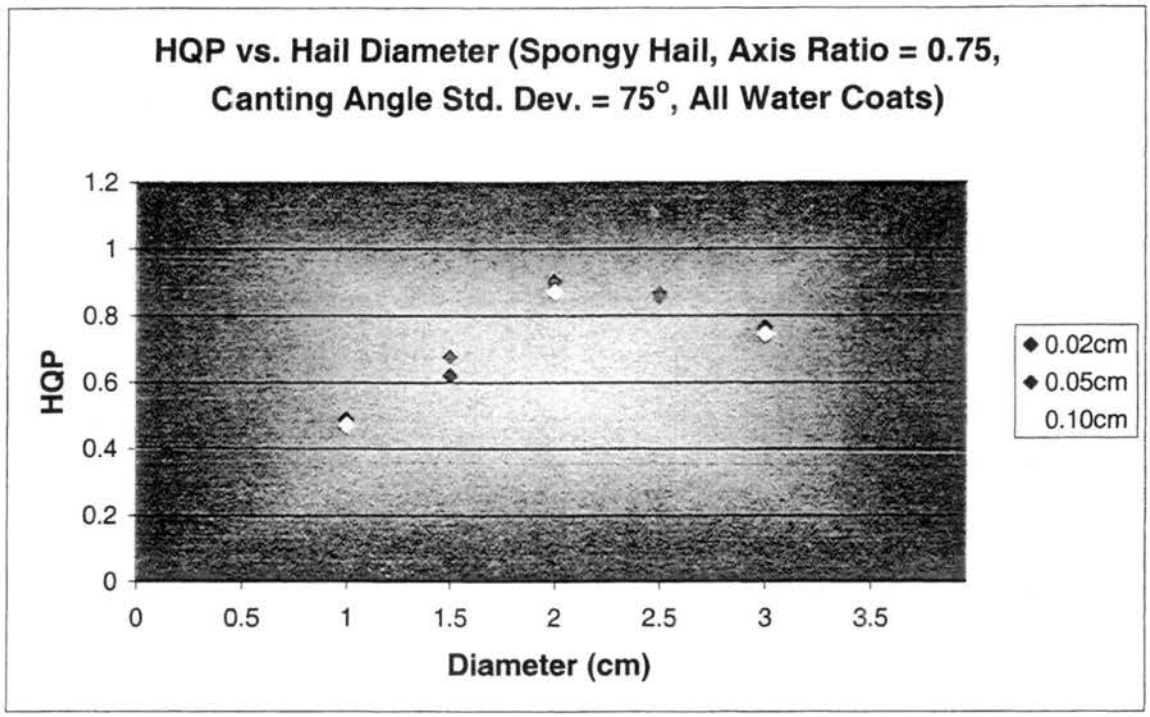

d)

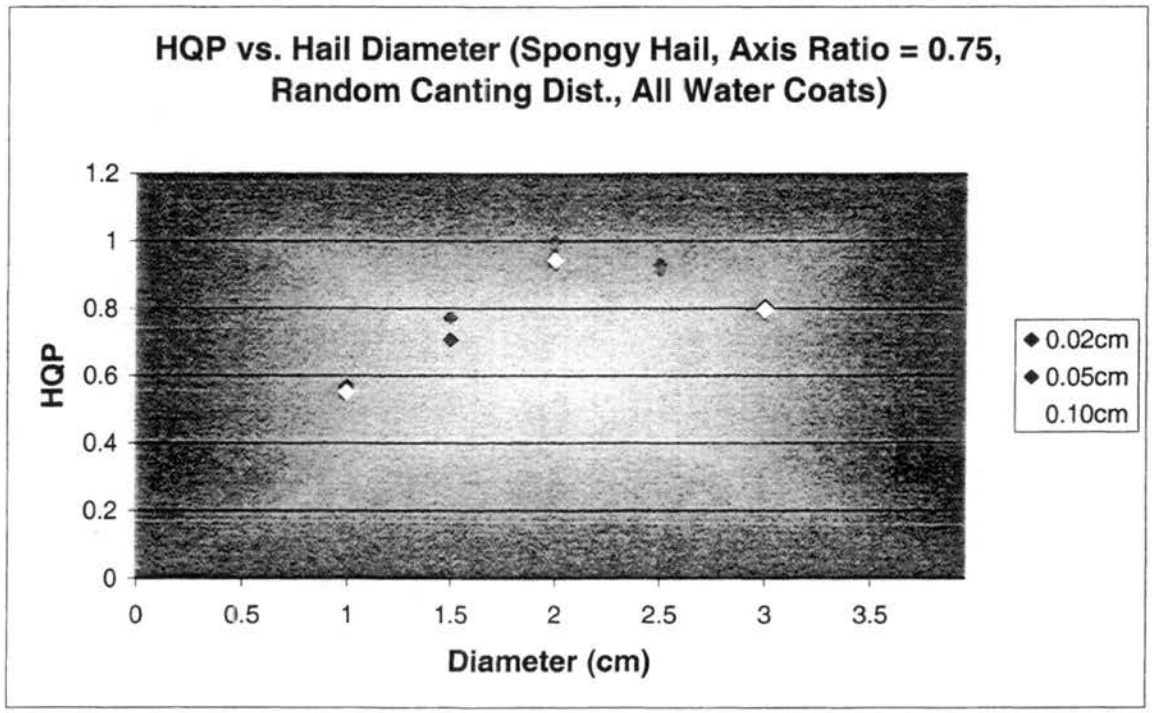

Figure 3.18: (Cont.)

a)

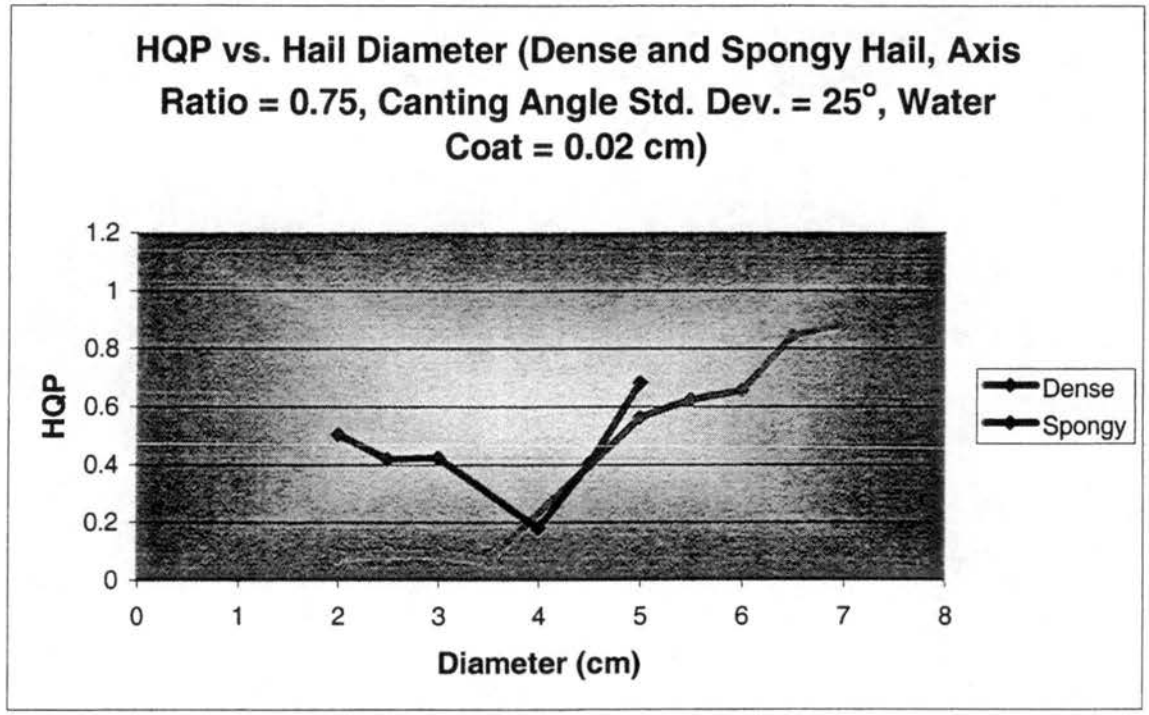

b)

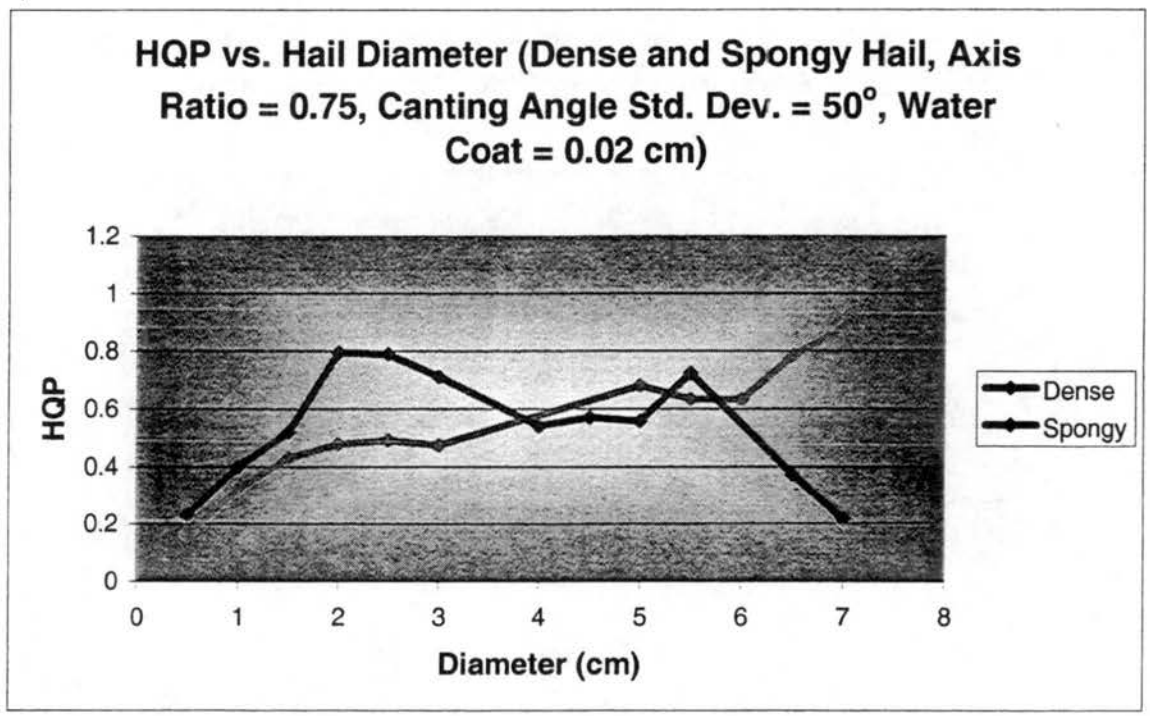

Figure 3.19: HQP vs. hail diameter for ice densities of 0.91 g cm^{-3} and 40% water volume. Axis ratio of 0.75 and canting angle standard deviation of a) 25°, b) 50°, c) 75°, and d) random distribution.

c)

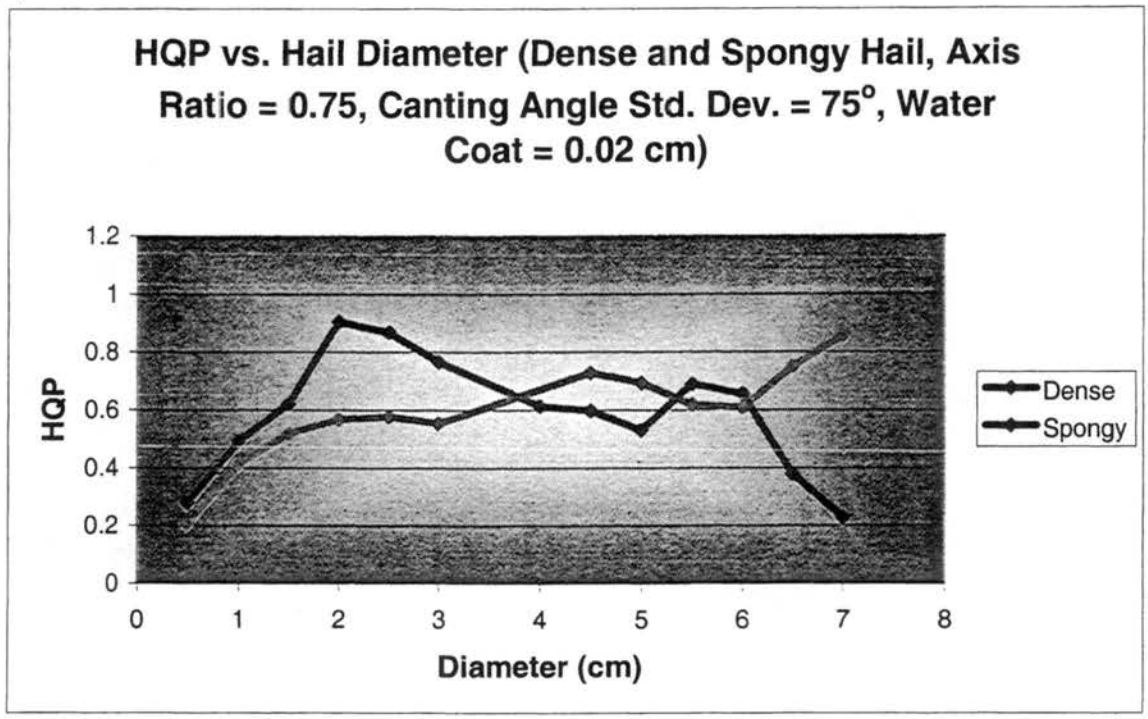

d)

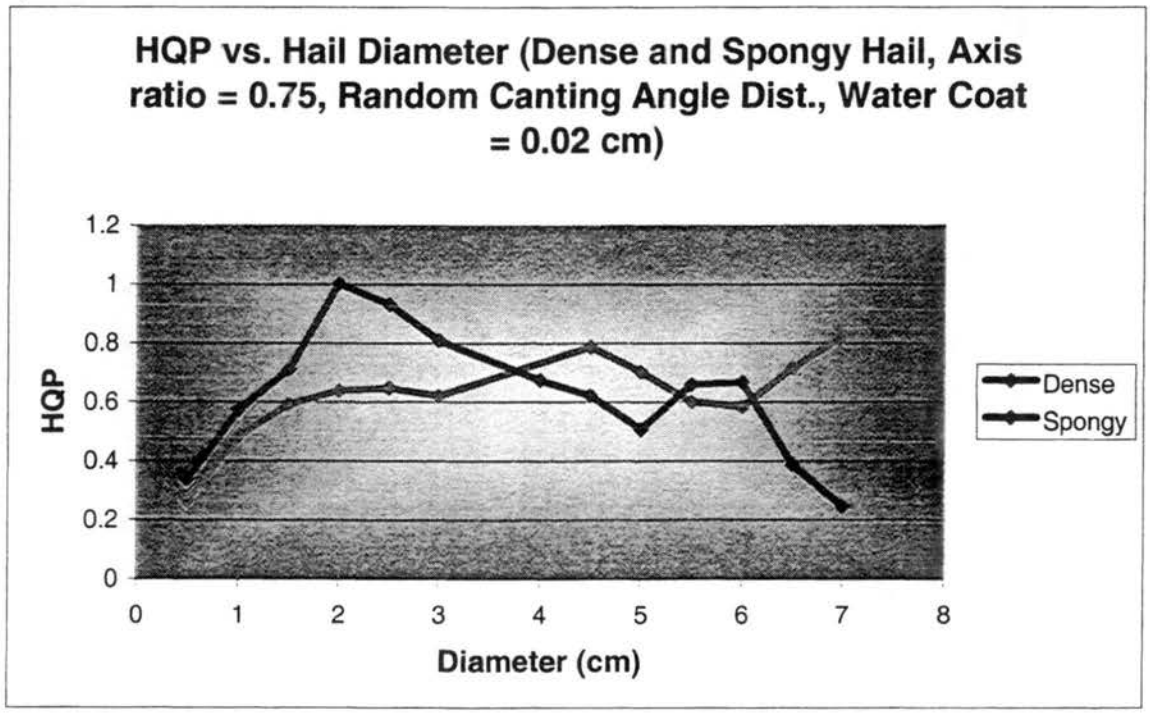

Figure 3.19: (Cont.)

e)

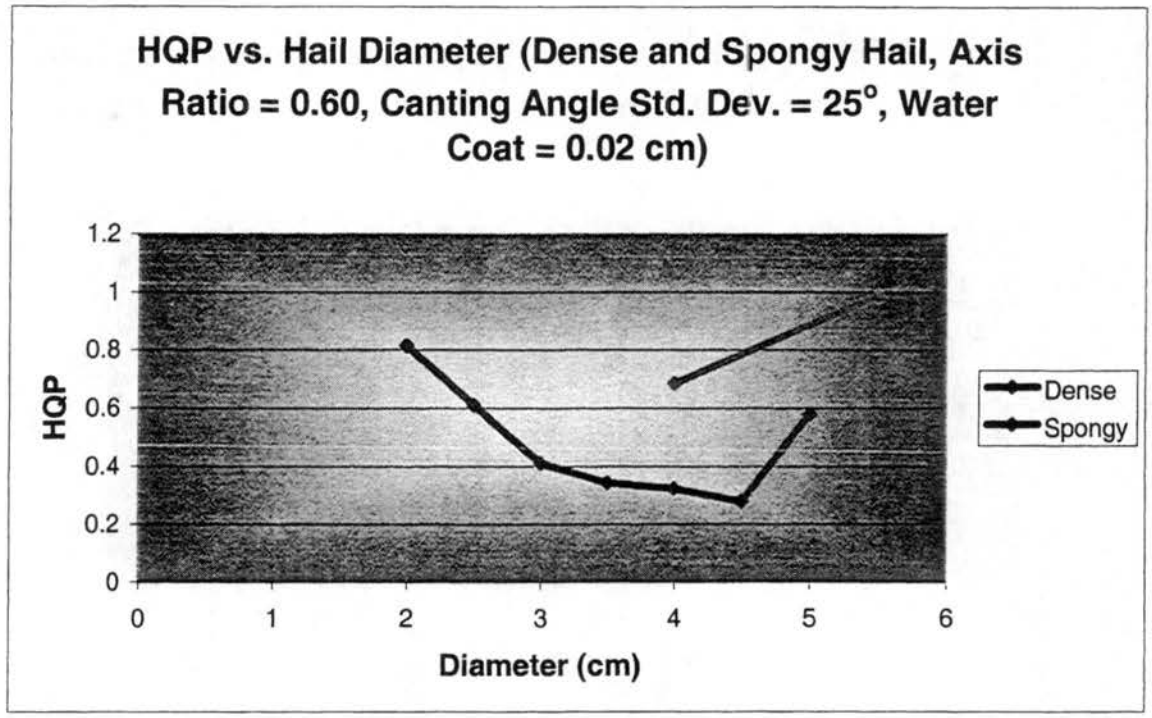

f)

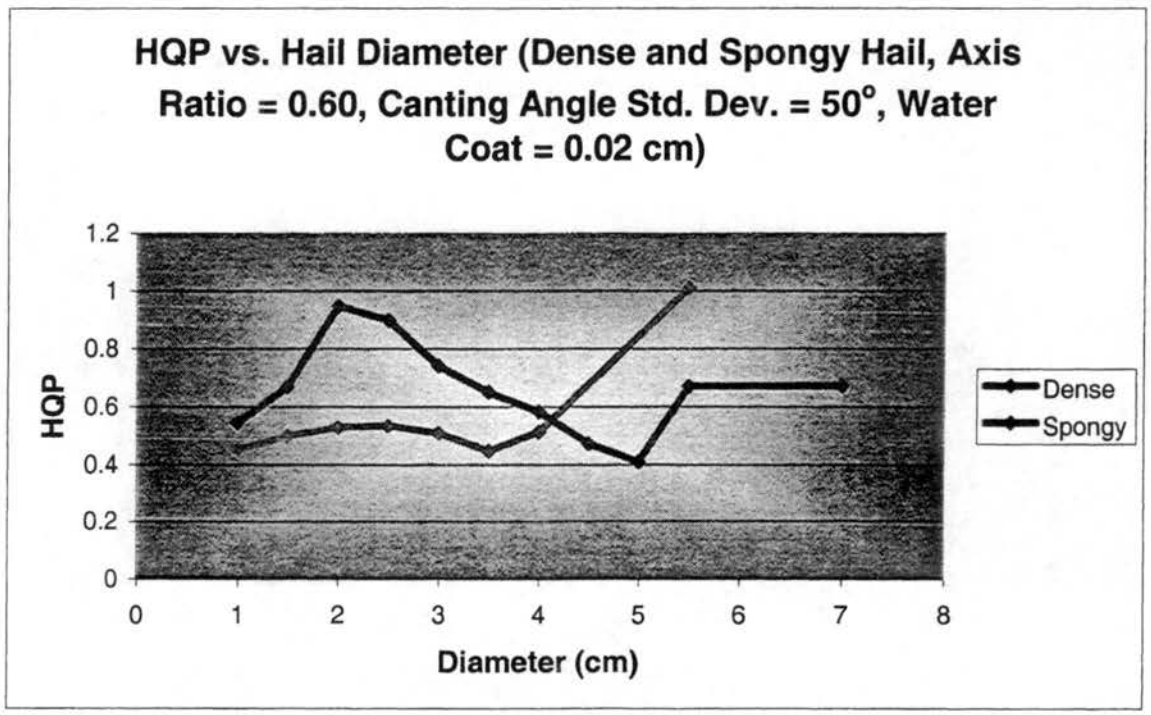

Figure 3.19 (Cont.): HQP vs. hail diameter for ice densities of 0.91 g cm^{-3} and 40% water volume. Axis ratio of 0.60 and canting angle standard deviation of a) 25°, b) 50°, c) 75°, and d) random distribution.

g)

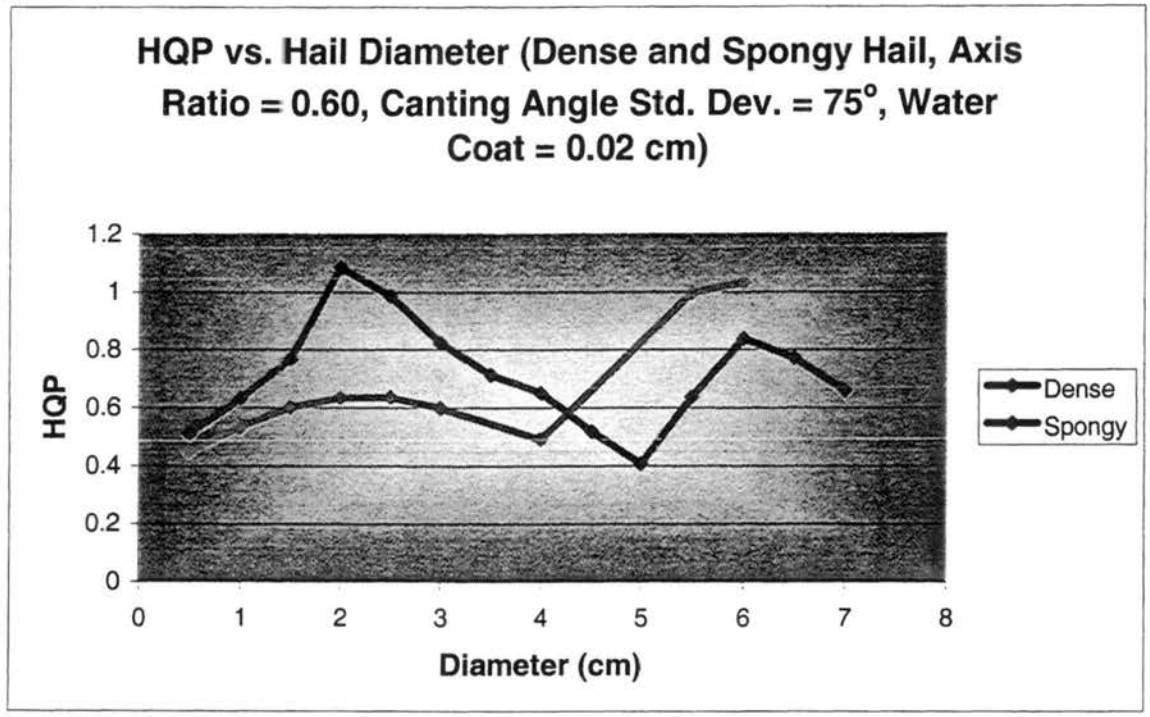

h)

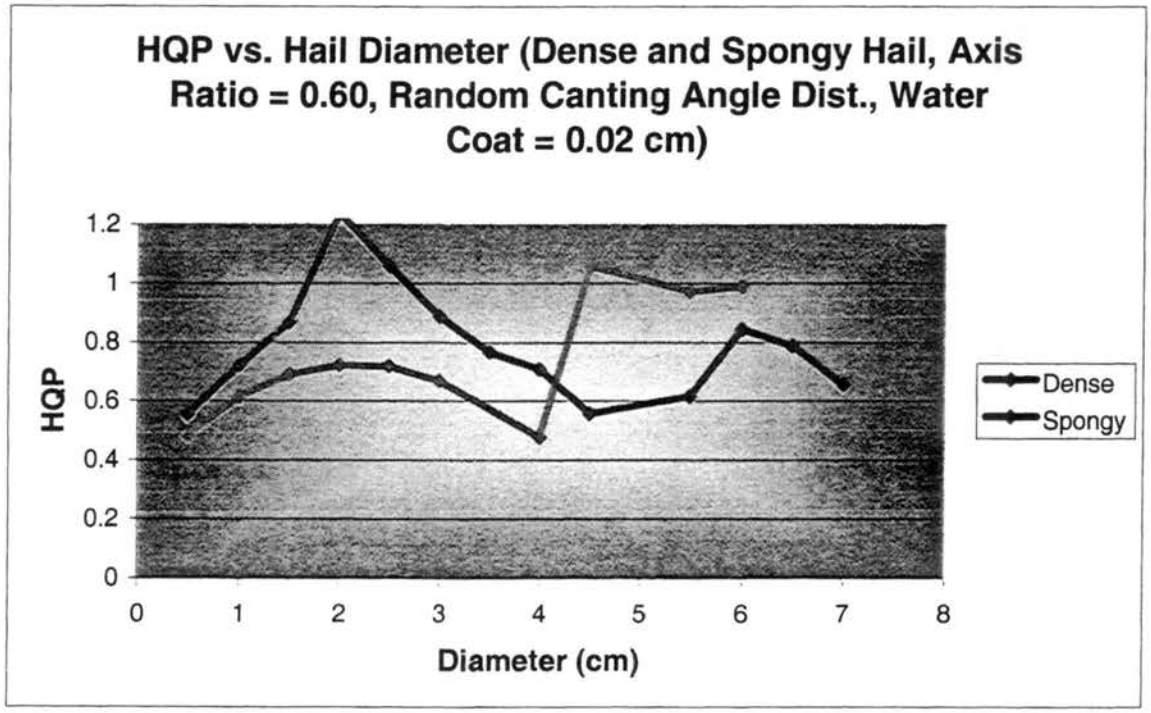

Figure 3.19: (Cont.)

CHAPTER FOUR

Observations

4.1 Surveys

In order to test the representativeness of HQP in diagnosing the presence of large hail, extensive ground-truth data were collected to compare with the results from the radar. Ground truth data were collected in northern and eastern Colorado during the summer of 2002. One storm from 2001 and one from 2003 were also included. A procedure (outlined below) was developed and followed for determining the best areas to cover and the methods for conducting surveys of potential hail cases. A list of questions was asked of people who had direct experience with the storms in question. Their answers were recorded, and later given alpha-numeric codes to facilitate processing through a computer program that extracted the necessary information for comparison with the radar data. See Appendix B for definitions of the alpha-numeric codes and detailed summaries of all surveys.

4.1.1 Pre-survey procedures

After an active storm day, CHILL radar data were studied in detail and each relevant polarimetric parameter (Z_h, Z_{dr}, and LDR) was examined to determine if hail was likely present. Areas of high reflectivity were inspected to determine whether they also possessed low Z_{dr} values (a Z_{dr} "hole") and elevated LDR values. An HQP map was

made, with contour levels indicating potential hail presence, warning-class hail, and very damaging hail. If the raw volume scans looked to be uncontaminated (free of clutter, anomalous propagation, and other noise effects), the contours were sketched onto a Colorado road atlas. If it appeared that the main part of the storm occurred in an unpopulated area, then the case was not considered for further study, as it would not be possible to interview enough observers to determine the severity of the storm. If the storm occurred in a populated area, then CSU personnel drove to the area and began conducting storm surveys.

4.1.2 Survey procedures

The surveys were conducted according to the following guidelines.

4.1.2.1 Where to Go

As stated above, the first criterion that had to be met before a survey was even considered was that the storm occurred in a populated area, having roads and at least a modicum of potential observers. Once that had been satisfied, GPS software was used to create routes along the major roads that would be traveled during the survey, and those routes were added to the HQP map using IDL. This ensured that surveys were done along the main points of interest in the storm. We attempted to survey subjects within all HQP contour levels to determine differences in the severity of the storm. Attempts were also made when possible to establish the perimeters of the storm. Sparse population and a lack of available survey subjects made the latter very difficult and at times impossible. Generally, we began on a road near the perimeter of the hail signature and moved back

and forth in a cross-cutting fashion, in an attempt to acquire ground truth data points at resolutions corresponding to the radar's resolution at the distance of the storm in question.

4.1.2.2 Whom to Ask

In general, the personal interviews were conducted with a wide range of individuals. Only two basic criteria were used when selecting subjects: 1) They had to be adults, and 2) they had to be outside when contacted for the interview. It was decided at the beginning that it was inappropriately invasive to knock on doors and disturb people in their homes. So, interviews were conducted with several farmers, people arriving home from work or the store, people doing yard work, and construction workers. We did go inside and inquire at local businesses if they were located in the area of interest. In general people were very cooperative. Of the many surveys conducted, only one person declined to answer questions. The surveys conducted with farmers were usually particularly informative, given their strong interest in and dependence upon the weather.

4.1.2.3 What to Ask

The personal interviews consisted of several standardized questions:

1) How large was the hail?
2) How hard was the hail?
3) How completely did the hail cover the ground?
4) What was the duration of the hail fall?
5) How strong was the wind?

6) How much rain fell, and is there a rain gauge record?

7) Did any damage occur?

8) Are there any other comments about the storm?

Questions were asked about several specific types of damage.

1) Structural damage, including roofs, windows, screens, and house siding (see Figures 4.1 through 4.3).

2) Vegetation damage, including gardens, flowers, trees, and crops.

3) Vehicle damage, including dents in the body or trim, and broken windows or sideview mirrors (see Figure 4.4).

4) Injuries to either animals or humans on the premises at the time.

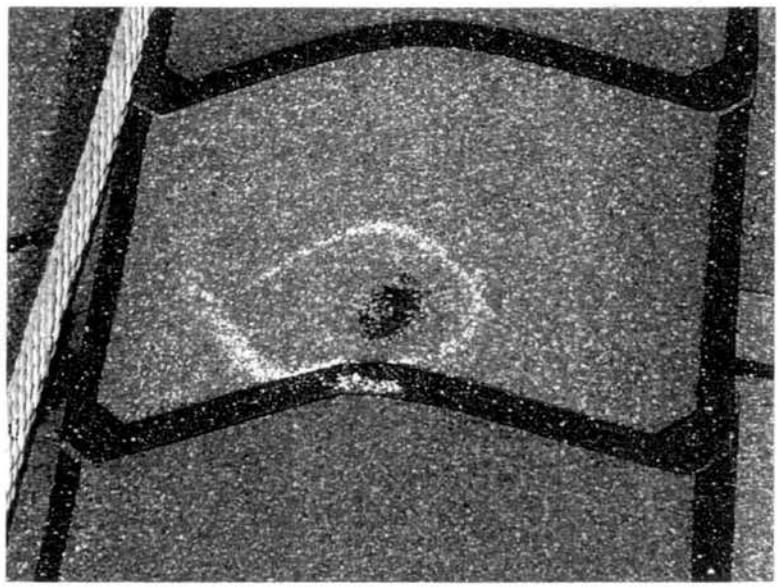

Figure 4.1: Damaged roof shingles in Parker.

Figure 4.2: Torn window screens in Parker.

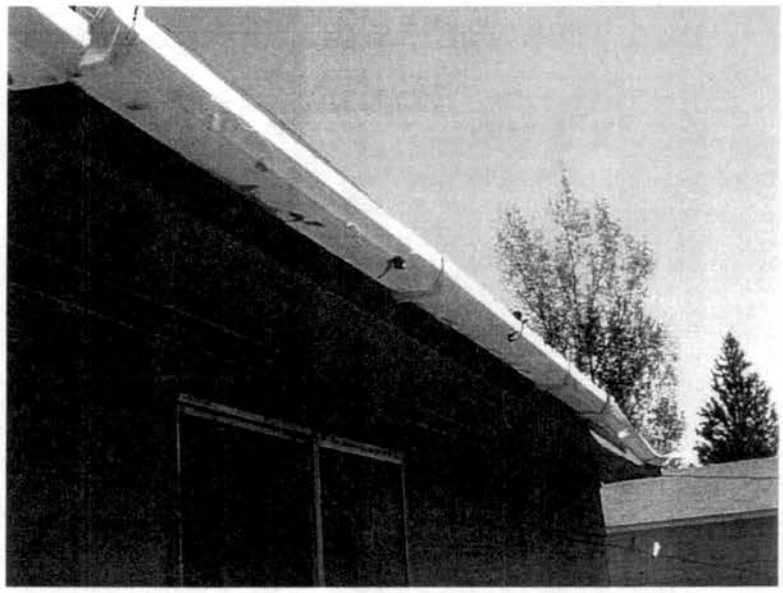

Figure 4.3: Gutter in Merino cracked and punctured completely in several places.

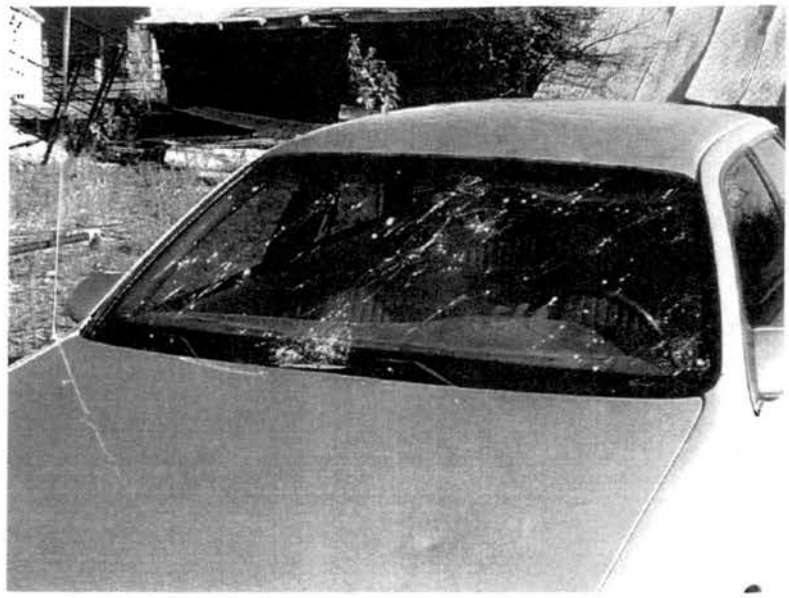

Figure 4.4: Car in Merino with shattered windshield and dented body.

4.1.2.4 What to Look For

On many occasions, it was not possible to interview people in areas of interest, either due to the sparse population or a lack of people outside their homes. In these cases, vegetation was surveyed for damage. The main types of vegetation considered were crops, trees, broad-leafed weeds, and grassland vegetation. The main crops observed were corn (which had shredded and curled leaves if damaged by hail, see Figure 4.5) and wheat and wheat-like weeds (which had broken or bent stalks or heads if damaged by hail). Tree damage observed included individual leaves found scattered under or near the trees (see Figure 4.6). Branches found under trees indicated that damage was likely due to wind, not hail. Holes and tears found in the broad-leafed weeds were indicators of hail early in the summer. Later in the season, however, only tears could be considered due to the increased insect population contributing to holes in the leaves. The main indicator in grassland vegetation was cactus. Pads knocked off the

plant and found either near the plant or downstream of the plant (if there were indications of heavy rain) were a likely indication of hail (see Figure 4.7). This was a less reliable indicator if cattle were present, as they could cause similar damage. When cattle were present, it was possible to inspect their byproducts, which showed dents if the hail was of sufficient size and fall speed.

Figure 4.5: Badly damaged corn in Merino. Note completely shredded stalks and leaves laying on the ground.

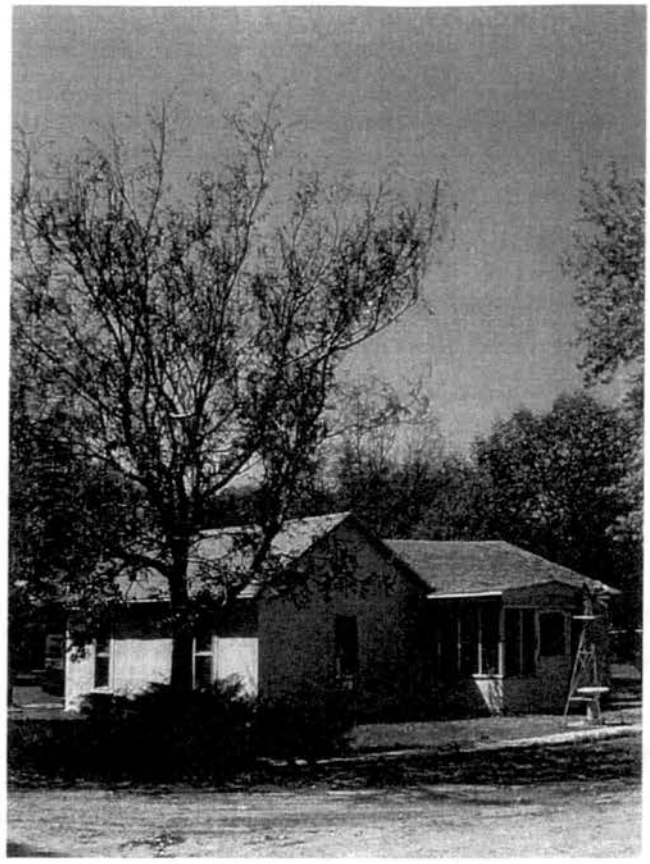

Figure 4.6: Damaged tree in Merino. Note leaves spread across both the ground and the roof of the house.

Figure 4.7: Damaged cactus plant in Parker. Note pads that have been knocked off and are laying near the plant.

4.1.3 Post-Survey Procedures

The results from each survey were later typed and recorded. Alpha-numeric codes were assigned to each answer so that the results could be quantitatively compared with the radar values at each ground truth data point. (The numeric values used in these codes are discussed below and the specific codes are given in Appendix B). Once the codes were determined for each survey point, a text file was created that contained both the codes and the GPS locations for each point. The data were entered in such a way as to make it easily extractable by the program used to combine the ground-truth results with the radar parameters.

Size

The size of the hail was determined by asking each interviewee to select from a collection of different sized wooden spheres that which most closely matched the size of hail they observed. This was found to be a more accurate method than simply asking for raw sizes or comparisons to "golf balls" or "marbles." The sizes were in quarter inch increments and the largest size selected was used for the quantitative comparison.

Hardness

The hardness of the hail was set to 1 if it was soft and became deformed on impact, 3 if it was hard and/or bounced, and 2 if it was between, or a combination of, the two.

Ground Coverage

The amount of ground coverage was set to 1 if the hail only accumulated in low spots and around bushes, 2 if drifts occurred but the ground was not completely covered, and 3 if the ground was completely covered and "it looked like snow."

Duration

The value used for this was simply the numeric value in minutes of the time the hail lasted.

Wind Strength

The strength of the wind was set to 1 if it was negligible, 2 if it was noticeable but not very strong, and 3 if it was very strong or damaging.

Wind Effect

This parameter was used to describe how much the wind affected how the hail fell and the amount of damage the hail caused. It was set to 1 if damage was caused by the hail alone, 2 if it was a combined effect, and 3 if the wind had a strong influence, such as blowing the hail sideways into windows, under overhangs, etc.

Rain Amount

The amount of rain was set to 1 if there was only light rain, 2 if it was moderate, and 3 if it was heavy.

Rain Order

This was used to determine if the rain and hail fell together, or separately, and which came first. This was set to 1 if the rain fell first, 2 if the rain and hail fell simultaneously, and 3 if the hail fell first.

Damage

Several categories of damage were considered. Some were determined by asking people and observing the damage they pointed out. Other categories were based on the vegetation surveys conducted by the authors. All damage categories were given a value of 1 if there was no damage of that type.

1) Vehicle damage was classified as 2 if the vehicles had light dents or broken sideview mirrors, and as 3 if they had large dents or broken windows.
2) Structural damage was classified as 2 if the damage was not obvious and had to be pointed out by the owner (such as roof dents or small chips in paint), and as 3 if the damage was obvious (such as large holes in screens, broken windows, broken siding) or if a roof required a full replacement.
3) Crop damage was classified as a 2 if moderate shredding and holes were apparent, and as 3 if the crop was destroyed.
4) Wheat and wheat-like weed damage was classified as a 2 if a few percent of the stalks were bent, 3 if the damage was obvious while driving along the road, and 4 if it was flattened or destroyed.
5) Tree damage was classified as 2 if some leaves were found on the ground, and as 3 if there was substantial leaf coverage.
6) Yard plant damage (including vegetable gardens and flowers) was classified as 2 if some leaves or flowers were knocked off, and as 3 if the plants were reduced to stripped stalks.
7) Large animal injuries were classified as 2 if an injury occurred to a large animal (such as a cow or horse) or human, such as bruising or lumps, and as 3 if either a large animal or human was killed.
8) Small animal injuries were classified as 2 if an injury occurred to a small animal (such as a dog, cat, chicken, yard animal) or child, and as 3 if either a small animal or child was killed.

Hail Shape

Hail shape was classified as 1 if it was spherical, 2 if it was obviously not spherical (flattened or pointed on one end or obviously oblate), and 3 if it had lobes or protrusions of some sort.

Quality of Observation

This final parameter was used to give a weight to each observation when necessary. A classification of 1 was given if the observer appeared very unobservant or had very unclear recollections about the storm, 2 was given if the observer appeared reliable, 3 if the observer was someone with extensive weather observing experience, such as a farmer or pilot, and 4 if the observation occurred after the fact (such as the vegetation surveys).

4.2 Radar Data

Each volume scan was recorded in universal format. A program was created that enabled the user to input desired volume scans and sweep levels over a user-specified grid. The output consisted of the distance of each range gate from the radar, in both x- and y-coordinates, as well as the radial range. The elevation angle and height of each gate (in km MSL) were also included. Finally, each range gate was assigned each polarimetric variable considered in this study (HQP, H_{dr}, Z_h, Z_{dr}, and LDR) as well as velocity and ρ_{hv}.

As discussed in Section 2.6, one of the major drawbacks to HQP is the low signal-to-noise ratio of LDR. This issue was encountered while processing the data sets. Two storms in particular were found to have abnormally high LDR values – generally unphysical for meteorological targets. The data had to be inspected more carefully to

determine whether these values were caused by noise or legitimate meteorological phenomena. It was determined that one case was corrupted by a three-body-scatter-spike and the other by a second-trip echo. There was no way to remove the contamination from the data, so the cases were removed from the data set.

Not only did these spurious effects cause problems with our experimental data set, but it brings up the point that if HQP were to be used operationally, one would need to monitor the data for noise and other misleading sources such as those described above. This might be done by simply being alerted when abnormally large LDR values are recorded.

4.3 Data Synthesis

A program was developed in Matlab to take the text file with the survey results and survey point locations and combine these data with the raw range gate data provided by the Hailmap code. The program first determined the distance of each survey point from the radar. All range gates within a specified radius of influence (based on distance from the radar) were found and saved. Points further from the radar were given a larger radius of influence, due to the larger azimuthal distance between gates. A Cressman-weighted function was then used to average the polarimetric values over all these points. The averaged reflectivity and Z_{dr} values were used to calculate H_{dr}. This H_{dr} value and the averaged LDR value were then used to calculate HQP. The program iterated through the specified volume scans (to ensure the entire duration of the storm was covered) and the highest reflectivity, LDR, H_{dr} and HQP were retained, while the lowest Z_{dr} was retained. Values at specific times were not of interest due to observers' inability to

remember exactly when storms occurred. Instead, it was assumed that the largest hail they observed fell during the most intense part of the storm, thus the reason for recording only the highest (or lowest) values throughout the entire event. These final values obtained after processing all volume scans were those used in the statistical analyses.

4.4 Analysis

Once each survey point had been assigned the necessary polarimetric values, it was possible to do both a visual and a statistical analysis to determine the skill of each chosen algorithm for detecting hail. It was decided that the main concentration would be on comparing HQP and H_{dr}, since the purpose of HQP is to possibly improve upon the information contained in H_{dr} alone. It was also decided that hail size and vehicle/structural damage would be the only survey data used in the analysis. These two aspects were the most verifiable and relevant pieces of information obtained in the surveys.

4.4.1 Data Plots

Figures 4.8 (b and c) and 4.9 (b and c) show the relationship between H_{dr}/HQP and size/damage, respectively. Both H_{dr} and HQP have a more or less linear relationship with size and damage – smaller hail sizes correspond to smaller values of both H_{dr} and HQP. Neither H_{dr} nor HQP, however, shows a better correlation with either size or damage. This indicates that perhaps neither one performs much better than the other.

Figures 4.10 (b and c) and 4.11 (b and c) show histogram plots of H_{dr} and HQP values broken into size and damage categories. Figures 4.10 (b and c) are broken down

by size with different colors representing each size category. Figures 4.11 (b and c) are broken into damaging and non-damaging cases. The ideal appearance for these plots would be to have all the small-sized/non-damaging points at the small H_{dr}/HQP values, with all the large-sized/damaging points at the large H_{dr}/HQP values. These plots do not appear ideal, but there is definitely a larger percentage of small-sized/non-damaging hail at small values and large-sized/damaging hail at large values. Once again, however, neither H_{dr} nor HQP conform more to the ideal shape, indicating that neither one outperforms the other.

Figures 4.8a and 4.9a (also discussed in Section 5.3.1) give some explanation as to why HQP does not detect hail more effectively than H_{dr}. Figure 4.8a shows that LDR does not have a linear relationship with size. The larger hail sizes are found to have larger LDR values. However, large LDR values are also found at much smaller sizes as well. In fact, large LDR values span the entire range of hail sizes, creating the visibly flattened, not sloped, appearance across the top of the graph. The same pattern is seen in the damage data as shown in Figure 4.9a. This is most likely due to Mie effects, such as those found in the modeling aspect of this study, discussed in Section 3.6.3. It is possible that a combination of surface irregularities, oblateness, canting and sufficient water-coat thickness are present on enough of the small hailstones to cause elevated LDR values.

Figures 4.11a and 4.12a are the same type of histogram for LDR as those shown for H_{dr} and HQP. Once again, it can be seen that small/non-damaging hail points span the entire hail size spectrum, with some showing up at even the largest LDR values.

The LDR results shown in Figures 4.8 – 4.11 show why LDR may render the interpretation of HQP, for the detection of large hail, somewhat difficult. As theory

indicates, LDR values are indeed greater for larger hail since larger hail has the expected characteristics necessary to increase LDR such as increased oblateness, canting and irregular surface features. Since small hail also can be found with large LDR values, Mie and dielectric effects due to melting must be contributing significantly.

In an attempt to determine whether any hail-detection information could still be retrieved from the data, Figures 4.8 (a and b) were inspected more closely. It became apparent that all hail larger than 1 inch had LDR values greater than -20 dB and H_{dr} values greater than 22 dB. An experiment was done to determine whether this information could be used to create an alternative method for differentiating between hail size/damage. Results from this experiment are discussed in Section 4.5 below.

4.4.2 Contingency Tables

The contingency table method was decided upon as the best statistical tool to use, since most severe weather and hail detection algorithms have been analyzed in this manner. Using this method, four basic categories are created: hits, false alarms, misses, and nulls. Please see table below for an example of the contingency table.

Table 4.1 Contingency table.

	Occurred	Did Not Occur
Detected	**Hit**	**False Alarm**
Not Detected	**Miss**	**Null**

Several different thresholds were tested (See Section 4.5), and each ground truth point was defined as a hit, false alarm, miss or null, based on these thresholds. Statistical formulas were then used to calculate the skill of each algorithm.

4.4.3 Statistical Formulas

Five different statistical formulas were used to ascertain the skill of both H_{dr} and HQP. These were the Probability of Detection (POD), False Alarm Ratio (FAR), Critical Success Index (CSI), Heidke Skill Score (HSS) and the Hanssen and Kuipers Score (HK) also known as the True Skill Score (TSS). Below, each equation is given, with an explanation of the utility of each statistic. For each equation, h = hit, f = false alarm, m = miss, and n = null.

$$POD = h/(h+m)$$

This is used to measure the skill of the algorithm in correctly predicting the detection of hail. It is the ratio of hits to the total number of hail events that occurred. A perfect score of 1 would occur if the algorithm in question detected every hail event. It is only sensitive to missed occurrences, not false alarms, so the POD can be increased by lowering the threshold so that more events are detected. This will, however, increase the likelihood of false alarms. It is possible to have a perfect POD with a very large number of false alarms.

$$FAR = f/(h+f)$$

Similar to the POD, this is a ratio of false alarms to total instances of detection. A perfect score of 0 would occur only if hail actually occurred at every point where hail was detected. This statistic is not sensitive to misses, so it can be lowered by raising a threshold so less events are detected. This will, however, increase the occurrence of missed detections. It is possible to have a FAR of zero, but at the expense of missing many cases of hail.

CSI = h/(h+f+m)

The CSI is the ratio of all correct detections to all detections and occurrences. A perfect score of 1 would occur if all hail events were detected, and all indications of hail were verified. This is a more representative statistic, since it is sensitive to both misses and false alarms. The value cannot simply be increased by changing the threshold, as the increase in either false alarms or misses will be detected.

HSS = 2*(n*h – f*m)/((n+m)(m+h) + (n+f)(f+h))

The HSS is useful because it accounts for accurate detections that may be due solely to chance. Since nulls are taken into consideration in this statistic, a perfect score of 1 would occur if hail occurred in all cases in which it was detected, and if no hail occurred in all cases in which no hail was detected.

TSS = (n*h – f*m)/((n+f)*(m+h))

The TSS is useful, because it, too, eliminates correct detections based just on chance. Like the HSS, a perfect score of 1 would occur only if both detections and non-detections

were accurate. The advantage of the TSS, however, is that it does not depend on whether there were more occurrences of hail, or non-hail. Other indices may be biased if, as in this case, there are many more cases of hail than non-hail.

4.4.4 Statistical Results

Hail sizes ranging from 0.25 in to 2.00 in were chosen at 0.25 in intervals. Thresholds of 0 to 1.0 were used for HQP and 0 to 35 for H_{dr}. All intervals were tested for all possible hail sizes (see Tables C.1 and C.2 in Appendix C). This method allowed a close inspection of various threshold values for each parameter. It could then be determined which thresholds were most effective for detecting different sizes or size categories of hail.

Tables C.1 and C.2 show a summary of the statistical results for each experiment. Figures C.1 through C.16 of Appendix C show the difference between the Heidke Skill Score and the True Skill Score for each threshold of both HQP and H_{dr}. As can be seen in Tables C.1 and C.2 (also in Appendix B), for many hail sizes the TSS and HSS gave conflicting results as to which algorithm performed better. For several sizes, there was no significant difference between the algorithms in either score. This appears to reinforce the conclusion from the data plots indicating that neither HQP nor H_{dr} performs significantly better than the other.

4.5 Additional Experiment

After observing the trend in Figure 4.8a, in which all large hail possessed large LDR values, but small hail ranged from small to equally large LDR values, an attempt

was make to determine whether this information could still be useful for hail detection or size descrimination. Upon careful inspection of Figure 4.8 (a and b) it was determined that all but two points corresponding to hail size > 1 inch were found at LDR > -20 dB and H_{dr} > 22 dB. This information was combined with the best-performing thresholds (according to the CSI, HSS and TSS) for H_{dr} and LDR (Appendix B) and combined LDR/H_{dr} thresholds were chosen for two hail size thresholds. The hail size threshold of ≥ 1.25 in was chosen because this seemed a natural delineation in the data. The size threshold of ≥ 0.75 in was also chosen because this is the threshold of greatest interest operationally.

In a more thorough treatment of this issue, an independent data set would be used to determine the threshold values and then those values would be tested on the remaining data points. This was not done in this case because it was desirable to first know whether even under the most favorable (and even biased) circumstances these threshold values would prove useful.

The same statistical analyses described in 4.4.2 and 4.4.3 were performed on the experimental algorithms using only selected LDR/H_{dr} thresholds over the entire range of hail sizes tested for HQP and H_{dr}. Table 4.2 shows the experimental LDR/H_{dr} algorithm thresholds chosen for each hail-size threshold of greatest interest. In addition, it shows the statistical performance of each experimental algorithm compared to the best statistical performance of HQP and H_{dr} for those size thresholds.

Table 4.2:Comparison between statistical results from experimental algorithm, HQP and H_{dr}.

Algorithm	Threshold	Hail Size	POD	FAR	CSI	TSS	HSS
Experimental	LDR = -22 dB H_{dr} = 22 dB	≥0.75 in	0.77	0.08	0.72	0.61	0.64
HQP	0.6	≥0.75 in	0.77	0.11	0.70	0.56	0.59
H_{dr}	22	≥0.75 in	0.83	0.15	0.72	0.57	0.57
Experimental	LDR = -20 dB H_{dr} = 22 dB	≥1.25 in	0.94	0.36	0.62	0.61	0.68
HQP	0.7	≥1.25 in	0.81	0.32	0.58	0.58	0.62
H_{dr}	32	≥1.25 in	0.71	0.31	0.54	0.55	0.55

It can be seen that the experimental algorithm does consistently (from all skill scores) perform slightly better than both HQP and H_{dr} for both hail size thresholds investigated. It does not, however, offer a very large improvement. In fact, most of the improved performance can likely be attributed to the highly biased method of arriving at each algorithm threshold. The results of this experiment appear to verify the original conclusion that LDR does not offer a significant amount of additional hail detection/classification information. (The same experiment was performed to determine whether an experimental algorithm existed which would provide a better method for detecting damaging hail, but the results showed no statistical improvement at all, so they are omitted from this discussion).

a)

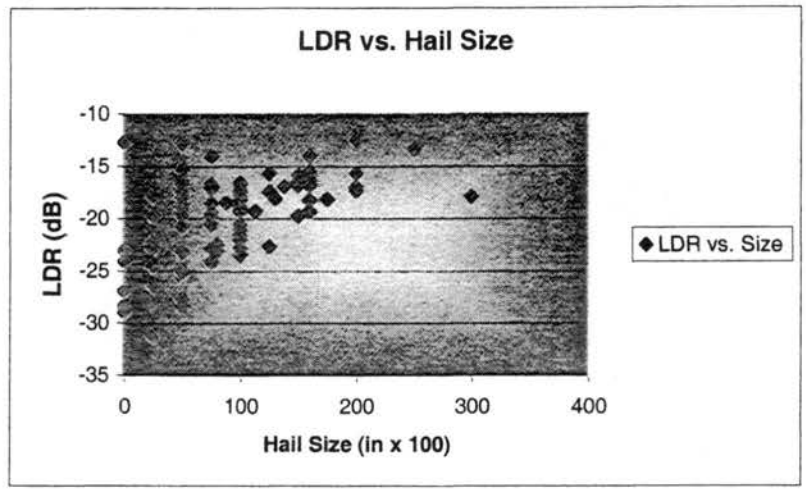

b)

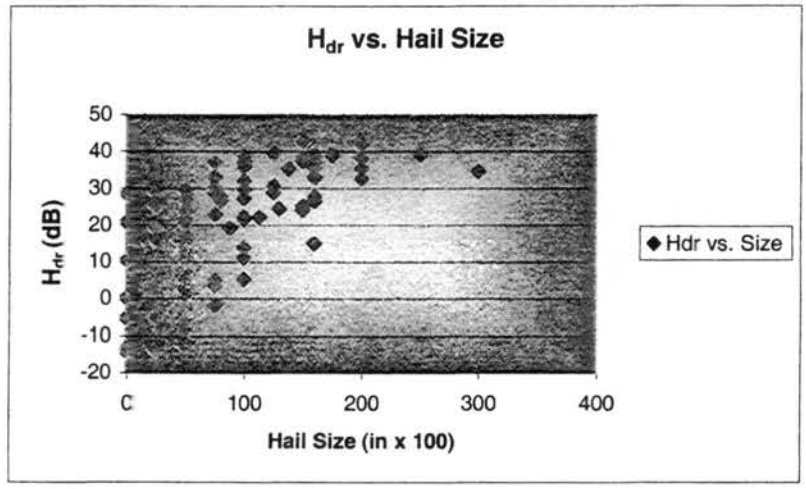

c)

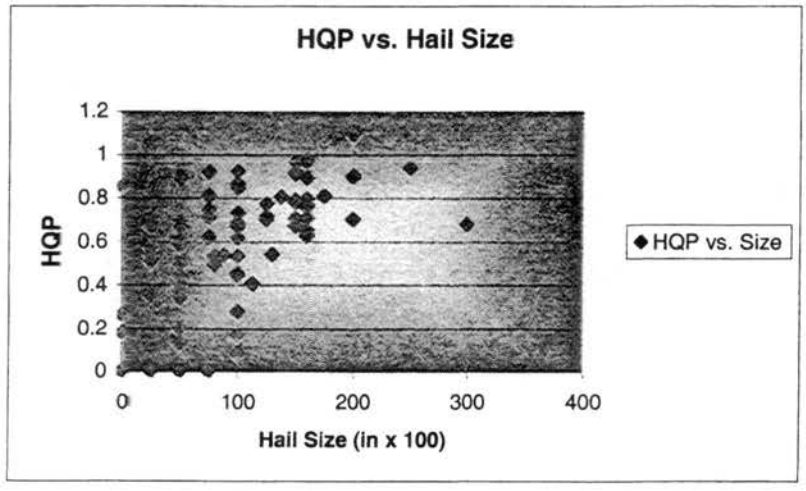

Figure 4.8 a)LDR, b)H_{dr}, and c)HQP values vs. hail size.

a)

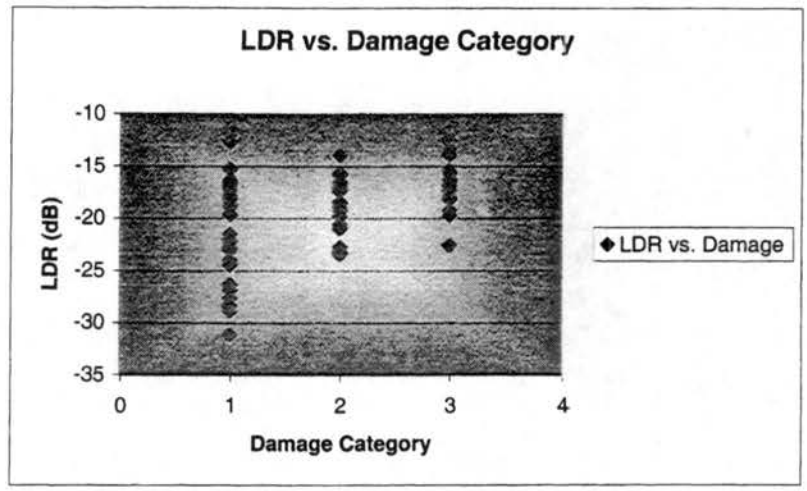

b)

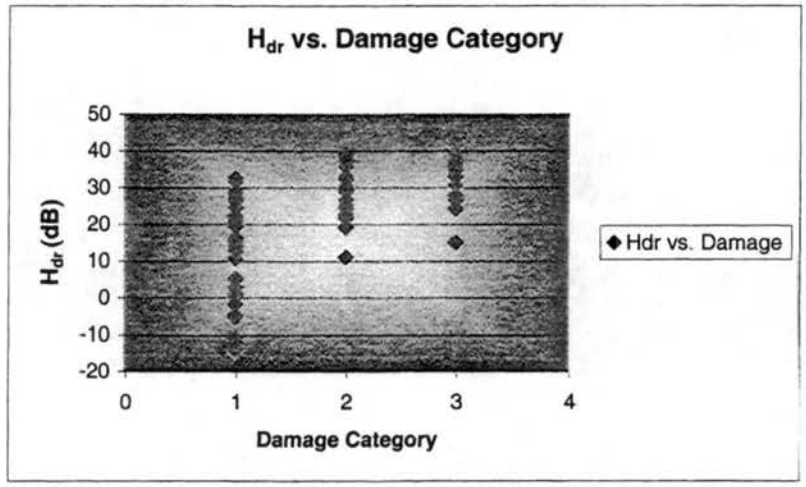

c)

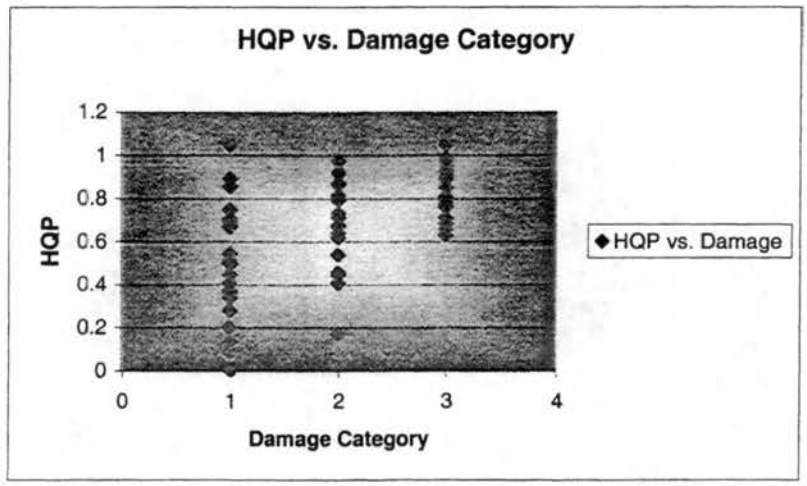

Figure 4.9 a)LDR, b)H_{dr}, and c)HQP values vs. damage category. Damage category values are either structural or vehicular damage, whichever is larger.

a)

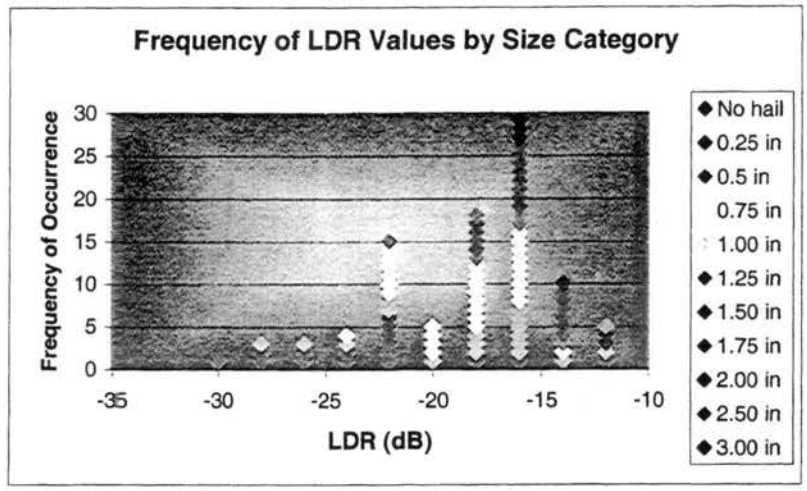

b)

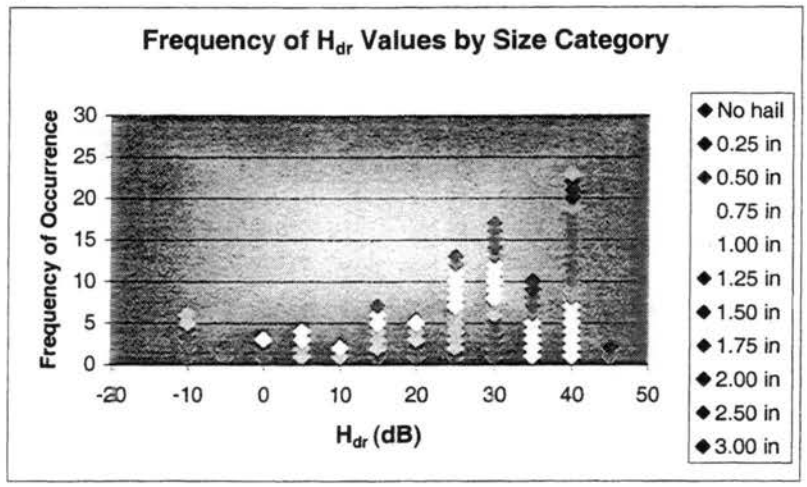

c)

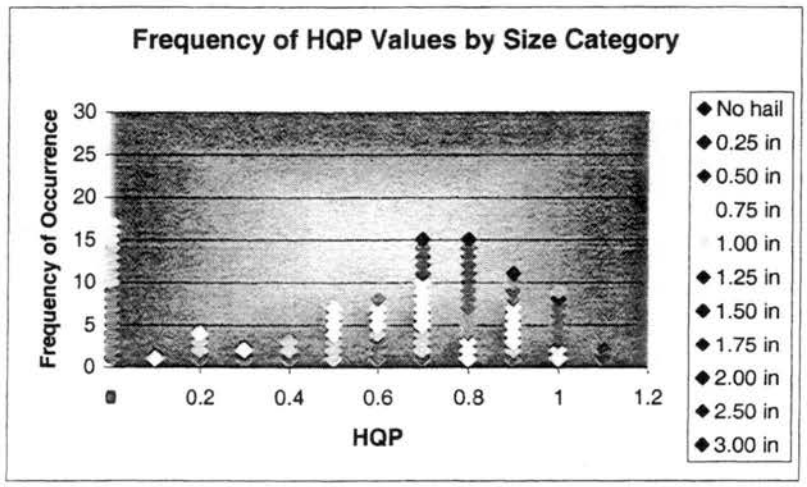

Figure 4.10 Histograms of the frequency of occurrence of binned a)LDR, b)H_{dr} and c)HQP values color-coded by binned size category. LDR bin size = 2, H_{dr} bin size = 5, HQP bin size = 0.1. Hail bin size = 0.25 in.

a)

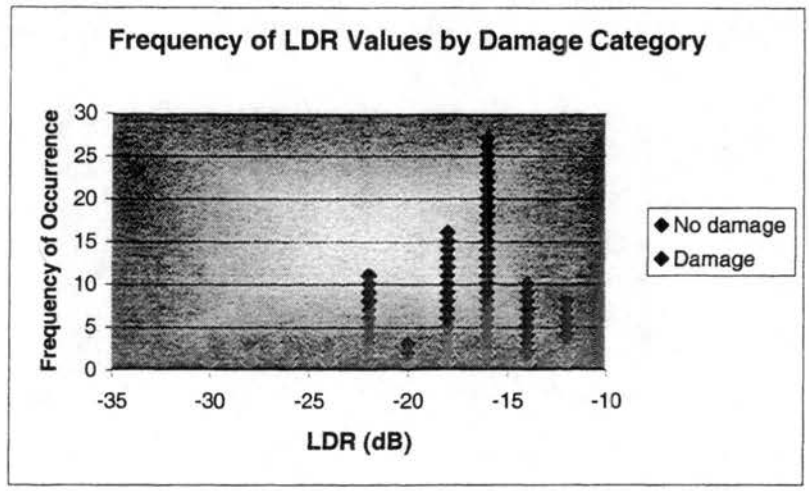

b)

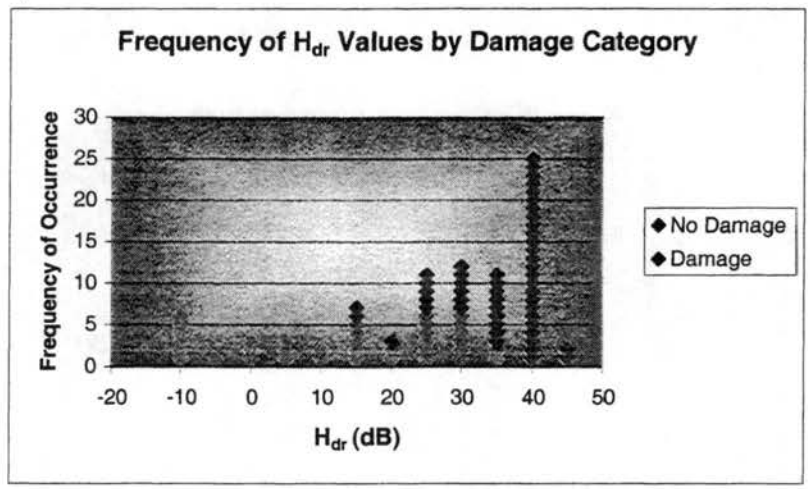

c)

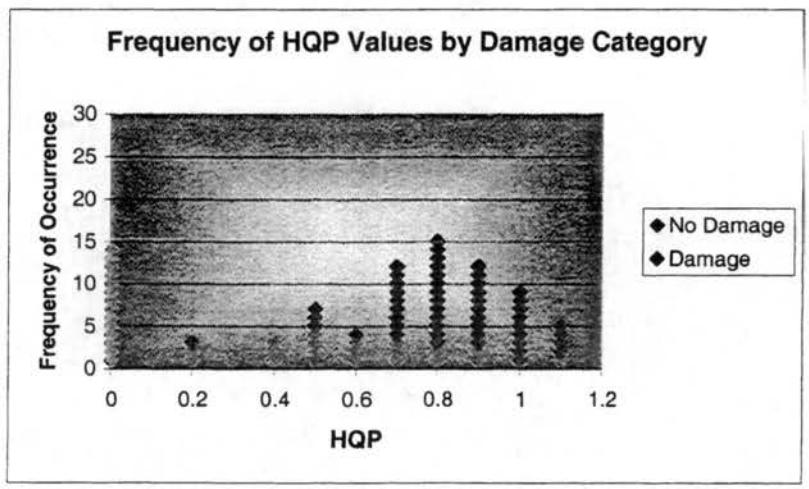

Figure 4.11 Histograms of the frequency of occurrence of binned a)LDR, b)H_{dr} and c)HQP values color-coded according to damaging and non-damaging hail. LDR bin size = 2, H_{dr} bin size = 5, HQP bin size = 0.1.

CHAPTER FIVE

Conclusions

5.1 Theoretical Conclusions

From polarimetric theory it is apparent that there is a theoretical basis for the effectiveness of HQP. The use of LDR should be able to provide at least some additional information to that found in H_{dr}. Several studies show that large hail should possess physical characteristics (increased oblateness, irregular shapes, canting) that would lead to increased LDR values. These increased LDR values would increase HQP values and possibly provide more information about hail size and damage capability than provided by H_{dr}. The modeling and ground-truth verification aspects of this study were conducted to determine whether theoretical issues such as Mie resonance and dielectric effects (e.g., associated with melting hail) are enough of a problem to interfere with the effectiveness of HQP in diagnosing hail size and the propensity for hail damage.

5.2 Modeling Conclusions

The modeling results show that the interpretation of HQP is hindered by both melting and Mie resonance effects. After running the *T*-matrix model on many combinations of hailstone characteristics, it is apparent that individual HQP values cannot be directly linked to unique hail sizes. In addition, it is possible to predict with certainty that at times HQP will fail to detect hail that is present (i.e., if hail is perfectly spherical

or completely dry). Certain mitigating factors exist, however, to decrease the likelihood of HQP failures, such as the rare occurrence of hailstones with these characteristics. For instance irregular and oblate hailstones would likely be mixed in with the spherical and dry hailstones, and the hail would still be detectable by HQP. In addition, completely uniform populations of hailstones are highly unlikely.

5.3 Observational Conclusions

5.3.1 Plots

From Figure 4.8a in Section 4.6, it was evident that LDR does not offer as much additional information as was originally hypothesized. In order to gain truly useful diagnostic information from LDR, it would need to have a quasi-linear relationship with hail size and/or damage. Figure 4.8a however, shows that while large LDR values are found in all cases of large hail (> 1 inch.), similarly large LDR values accompany all sizes of hail. This indicates that, as theoretically predicted, large hail does have physical properties (oblateness, irregularities, etc.) that increase LDR values. It also shows, however, that small hail may also possess physical attributes that increase LDR values (water coating contributing to Mie effects, irregular shapes, sponginess). The findings of this study confirm the theory that larger hail does correspond to larger LDR values. The opposite, however, cannot be said, that is, smaller hail (i.e., D < ~1.9 cm) is not uniquely associated with smaller LDR values (i.e., LDR < -20 dB). Since large LDR values can be found across the entire spectrum of hail sizes, LDR cannot be used to detect or predict when large hail may be present in a storm.

5.3.2 Statistics

Selected values from the statistical tests were shown in Table 4.2. Two main results appeared in the statistics. 1) The differences between H_{dr} and HQP are shown to be insignificant using a single statistic , or 2) the True Skill Score (TSS) and Heidke Skill Score completely contradict each other. See Table 5.1 below for examples (hail size threshold and algorithm threshold are listed on the second line of the first row of cells). (Due to the small number of no-hail data points collected, the statistics for hail size $\geq$ 0.25 in may be suspect). Since HQP and H_{dr} do not appear to be statistically different, this supports the conclusion that HQP does not offer significantly more information about hail size/damage potential than H_{dr}.

Table 5.1 – Comparison of statistics for H_{dr} and HQP. Note that in the 1st and 3rd cases, the CSI and HSS are better for H_{dr}, but the TSS is better for HQP, and in the 2nd case, there is no significant difference between the H_{dr} and HQP for any of the statistics.

Hail size $\geq$ 0.25 in	H_{dr} 1	HQP 0.3		Hail size $\geq$ 0.75 in	H_{dr} 26	HQP 0.6		Hail Size $\geq$ 1.50 in	H_{dr} 32	HQP 0.6
CSI	0.90	0.80		CSI	0.68	0.70		CSI	0.53	0.50
HSS	0.52	0.40		HSS	0.55	0.56		HSS	0.55	0.47
TSS	0.62	0.70		TSS	0.59	0.59		TSS	0.59	0.62

An additional statistical experiment was performed using H_{dr} and LDR threshold values tailored to selected hail size thresholds. This was intended to discover if perhaps the HQP algorithm as constructed was not the most efficient and whether useful hail detection/size information could still be obtained from the addition of LDR. This was

found not to be the case since only a small improvement over HQP and H_{dr} was noted, and was likely due to the biased method of threshold selection.

5.3.3 Operational Algorithm Comparisons

During the summers of 1992 and 1993, the National Center for Atmospheric Research (NCAR) Research Applications Program (RAP) conducted a hail study in northeastern Colorado. The purpose of this study was to test the effectiveness of the then-current Next Generation Radar (NEXRAD) hail detection algorithms and the newer National Severe Storms Laboratory (NSSL) Hail Detection Algorithm (HDA) (Kessinger and Brandes, 1995). Due to the quality of observations during this study (not simply relying on storm spotter reports and information from *Storm Data*) as well as the location, these results were chosen to compare with the results from both H_{dr} and HQP. The NCAR study examined several thresholds for probabilities of both hail and large hail, and calculated many of the same statistics used in this study. The statistics from the best-performing threshold for each algorithm (POH, POSH, H_{dr}, and HQP) are included in Table 5.2 below. Due to the outdated nature of the NEXRAD algorithm used in the NCAR study, it is not included here. For the POH and POSH, a 15 km influence radius was used. The threshold value for each algorithm is listed below each algorithm name. For the polarimetric values, very few no-hail data points were collected (<10), so the statistics for hail size > 0 mm (existence of any hail) are suspect. For the detection of severe hail, however, it can be seen that the polarimetric algorithms far exceed the current NWS algorithms in skill. For example, for hail larger than 19 mm (or 0.75 in) the POSH algorithm has a Critical Success Index (CSI) of 0.36 and a HSS of 0.42. For the same

hail-size threshold H_{dr} has a CSI of 0.72 and a HSS of 0.57. HQP has very similar values for the algorithms. These skill scores are significantly better than those for the NWS algorithms.

Table 5.2 – Comparison of NWS and polarimetric hail-detection algorithms.

Hail size > 0 mm	POH 20%	POSH 20%	H_{dr} 1	HQP 0.3		Hail size > 19 mm	POH 100%	POSH 100%	H_{dr} 22	HQP 0.6
POD	0.95	0.88	0.93	0.81		POD	0.75	0.65	0.83	0.77
FAR	0.07	0.04	0.04	0.01		FAR	0.71	0.55	0.15	0.12
CSI	0.89	0.85	0.90	0.80		CSI	0.27	0.36	0.72	0.70
HSS	0.79	0.74	0.52	0.40		HSS	0.25	0.42	0.57	0.56

5.4 Final Conclusions

The modeling and observational results reinforce each other in that each seems to show more of a "fan-shaped" than linear relationship between LDR and size. Figures 3.6 and 3.13 show that Mie resonance effects begin at smaller sizes for hailstones either coated with or containing a larger amount of liquid water. Figures 3.5 - 3.7 show a very similar shape to that seen in Figure 4.8a, in which the LDR values for large hail are all large, but similarly large LDR values can be found at all sizes tested (0.25 in $\leq D \leq$ 7.0 in). The modeling results show that these larger LDR values at smaller hail sizes are due primarily to Mie effects brought on at smaller hail sizes by progressively thicker water coatings. It can be concluded then that while large hail possesses physical attributes that cause it to have large LDR values, small hail possesses physical attributes that can yield

both small and large LDR values. This severely limits any diagnostic capability of LDR, and therefore HQP as well.

Regardless of the lack of skill shown by LDR, HQP and H_{dr} are still quite comparable. As seen in Sections 4.5 and 4.6 and Table 5.2 above, both algorithms show significant skill in detecting hail. In addition, each of these algorithms can give detailed information regarding the location of hail, and can be calculated using only the lowest one or two sweep levels. These factors combine to show that these algorithms have tremendous advantages over current operational algorithms using reflectivity and environmental temperature data. As for the lack of LDR capability on the proposed upgraded WSR-88D radars, it is apparent from this study that this will not be a problem for hail detection. Based on this study, the use of Z_h and Z_{dr} (combined as H_{dr}) seems sufficient to detect hail without the need for any additional depolarization information.

5.5 Future Work

Although the results from this study appear to be fairly conclusive, more investigation can and should be done. In this study, data were only collected in the area of northeast Colorado. No attempt was made to collect data in other climate regimes or regions of the country. It is possible that depolarization may yield more information in areas with different types of hail, such as in the southern plains where much larger hail is common, or in the southeast where hail is more likely to originate as frozen raindrops. LDR may also yield additional information in discriminating hail from rain when small, nearly-spherical raindrops are present that might lead to Z_{dr} values more indicative of hail (such as in the tropics).

The data sets used in this study all contained hail, because specifically locating hail was the goal of the researchers. Attempts were made to find reports of no hail during these surveys (beyond the perimeter of the storm, for instance), but no strictly rain cases were investigated. This caused problems in determining the true skill of the algorithm to discriminate between hail and no-hail events. More attempts should be made to collect and verify data in storms believed to contain mostly rain in order to facilitate a more reliable statistical analysis. It would be interesting to collect data from a few more storms, and perhaps in a different region of the country before it is determined conclusively that LDR has no usefulness for hail identification.

REFERENCES

Atlas, D., 1964: Advances in radar meteorology. *Adv. in Geophys.*, **10**, 317-478.

Auer, A. H., 1994: Hail recognition through the combined use of radar reflectivity and cloud-top temperatures. *Mon. Wea. Rev.*, **122**, 2218-2221.

Aydin, K., T. A. Seliga, V. Balaji, 1986: Remote sensing of hail with a dual linear polarization radar. *J. Climate Appl. Meteor.*, **25**, 1475-1484.

Aydin, K., Y. Zhao, T. A. Seliga, 1990: A differential reflectivity radar hail measurement technique: Observations during the Denver hailstorm of 13 June 1984. *J. Atmos. Oceanic Tech.*, **7**, 104-113.

Bailey, I.. H., and W. C. Macklin, 1968: The surface configuration and internal structure of artificial hailstones. *Quart. J. Roy. Meteor. Soc.*, **94**, 1-11.

Balakrishnan N., and D. S. Zrnić, 1990: Use of polarization to characterize precipitation and discriminate large hail. *J. Atmos. Sci.*, **47**, 1525-1540.

Barber P., and C. Yeh, 1975: Scattering of electromagnetic waves by arbitrarily shaped dielectric bodies. *Appl. Opt.*, **14**, 2864-2872.

Barge, B. L., and G. A. Isaac, 1973: The shape of Alberta hailstones. *J. Rech. Atmos.*, **7**, 11-20.

Battan, L. J., 1973: Radar Observations of the Atmosphere. The University of Chicago Press, Chicago, Illinois, 324 pp.

Brandes, E. A., and Vivekanandan, J., 1998: An exploratory study in hail detection with polarimetric radar, *Preprints, 14th International Conference on Interactive Information and Processing Systems*, Phoenix, AZ, Amer. Meteor. Soc., 287-290.

Breidenbach, J. P., Kitzmiller, D. H., McGovern, W. E., Saffle, R. E., 1995: The use of volumetric radar reflectivity predictors in the development of a second-generation severe weather potential algorithm. *Wea. Forecasting*, **10**, 369-379.

Bringi, V. N., J. Vivekanandan, J. D. Tuttle, 1986: Multiparameter radar measurements in Colorado convective storms. Part II: Hail detection studies. *J. Atmos. Sci.*, **43**, 2564-2577.

Bringi, V. N., and A. Hendry, 1990: Technology of polarization diversity radars for meteorology. *Radar in Meteorology: Battan Memorial and 40th Anniversary Radar Meteorology Conference,* Amer. Meteor. Soc., 109-114.

Bringi, V. N., and V. Chandrasekar, 2001: Polarimetric Doppler Weather Radar: Principles and Applications. Cambridge University Press, Cambridge, United Kingdom, 636 pp.

Browning, K. A., and J. G D. Beimers, 1967: The oblateness of large hailstones. *J. Appl. Meteor.*, **6**, 1075-1081.

Browning, K., A., J. Hallett, T. W. Harrold, D. Johnson, 1968: The collection and analysis of freshly fallen hailstones. *J. Appl. Meteor.*, **7,** 603-612.

Carbone, R. E., D. Atlas, P. Eccles, R. Fetter, E. Mueller, 1973: Dual wavelength radar hail detection. *Bull. Amer. Meteor. Soc.*, **54**, 921-924.

Cheng, L., and M. English, 1983: A relationship between hailstone concentration and size. *J. Atmos. Sci.*, **40**, 204-213.

Chong, S., and C. S. Chen, 1974: Water shells on ice pellets and hailstones. *J. Atmos. Sci.*, **31**, 1384-1391.

Doviak, R. J., and Zrnic, D. S., 1993: Doppler Radar and Weather Observations. Academic Press, San Diego, CA, 562 pp.

Doviak, R. J., V. Bringi, A. Ryzhkov, A. Zahrai, D. Zrnić, 2000: Considerations for polarimetric upgrades to operational WSR-88D radars. *J. Atmos. Oceanic Technol.*, **17**, 257-278.

Eccles, P. J., and D. Atlas, 1973: A dual-wavelength radar hail detector. *J. Appl. Meteor.*, **12**, 847-854.

Féral, L., H. Sauvageot, S. Soula, 2003: Hail detection using S- and C- band radar reflectivity difference. *J. Atmos. Oceanic Technol.*, **20**, 233-248.

Herzegh, P. H., and A. R. Jameson, 1992: Observing precipitation through dual-polarization radar measurements. *Bull. Amer. Meteor. Soc.*, **73**, 1365-1374.

Hubbert, J., V. N. Bringi, L. D. Carey, 1998: CSU-CHILL polarimetric radar measurements from a severe hail storm in eastern Colorado. *J. Appl. Meteor.*, **37**, 749-775.

Husson, D., and Y. Pointin, 1989: Quantitative estimation of hailfall intensity with dual polarization radar and a hailpad network. *Preprints, 24th Conference on Radar Meteorology*, Tallahassee, FL., Amer. Meteor. Soc., 318-321.

Kennedy, P. C., S. A. Rutledge, W. A. Petersen, 2001: Polarimetric radar observations of hail formation. *J. Appl. Meteor.*, **40**, 1347-1366.

Kennedy, P. C., V. N. Bringi, D. A. Brunkow, S. A. Rutledge, and N. J. Doesken, 2001: Hail characterization via the joint utilization of reflectivity, differential reflectivity, and linear depolarization ratio data. *Preprints, 30th International Conference on Radar Meteorology*, Munich, Germany, Amer. Meteor. Soc.,

Kessinger, C. J., and E. A. Brandes, 1995: A comparison of hail detection algorithms. Summary project report prepared for the FAA, 31 January 1995, 52pp.

Kitzmiller, D. H., McGovern, W. E., Saffle, R. E., 1995. The WSR-88D severe weather potential algorithm. *Wea. Forecasting*, **10**, 141-159.

Knight, C. A., and N. C. Knight, 1970a: Lobe structures of hailstones. *J. Atmos. Sci.*, **27**, 667-671.

Knight, C. A., and N. C. Knight, 1970b: The falling behavior of hailstones. *J. Atmos. Sci.*, **27**, 672-681.

Knight, C. A., and N. C. Knight, 1973: Quenched, spongy hail. *J. Atmos. Sci.*, **30**, 1665-1671.

Knight, N. C., 1986: Hailstone shape factor and its relation to radar interpretation of hail. *J. Climate Appl. Meteor.*, **25**, 1956-1958.

Lemon, L. R., 1998: The radar "Three-Body Scatter Spike": an operational large-hail signature. *Wea. Forecasting*, **13**, 327-340.

Lesins, G. B., and R. List, 1986: Sponginess and drop shedding of gyrating hailstones in a pressure-controlled icing wind tunnel. *J. Atmos. Sci.*, **43**, 2813-2825.

List, R., 1959: Zur Aerodynamik von Hagelkoernern. *Z. Angew. Math. Phys.*, **10**, 143-159.

List, R., U. W. Rentsch, A.C. Byram, 1973: On the aerodynamics of spheroidal hailstone models. *J. Atmos. Sci.*, **30**, 654-661.

List, R., and R. S. Schemenauer, 1971: Free-fall behavior of planar snow crystals, conical graupel and small hail. *J. Atmos. Sci.*, **28**, 110-115.

Macklin, W. C., 1963: Heat transfer from hailstones. *Quart. J. Roy. Meteor. Soc.*, **89**, 360-369.

Macklin, W. C., and F. H. Ludlam, 1961: The fallspeeds of hailstones. *Quart. J. Roy. Meteor. Soc.*, **87**, 72-81.

Marzban, C., A. Witt, 2001: A Bayesian neural network for severe-hail size prediction. *Wea. Forecasting*, **16**, 600-610.

Mason, B. J., 1956: On the melting of hailstones. *Quart. J. Roy. Meteor. Soc.*, **82**, 209-216.

Mason, B. J., 1971: The Physics of Clouds.2d ed. Oxford University Press, 671 pp.

Matson, R. J., and A. W. Huggins, 1980: The direct measurement of the sizes, shapes and kinematics of falling hailstones. *J. Atmos. Sci.*, **37**, 1107-1125.

Mitchell, E. D., S. V. Vasiloff, G. J. Stumpf, A.Witt, M. D. Eilts, J.T. Johnson, K. W. Thomas, 1998: The National Severe Storms Laboratory tornado detection algorithm. *Wea. Forecasting*, **13**, 352-366.

Pruppacher, H. R., and K. V. Beard, 1970: A wind tunnel investigation of the internal circulations and shape of water drops falling at terminal velocity in air. *Quart. J. Roy. Meteorol. Soc.*, **96**, 247-256

Rasmussen, R. M., and A. J. Heymsfield, 1987: Melting and shedding of graupel and hail. Part I: Model physics. *J. Atmos. Sci.*, **44**, 2754-2763.

Rasmussen, R. M., and A. J. Heymsfield, 1987: Melting and shedding of graupel and hail. Part II: Sensitivity study. *J. Atmos. Sci.*, **44**, 2764-2782.

Rasmussen, R. M., V. Levizzani, H. R. Pruppacher, 1984: A wind tunnel and theoretical study on the melting behavior of atmospheric ice particles: III. Experiment and theory for spherical ice particles of radius > 500 μm. *J. Atmos. Sci.*, **41**, 381-388.

Rinehart, R. E., and J. D. Tuttle, 1982: Antenna beam patterns and dual wavelength processing. *J. Appl. Meteor.*, **15**, 69-76.

Roos, D., 1972: A giant hailstone from Kansas in free fall. *J. Appl. Meteor.*, **11**, 1008-1011.

Seliga, T. A., and V. N. Bringi, 1976: Polarimetric use of radar differential reflectivity measurement at orthogonal polarizations for measuring precipitation. *J. Appl. Meteor.*, **15**, 69-76.

Seliga, T. A., and V. N. Bringi, 1978: Differential reflectivity and differential phase shift: Applications in radar meteorology. *Radio Sci.*, **13**, 271-275.

Seliga, T. A., R. G. Humphries, J. I. Metcalf, 1990: Polarization diversity in radar meteorology: Early developments. *Radar in Meteorology: Battan Memorial and 40th Anniversary Radar Meteorology Conference,* Amer. Meteor. Soc., 109-114.

Schuur, T. J., D. S. Zrnić, R. E. Saffle, 2001: The Joint Polarization Experiment – An operational test of weather radar polarimetry, *Preprints, 30th International Conference on Radar Meteorology*, Munich, Germany, Amer. Meteor. Soc., 722-723.

Straka, J. M., D. S. Zrnić, A. V. Ryzhkov, 2000: Bulk hydrometeor classification and quantification using polarimetric radar data: Synthesis of relations. *J. Appl. Meteor.*, **39**, 1341-1372.

Thwaites, S., J. N. Carras, W. C. Macklin, 1977: The aerodynamics of oblate hailstones. *Quart. J. Roy. Meteor. Soc.*, **103**, 803-808.

Tuttle, J. D., and R. E. Rinehart, 1983: Attenuation correction in dual-wavelength analysis. J. Climate Appl. Meteor., **22**, 1914-1921.

Vivekanandan, J., W. M. Adams, V. N. Bringi, 1991: Rigorous approach to polarimetric radar modeling of hydrometeor orientation distributions. *J. Appl. Meteor.*, **30**, 1053-1063.

Wang, D. Y., 1979: Light scattering by nonspherical multilayered particles, Doctoral Thesis, University of Utah, 40-51 pp.

Waterman, P. C., 1969: Scattering by dielectric obstacles. *Alta Frequenza*, (Speciale), 348-352.

Witt, A., M. D. Eilts, G. J. Stumpf, J. T. Johnson, E. D. Mitchell, K. W. Thomas, 1998: A enhanced hail detection algorithm for the WSR-88D. *Wea. Forecasting*, **13**, 286-303.

Ziegler, C. L., P. S. Ray, N. C. Knight, 1983: Hail growth in an Oklahoma multicell storm. *J. Atmos. Sci.*, **40**, 1768-1791.

Zrnić, D. S., 1996: Weather radar polarimetry – trends toward operational applications. *Bull. Amer. Meteor. Soc.*, **77**, 1529-1534.

Zrnić, D. S., V. N. Bringi, N. Balakrishnan, K. Aydin, V. Chandrasekar, J. Hubbert, 1993: Polarmetric measurements in a severe hailstorm. *Mon. Wea. Rev.*, **121**, 2223-2238.

Zrnić, D. S., and A. V. Ryzhkov, 1999: Polarimetry for weather surveillance radars. *Bull. Amer. Meteor. Soc.*, **80**, 389-406.

APPENDICES

APPENDIX A

Stokes' Parameters

Stokes parameters (From Bringi and Chandrasekar, 2001):

The elements of the Stokes' vector corresponding to a plane wave with electric field $\vec{E}^i(O) = E_h^i \hat{h}_i + E_v^i \hat{v}_i$, are defined as,

$$I = \left|E_h^i\right|^2 + \left|E_v^i\right|^2 = \left|\vec{E}^i(O)\right|^2$$

$$Q = \left|E_h^i\right|^2 - \left|E_v^i\right|^2 = I\cos 2\psi \cos 2\tau = I\cos 2\varepsilon$$

$$U = 2\,\mathrm{Re}(E_h^{i*} E_v^i) = I\sin 2\psi \cos 2\tau = I\sin 2\varepsilon\cos\delta$$

$$V = 2\,\mathrm{Im}(E_h^{i*} E_v^i) = I\sin 2\tau = I\sin 2\varepsilon\sin\delta$$

Where: $\vec{E}^i$ is the incident electric field vector

E_h^i and E_v^i are incident wave components of the electric field in the (h,v)-basis

$\hat{h}_i$ and $\hat{h}_v$ are the unit horizontal (vertical) polarization vectors of incident electric field

ψ and τ are geometrical ellipse angles

$\delta = \theta_v - \theta_h$ and

$\tan\varepsilon = \left|E_v^i\right| / \left|E_h^i\right|$

APPENDIX B

Alpha-numeric Survey Codes

Codes are a combination of the letter in parenthesis and the number described to the right.

(S)ize	hundreds of an inch
(H)ardness	1-soft; 2-in between; 3-hard
(G)round Coverage	1-hail accum. in low spots and bushes; 2-high drifts; 3-total coverage
(D)uration	time in minutes
(W)ind strength	1-negligible; 2-noticeable; 3-damaging
(w)ind effect	1-damage from hail alone; 2-damage from hail and wind; 3-wind strongly influenced damage
(R)ain amount	1-light; 2-moderate; 3-heavy
(r)ain order	1-rain first; 2-rain and hail together; 3-hail first
(O)ther	1-spherical; 2-obviously not spherical; 3-lobes, protuberances
(Q)uality of observer	1-highly questionable; 2-reliable; 3-expert; 4-after the fact

Damage:

(V)ehicle	1-no damage; 2-light dents, broken mirrors; 3-large dents, broken windows
(S)tructural	1-no damage; 2-non-obvious; 3-obvious, roof replacement
(C)rops	1-no damage; 2-moderate shredding, holes; 3-destroyed
(P)lants	1-no damage; 2-few % broken stalks, 3-can see broken stalks from road; 4-destroyed, laid flat
(T)ree	1-no damage; 2-some leaves on ground; 3-substantial leaf coverage on ground
(Y)ard plants	1-no damage; 2-some leaves knocked off; 3-stripped stalks
Small (a)nimals	1-no injury; 2-injury, 3-death
Large (A)nimals	1-no injury; 2-injury; 3-death

In the surveys below, a code letter with no number following indicates that no information was obtained about that storm/hail characteristic.

Denver International Airport, CO Storm 6/20/01

Point	Code	GPS	Description
DN001	S3,V3	536780 4399997	Hail size: G-ball - 2 in size Damage: Svr car and trailer damage, ground impact marks.
DN002	V3,S3	535591 4400359	Damage: Svr house + camper damage, ground marks.
DN003	V3,S3	538680 4404724	Hail size: 2 in Damage: Severe building and aircraft damage at FTG
DN004	S3	532435 4399178	Hail size: >G-ball Ground coverage: sparse Damage: Broke outer window pane on E side of house only.
DN005	No Code	529637 4398568	Hail size: 0 Other descriptions: No hail observed at Aurora Airpark
DN006	V3	540526 4399902	Hail size: Few G-ball sized stones Damage: No damage at site. But, cars pulled off of I-70 w/ broken windshields.
DN007	V3	539100 4400046	Hail size: G-ball to approaching tennis ball size.
DN008	V2	542736 4400721	Hail size: Approx .75 inch stones displayed from freezer; probably melted somewhat. Ground coverage: Ground not fully covered Damage: Dented cars, no broken glass.
DN 009	S3	534847 4402091	Damage: Hailstones blew in through broken window in house
DN010	V3	533970 4399227	Damage: DEN Post had picture of car w/ completely destroyed rear window at Biscuit Café
DN011	V3,S3	528483 4412095	Hail size: 2 inch hail Damage: Significant car and terminal roof damage.

Fort Morgan,CO Storm 6/03/02

Point	Code	GPS	Description
AM001	H1,G1, D5,W2, R2,r3, V1,S1, T1,Y1, Q2	0596850 4452492	Hail size: 0.5in to 1in Hardness: Soft Ground coverage: Visible coverage, didn't cover ground completely Duration: Few minutes Wind: Some wind Rain: Rained for awhile longer Rain gauge: no Damage: no truck damage No leaves locally visible down
AM002		0595073 4452532	Letter drop. Unknown leaf debris, maybe raked.
AM003	R2,Q4	0594577 4452878	Hail size: unknown Hardness: unknown Ground coverage: unknown Duration: unknown Wind: unknown Rain: yes Rain gauge: 0.6 in Damage: unknown Other descriptions: John was at point 4 during the storm
AM004	H1,G3, D10, W1,R1, C1,Y1, S1,Q2	0592184 4454111	Hail size: Dime to nickel Hardness: Hail softer than normal Ground coverage: ground evenly covered Duration: Straight hail for 5-10 min Wind: Little wind Rain: yes Rain gauge: 0.3in Damage: No crop damage
n/a		None	Was at Grandma's house on S edge of town on Sherman St. Small hail only, no plant damage.
AM006	G3, D18, r3,R3, Q2	0594323 4454193	Hail size: Pea sized max Hardness: unknown Ground coverage: Covered ground Duration: 15-20 min Wind: unknown Rain: both before and after, separate from hail Rain gauge: no Damage: unknown Other descriptions: Saw rotation in storm. 1)Rotation, 2)Freight train hail (roar), 3)Rain separate from hail, 3-4 rain episodes after. Order: Intermittent rain, hard

			rain, soft hail, heavy hail.
AM007	H1,G2, R3,Q2	0594317 4451722	Hail size: Marble sized Hardness: Soft Ground coverage: piled up in ditches and low spots Duration: unknown Wind: unknown Rain: yes Rain gauge: see below Damage: unknown Other descriptions: Hailed from Rd 12 to Rd 14. Came on as a sheet moving W to E. Raingauge: at house gauge (location below)
AM008	R3,Q4	0594663 4451983	Hail size: unknown Hardness: unknown Ground coverage: unknown Duration: unknown Wind: unknown Rain: yes Rain gauge: 1-1.2 in Damage: unknown Other descriptions: Raingauge location Pix:
AM009	H3,W1, w1,R1, T2,S1, Q2	0596305 4450860	Hail size: Some ~1 in sized hail Hardness: hard Ground coverage: unknown Duration: unknown Wind: little wind Rain: Not much rain Rain gauge: no Damage: Obvious leaf debris immediately upon turning along O from 15 Other descriptions: Picked up rock to show size
AM010	G1,D4, R2,r3, Q2	0596894 4450851	Hail size: ~ 1 in diameter Hardness: unknown Ground coverage: Ground not covered Duration: 3-4 min Wind: unknown Rain: Hail first, then rain longer afterward Rain gauge: 0.8 in at office. Damage: Little damage (few) car dents reported
AM011	H2,G3, D8, W2,r3, T2,S1, Q2	0597929 4453280	Hail size: Pea & slightly bigger Hardness: Stones not that hard Ground coverage: Covered ground. Field white east of house Duration: 5-10 min Wind: Strong NW wind

			Rain: After hail Rain gauge: no Damage: Some leaves off trees No damage
AM014	H3,G1, D10, R2,S1, C1,Q2	0599584 4450135	Hail size: Shooter marble Hardness: hard (hit on head by one) Ground coverage: 50% ground coverage Duration: ~10 min Wind: unknown Rain: yes Rain gauge: 0.9in Damage: No crop damage
AM015	C2,P3, Q4	0599514 4450945	Hail size: unknown Hardness: unknown Ground coverage: unknown Duration: unknown Wind: unknown Rain: unknown Rain gauge: no Damage: corn shredded, but will recover, leaf hole in wild sunflower Pix: 2 pix of corn damage. Leaf hole in wild sunflower.
AM016	C2,P2, Q2	0601988 4451381	Hail size: Mothball sized Hardness: unknown Ground coverage: unknown Duration: unknown Wind: unknown Rain: unknown Rain gauge: Damage: Crop damage (corn and wheat). Few % of wheat stalks broken and bent over.
AM017	H3,G1, W2,R3, S1,Y2, Q2	0601157 4452482	Hail size: Finger tip diameter Hardness: Hard, didn't smash on concrete Ground coverage: Partial ground coverage Duration: unknown Wind: Breezy Rain: yes Rain gauge: a little over 1 in Damage: Some plant damage, but not wiped out.
AM018	G2,D5, R3,r3, V1,S1, A1,Q2	0602756 4454249	Hail size: Pencil eraser sized Smaller than pea Hardness: unknown Ground coverage: Piles of hail next to bldgs Didn't cover ground Duration: 5 min Wind: unknown Rain: heavy rain, after hail

			Rain gauge: no Damage: No damage
AM019	H3,V2, Q1	0602758 4450244	Hail size: 0.5 in diameter Hardness: Not too soft – bounced off of windshield Ground coverage: unknown Duration: unknown Wind: unknown Rain: unknown Rain gauge: unknown Damage: Slight windshield damage
AM020	G1, D18, W2,R1, S1,Y1, Q2	0604788 4449454	Hail size: Pea to marble sized Hardness: unknown Ground coverage: Ground not covered Duration: 15-20 min Wind: Did beat things ? by wind Rain: yes Rain gauge: 0.25 in storm total Damage: unknown Other descriptions: Not that bad of a hailstorm
AM021	Q2	0602953 4447776	Hail size: Large marble sized "around here" (pointed E). Hardness: unknown Ground coverage: unknown Duration: unknown Wind: unknown Rain: unknown Rain gauge: no Damage: unknown

Fort Lupton/Brighton, CO Storm 6/03/02

Point	**Code**	**GPS**	Description
AL024	H3,G3, D18, W2,w2, R3,S3, T3,Y2, O1,Q2	0519378 4429250	Hail size: Golf ball and large marble sized hail. Hardness: Hard Ground coverage: Total ground coverage, 2"in deep, didn't melt until sometime that night. Duration: 15-20 min Wind: Out of W and N Rain: Heavy, leaked into porch Rain gauge: No Damage: Obvious tree and plant damage. Machete chopped tree branches. Total roof replacement needed. Other descriptions:Worst she's seen in 6-8 yrs.

			Sudden onset of hail. Pix: 1)Locus leaves (?) w/rock pile in front yard. 2)Pine tree w/dropped branches. 3)Hail dent in grass w/pen.
AL025	H2,V2, O1,T3, Y3,Q2	0519499 4429137	Pix:1)Vinyl roof of car, 2)Dented metal trim, 3)Partial hail "bite" on bumper cover w/metal ruler.
		Same as AL025	Hail size: ~1 in. some larger Hardness: Hard, but flattened some on impact Damage: Completely stripped tomato plants, severe pumpkin plant damage. Small dents in SUV. Other descriptions: Saved 4 cups of hail. Pix: Saved, frozen hail with ruler.
AL026	G3, D30, r2, S3, Q1	0520933 4429289	Hail size: Golf ball Hardness: unknown Ground coverage: Total ground coverage Duration: 30 min Damage: Some windows in stored trailers broken. Other descriptions: Was sure hail storm was on Tues. Said from 3:30-4:00pm Monday light rain, no hail. Rained all day Tues. with hail. Worse at mother's house 7 mi N of trailer site. Pix: 1&2)Broken windows in trailers.
AL027	D5,R3, V1,S1, Q2	0524106 4429474	Hail size: Pea sized Hardness: unknown Ground coverage: unknown Duration: 5 min Wind: unknown Rain: Lots Rain gauge: No Damage: None Other descriptions: Lightning strike in parking lot Pix: 1)Greenhouse covers, undamaged.
AL028	H3,G1, W2,R3, V1,S1, A1,Q2	0522555 4429524	Hail size: Pea sized Hardness: Hard Ground coverage: Barely covered ground Duration: unknown Wind: Stout breeze Rain: yes Rain gauge: 1 in Damage: None
AL029	T2,Q4	0517682 4429357	Obvious leaf damage. No one home.
AL030	H3,G1, D10,	0516552 4429504	Hail size: Marble size (shooter marble reported in Brighton)

	V1,S1, T2,Q2		Hardness: Hard Ground coverage: Not complete coverage on ground, built up on cars around wipers, etc. Duration: 5 min (also 15 min reported) Wind: unknown Rain: unknown Rain gauge: No Damage: Visible leaf debris. Green houses appeared undamaged. Other descriptions: Audible inside metal bldg. Pix: None
AL031	H3,G1, D3,W2, w3,R2, V1,S1, C1,T1, Q3	0516129 4431042	Hail size: Small pea, maybe some marble Hardness: Hard Ground coverage: No ground coverage. Duration: 2-3 min duration. Wind: Strong outflow from E Rain: yes Rain gauge: 0.8in storm total. Damage: No damage at this location. Other descriptions: Followed ridge (motion vector), noticeably larger on ridge to E, Pix: None
AL032	G3,Q4	0516988 4431036	Beginning point of damage and heavy hail from farmer's survey.
AL033	P3,Q4	0517484 4431043	Readily identifiable broken tall grass stalks gone to seed. Picture of broken stalks.
AL034	H3,G3, D10, W1,V2, S1,Y3, Q2	0520124 4431008	Hail size: 0.75 in max Hardness: Hard Ground coverage: Covered ground Duration: 10 min Wind: Wind with hail not too bad. Rain: unknown Rain gauge: No Damage: Truck damage despite blankets (many dents, but not too deep). Plant damage (plants stripped). No skylight damage.
AL035	G3,S1, T3,Q4	0519390 4432767	Hail size: unknown Hardness: unknown Ground coverage: Ground covered when wife came home. Duration: unknown Wind: unknown Rain: unknown Rain gauge: No Damage: Lots of leaves on ground and caught in fence

			Other descriptions: Retroactive report from wife
AL036	H3,G3, D20, R3,V1, S1,T2, Y2,A1, Q2	0521372 4431399	Hail size: Pea sized first, then larger, maybe 1 in max. Hardness: Hard Ground coverage: Ground covered. Duration: 20 min Wind: unknown Rain: Heavy rain washed out nearby road. Rain gauge: No Damage: Leaf damage only.
AL037	P2,T1, Q4	0523933 4432692	Few small holes in some broad leaves. No leaves under trees.
AL038	P2,Q4	0519979 4432687	Grass showed some broken stalks, more than at last stop, but less than further W.
AL039	H3,G1, W2,w2, R3,r2, S1,T2, A1,a3, Q2	0517400 4432675	Hail size: Marble sized and smaller Hardness: Hard Ground coverage: Patchy ground coverage Duration: unknown Wind: Wind blew hail and rain. Rain: Lots of rain Rain gauge: No Damage: Leaves down, killed 2 chickens Other descriptions: Heavier to E. "Stopped right here" (W edge of storm)
AL062	H3,G2, w2,V2, S3,A2, Q2	0517851 4432663	Hail size: Initially golf ball sized Hardness: Hard Ground coverage: Wind drifted hail around and caused uneven ground coverage at house Damage: Daughter's leg bruised (daughter at home), paint damage on side of house, broken truck mirror, broken glass in pump house (not house proper). Other descriptions: In a farm field unspecified distance N & E of farm office proper. Some hail there. More at her house. "One football field to E" along Rd 8, visibly more hail. Estimated 3-4 in even ground coverage. Pix: None
			Second survey, 6/14/02
AL049	H3,D1, W2,V1, S1,A1, Q2	0517857 4436827	Hail size: 1 in Hardness: Solid ice Ground coverage: unknown Duration: 45 sec Wind: 10 min gust Rain: unknown Rain gauge: No Damage: None

AL050	C2,Q4	0518570 4436419	Damage: Evidence of hail in corn field, some shredding, curling up of leaves. Looks like crop will recover. Pix: 2 of corn damage
AL053	P3,Q4	0520923 4435910	Damage: Tall grass damage (broken stalks) visible from moving van. Rough estimate, 20%.
AL055		0521822 4435914	Less grass damage, ~ 1%. Had to stop van to see.
AL058	H3,G3, W2,w2, R2,V1, S2,T3, Y3,Q2	0519421 4435082	Hail size: 1 – 1.25 in Hardness: Hard Ground coverage: Covered ground, 10 in deep on W side of house. Wind: 5 min strong wind Rain: Quite a bit Rain gauge: No Damage: Obvious plant damage, roof being checked by insurance Other descriptions: Locally approached from SE. Worried about windows breaking, but they didn't.
AL060	H3,G3, W3,w2, S3,C3, A2,Q2	0518493 4434058	Hail size: Golf ball Hardness: Hard Ground coverage: Ground covered, deep enough to make it difficult to open gate. Wind: Enough to break some limbs Damage: Roof to be checked on Sat., bruised in several places by hail stones (bruises still apparent), hit on head and dazed by hail stone. Knocked leaves off alfalfa, paint on house damaged, broken window.
AL064	w2,V2, T3,Y3, Q2	0519256 4433164	Hail size: 0.75 in Hardness: unknown Ground coverage: unknown Duration: unknown Wind: unknown Rain: unknown Rain gauge: No Damage: Truck sideview mirror broken, garden heavily damaged, pine branches knocked off on E side. Other descriptions: Said workers all rushed to put vehicles under hay barn to protect from hail. Pix: Broken truck mirror
AL063	G3,V2, S2,Y3, Q2	0519470 4434377	Hail size: 0.75 in Hardness: unknown Ground coverage: Ground covered in video. Duration: unknown Wind: unknown

			Rain: unknown Rain gauge: No Damage: Dented truck hood, plastic window broken, garden badly stripped. Other descriptions: Showed us video taken after storm. Pix: None
AL065	G3,D3, W2,w2, r2,S3, T3,Q2	0518746 4434574	Hail size: 1 -1.25 in Ground coverage: Ground covered Duration: 2-3 min Wind: After hail Rain: Yes, during hail Damage: Holes in house siding on E side of house, ins appraiser said part of roof needs to be redone Other descriptions: Very loud noise from hail while still across valley, could see wall of white coming toward them. Pix: 2 of Holes in siding
AL066	G3,Q4	0518306 4434281	Reported as W edge of accumulated hail. First white house W of previous location on Rd 12.

Hereford, CO Storm 6/03/02

Point	**Code**	**GPS**	Description
AH040	H1,G, D,W, w,R, r,V, S,C, P2, T2,Y, A,a, O,Q2	0556044 4533587	Hail size: 0.75 in, about 0.38 in when melting Hardness: soft Ground coverage: unknown Duration: unknown Wind: unknown Rain: unknown Rain gauge: no Damage: Tin off roof, probably from wind, Leaves down on trees, 10%-20% wheat damage across road. More damage reported at wheat field also owned by these people, about 2.5 mi W on 132 – about 40%-50% there. Other descriptions: Observers not here during event, arrived home later that evening. This house N edge of hail swath. Pix: Suspected window dings in car. Ended up being old and not related to this storm.
AH042	H, Q2	0558361 4536035	No hail here. Strong wind from E, then very strong gusts from W, blew unsecured items around.
AH043	P2	0555969	Crop: At most few % damage, mostly wheat head

		4534321	damage.
AH044	P3	0555971 4533651	Crop: Definitely more wheat damage (kinked stalks) than at point 43.
AH045		0554393 4532870	Crop: Obvious wheat damage. Missing heads, sheared off stalks. Estimated 50%-60% damage. Pix: Tracy pointing to damaged heads. Damage later ruled suspect, potentially eaten.
AH046	P2	0551189 4532734	Plants: Roadside weed/wheat tall grass, very little damage.
AH047		0549320 453725	Crop: Lots of damage to wheat. Animal droppings found all around area. Decided damage to wheat could be caused by being eaten. Pix: One picture of bent wheat head.

Pawnee Grasslands, CO Storm

Point	**Code**	**GPS**	Description
BP068	R3,P2, Q4	0523972 4517134	Dimpled surface. Evidence of sheet runoff. Pix: 1)Picture of cactus looking uphill 2) Broken cactus
BP069	H1,G3, w2, R3, S2, Q2	0518911 4518366	Size: 0.75in and smaller Hardness: Soft Ground coverage: Covered ground Damage: On S side of house, impacted S side of house, AC unit, etc.
			General plant damage increase
BP070	R1,Q2	0523978 4521189	0.16 in at Mark's office. Jeff Thomas was home at 19:00, hail piles.
BP071	H,G2, Q4	0525654 4517738	Size: 0.5in Ground coverage: Drift near knee high. Other description: Family arrived home after storm. Not here during storm.
BP072	T2,Q4	0523560 4515354	Trees: Few leaves under trees

Severance, CO Storm 7/03/02

Point	**Code**	**GPS**	Description
DS001	H,	0507813	Few downed tree leaves. Several branches down.

	T2,Q4	4492710	
DS002	H,C1, Q4	0506926 4493927	Corn field: no apparent damage
DS003	H,G1, D1, W2, R2, C1, Q2	0506511 4494016	Hail size: .5in Hardness: unknown Ground coverage: not covered Duration: 1 min Wind: noticeable Rain: sporadic, came in 2 or 3 shots Rain gauge: no Damage: none
DS004	H, W2, R1, Q2	0506218 4494709	Hail size: No hail Hardness: no hail Ground coverage: no hail Duration: ~ 2 hours Wind: windy first, then rain Rain: yes Rain gauge: 0.2 in Damage: none
DS005	H, S1, T1, Y1, Q4	0512936 4491563	Hail size: No hail Hardness: no hail Ground coverage: no hail Duration: unknown Wind: unknown Damage: none Other descriptions: Got home after storm, (a little after 5:00pm). No signs of hail or hail damage. No garden damage. Moved E to NW. Heard about hail in Severance.
DS006	H, R2, Q2	0513176 4491750	Hail size: No hail Hardness: no hail Ground coverage: no hail Duration: Hard rain for 20 min. Wind: unknown Rain: a little bit, not enough to soften ground significantly Rain gauge: no Damage: none
DS007	H3, G1, D5, W2, R1, S1, Y1, Q2	0513178 4488379	Hail size: pea/gravel, <0.5in Hardness: really hard Ground coverage: not at all Duration: few minutes Wind: strong Rain: yes Rain gauge: 0.3 in Damage: none

			Other descriptions: moved W to E then back again
DS008	H, W2, R1, S1, Y1, Q2	0512618 4490642	Hail size: No hail Hardness: no hail Ground coverage: no hail Duration: 45 min – 1 hour Wind: strong Rain: some, more lightning than wind Rain gauge: no Damage: none Other descriptions: lots of lightning, very close

Hudson, CO Storm 07/13/02

Point	**Code**	**GPS**	Description
DH001	H2,G1, D5,W2, w2,R3, r1,V1, S1,C, P,T,Y, A,a,O, Q2	0532066 4438277	Hail size: 0.5 in Hardness: unknown Ground coverage: Didn't cover ground Duration: 3-4 min Wind: unknown Rain: rained a lot, downpour Rain gauge: no Damage: none obvious Other descriptions: Nothing unusual
	H2,G1, D5,W2, w2,R3, r1,V1, S1,C,P, T,Y,A, a,O, Q2	Same	Hail size: 0.5 in Hardness: Exploded as it hit, some hard, some soft. Ground coverage: Didn't cover ground. Duration: 30 sec to 1 min (also said 5 min) Wind: Very windy from W, NW Rain: Hard rain. Sprinkled, then hard rain, then hail, all within about 4 min. Rain gauge: No, but reports from close by were 1in to 1.63 in Damage: none
DH002	H3,G1, D,W2, w,R2,r, V1,S1, C,P,T, Y,A,a, O,Q2	0530817 4440795	Hail size: < 0.5 in to 0.5 in Hardness: remained intact Ground coverage: Didn't cover. Hit and miss, not like snow, spaced out. Duration: unknown Wind: strong wind Rain: showery, not steady, but lots of rain, looked like a lake Rain gauge: no Damage: none Other descriptions: gave graphs of engine vibration,

			but suspect since can't tell rain from hail
DH003	H,G,D, W2,w, R1,r, V1,S1, C,P, T1,Y1, A1,a1, O,Q2	0530544 4435907	Hail size: No hail Hardness: no hail Ground coverage: no hail Duration: no hail Wind: some Rain: some, shower, nothing substantial, not enough to get muddy Rain gauge: no Damage: none Other descriptions: Watching for rainfall because of water restrictions and didn't see anything that made an impression.
DH004	H,G2, D5,W2, w,R3,r, V1,S, C,P,T, Y,A,a, O,Q2	0531004 4436592	Hail size: 0.5 in Hardness: unknown Ground coverage: Looked like snow in places, but didn't cover ground completely. Duration: Few minutes Wind: Some Rain: Very heavy, pouring Rain gauge: No Damage: No car damage
DH005	H,G,D, W3,w, R1,r, V1,S1, C,P, T1,Y, A1,a1, O,Q2	0533346 4438260	Hail size: No hail Hardness: no hail Ground coverage: no hail Duration: no hail Wind: Very strong wind Rain: No rain Rain gauge: no Damage: None Other descriptions: Worried about wind taking roof off (happened during another storm previously).
DH006	H3,G1, D,W2, w,R3, r,V,S1, C,P, T1,Y1, A,a,O, Q2	0533844 4438713	Hail size: 0.5 in to 0.75 in Hardness: Kept shape Ground coverage: Ground covered in areas, spotty, not coated. Duration: Came and went (came in one way then left, then came back from the other way). Wind: Very windy at first Rain: Lots Rain gauge: No Damage: None (no vegetation damage) Other descriptions: "Have seen worse." Came down fast and furious, then stopped, then came back from opposite direction.
DH011	H1,G1,	0534042	Hail size: Small 0.5 in

	D5,W2, w,R2, r3,V, S1,C, P,T, Y1,A, a,O, Q2	4441889	Hardness: Slushy Ground coverage: Not covered Duration: Few minutes Wind: A little wind before hail. Rain: Small hail before rain hit. Rain gauge: 0.6 in Damage: Didn't hurt anything (garden) Other descriptions: By the time the rain ended, there was no more hail visible. Pix:
DH013	H,G,D, W3,w, R,r,V, S1,C, P,T,Y, A,a,O, Q2	0532715 4444023	Hail size: about pea sized Hardness: unknown Ground coverage: unknown Duration: unknown Wind: more wind than hail, told his wife not to open the door during the storm out of concern that the wind might damage it Rain: unknown Rain gauge: unknown Damage: Main crop hail damage that he was aware of was in his alfalfa field on the west side of Klug lake (see later GPS point) Other descriptions: was aware of crop damage to his south
DH014	H3,G3, D20, W2,w2, R3,r2, V,S,C, P,T,A1, a,O,Q2	0535368 4445599 (Should be shifted a bit east)	Hail size: 1 in Hardness: some stones were hard. He was caught outside and took shelter at a power company work trailer. Ground coverage: Partial ground coverage; heavier areas "looked like snow" Duration: Hail duration roughly 20 minutes. Total storm duration closer to 25 – 30 minutes. Wind: Strong winds with the hail Rain: Heavy rain with the hail Damage: Immediate area was all open pasture, thus no visible damage Other descriptions: Neighbor's information: More rain / less hail further west (distance not specified) "No storm" at Keensburg.
DH016	H,G,D, W,w,R, r,V,S, C2,P, T,Y,A, a,O,Q4	0533510 4439988	Hail size: unknown Hardness: unknown Ground coverage: unknown Duration: unknown Wind: unknown Rain: unknown Rain gauge: unknown

			Damage: Moderate damage to beets. Holes and/or tears in leaves of all plants. Other descriptions: Pix: 2 of holes and tears in beet leaves.
DH017	H3,G3, D8, W3,w3, R1,r, V2,S1, C,P,T, Y3,A,a, O,Q2	0533084 4442075	Hail size: 0.5 in, some between 0.75 in and 1.0 in Hardness: Could hear them when they hit Ground coverage: Pretty well white Duration: 5-10 min. Hailed, then quit, then reversed itself and came back. Wind: Terribly windy. Wind probably caused more damage than hail. Rain: Rained a little bit. Rain gauge: No, got knocked over. Damage: Garden completely knocked out. Few dents on camper. Cucumber has no leaves left, had to pick off all tomatoes. Other descriptions: Has seen a lot worse. Pix:
DH019	H,G,D, W,w,R, r,V,S, C3,P, T,Y,A, a,O,Q2	0533207 4444980	Patches 400-500 feet across, circles of completely dead alfalfa.

Parker, CO Storm 7/10/02

Point	**Code**	**GPS**	Description
EP001	S300, H3,G3, D45, W2,w2, R3,r2, V2,S3, C,P,T3, Y3,A, a,I2,O, Q3	0527302 4368030	Hail size: 3.0 in Hardness: Hard, aggregate Ground coverage: Covered Duration: 45 min Wind: Fairly strong Rain: Lots Damage: Roof totaled, trees very damaged, deck paint chipped, flowers destroyed, car slightly dented.
EP002	H,G3, D45, W,w2, R,r,V, S3,C, P,T,	0526050 4368180	Hail size: 35 mm collected (probable shrinkage) Hardness: unknown Ground coverage: Covered Duration: 45 min Damage: 2 broken windows to W (direction from which wind was coming)

	Y,A, a,I2, O,Q2		Other descriptions: Complete white out, couldn't see shed in back through storm. Worse seen in 30 yrs.
EP003	H3,G3, D75, W2,w2, R3,r2, V,S3, C,P,T, Y3,A,a, I,O,Q2	0525739 4367971	Hail size: 0.5 in, 0.75 in, and 1.0 in Hardness: Very hard, some smashed, but not most. Ground coverage: Looked like snow storm. Piled up. Duration: 1hr to 1.5 hr. "Thought it would never stop" Wind: From S, SW (back of the house) Rain: Heavy, continued to rain all night after the hail stopped. Lake developed to E of house, some water still there when we were. Rain gauge: 2.8 in (neighbor's gauge) Damage: Lots: Stucco, screens, holes in both. Have called insurance co. Paint chipped on deck, knocked lights out in driveway. Plants demolished. Knocked holes in plastic on grill cover. Bucket with remotes floating, not sure if hole in roof or skylight. Paint chipped off from inside under skylights from hard impacts. Flowers stripped in hanging pots. Deck paint just redone in April/May, paint badly chipped and even peeled up in one area. Destroyed plastic sign at driveway entrance and water uprooted post. Other descriptions: Very loud, sounded like a gun. At Singing Hills and Delbert rain but no hail. "Never seen hail last like that." Pix: Screens, decks.
EP004	H,G3, D30, W2,w2, R3,r2, V,S3, C,P,T3, Y,A,a, O,Q2	0523911 4367384	Hail size: Majority marble sized, up to 2.0 in (between golf ball and 2.0 in) son reported pool ball sized, matched size of hole in screen. Hardness: unknown Ground coverage: Covered an in or 2, snow plows out, drifts. Duration: 30 min Wind: Noticeable wind (rated an 80 out of 100) Rain: Rained before and after, very heavy rain with hail. Rain gauge: no Damage: Pitted wood siding, badly torn screens, roof totaled, shingles cracked, gravel off roof, could smell pine immediately after storm. Basement window well filled up about 18-24 inches and leaked. Other descriptions: Most he's ever seen, hail still around 24 hours later. Helicopters overhead. Son reported hailstones coming down chimney. Pix: Screen on RH side, 2 other windows.

EP005	H3,G3, D,W2, w2,R1, r,V,S2, C,P,T, Y,A,a, I,O,Q2	0523599 4367301	Hail size: 0.5 in to 1.0 in Hardness: Hard Ground coverage: Total coverage, had to shovel deck, looked like snow. Duration: Not here for whole thing, so not sure. Wind: Lots of damage to N side of house, but damage all around. Rain: Mostly just hail Rain gauge: No Damage: Roof, deck paint, yard light, AC unit (coil and netting on outside). No screen damage. Runoff damage to back path. Other descriptions: Smaller stones as coming home, then large ones on deck. Worst in 8 years. Mainly S and E.
EP006	H2,G2, D90, W2,w2, R3,r, V1,S1, C,P,T, Y2,A, a,I,O, Q2	0521390 4368167	Hail size: A few 2.0 in Hardness: Bouncing and splattering, not hard frozen. Ground coverage: Filled gutters, did not look like snow. Duration: 1.5 hr total rain and hail Wind: Came in from SW and S Rain: Heavy Rain gauge: No Damage: No car damage, banged up flowers, no roof damage, no screens to get ripped. Other descriptions: Hailed 1st (harder), quit for a bit, slushy rain, then hail back again, then heavy rain.
EP007	H3,G3, D60, W1,w, R1,r, V2,S2, C,P,T, Y,A,a, I2,O, Q2	0524295 4369546	Hail size: Bet 1.0 in and 1.25 in Hardness: Bounced, held shape Ground coverage: White gound, no drifts, even coverage. Duration: 1 hr Wind: No wind Rain: No rain Rain gauge: No Damage: Not extensive damage. A few cracked shingles. Couple dents in hood of vehicle. Other descriptions: Worst storm ever seen. Has lived in CO all her life (80 yrs). Pix: Hailstone
EP008	H3,G3, D,W, w,R3,r, V,S3, C,P,T3, Y3,A,a,	0524419 4367979	Hail size: Golf ball, majority marble Hardness: Kept shape Ground coverage: Looked like snow Duration: unknown Wind: unknown Rain: Lot of rain (washed-out driveway)

	I,O,Q2		Rain gauge: No Damage: Ruined vegetable garden, damaged chimney, gutters, roof needs complete replacement, damaged trees, lots of leaves on ground. Pock marked. Most damage from rain runoff. Other descriptions: Got home 2 hours after storm, hail piled up in ditch by road at end of property. Pix: Leaf debris under tree
EP009	H3,G3, D45, W,w, R,r,V1, S2,C,P, T,Y3, A,a,I, O,Q2	0524571 4367655	Hail size: Golf ball Hardness: Probably less dense than stones from ~10 yrs ago. Ground coverage: Covered ground Duration: 45 min Wind: unknown Rain: unknown Rain gauge: no Damage: Lots of shingles on ground. No truck or trailer damage. Shredded vegetation. Other descriptions: Was not there during storm. Wife was there. Suggested we call her.
EP010	H3,G3, D60, W2,w, R3,r, V1,S2, C,P,T, Y,A,a, I,O,Q2	0525592 4366645	Hail size: 1.25 to 1.50 in Hardness: Kept shape, hard Ground coverage: Totally covered, snow plows were out.. Duration: 1 hr Wind: So so, came and went Rain: Yes, heavy Rain gauge: No Damage: Insurance says roof is fine. Roofer says it totaled. Shingles on ground after storm. Other descriptions: So heavy, couldn't see close-by tree. Worst storm she's seen in her life, been here 20+ years. Channel 9 truck drove thru. Might e-mail pictures from digital camera.
EP011	H3,G3, D45, W2,w2, R,r1, V,S2, C,P,T, Y3,A,a, I,O,Q2	0524576 4366871	Hail size: 1.25 to 1.5 in Hardness: Hard, bounced when hit Ground coverage: Totally covered, still some hail next day, some 2-3 days later in shaded areas. Duration: 45 min Wind: some Rain: Rain for 15 min, then just hail Rain gauge: no Damage: Roof leaking in 2 places, had to shovel off roof. Have called ins agent, haven't heard anything yet. Lost veggie garden and flowers. Most damage on NW side, damage from leaks.

			Other descriptions: Roof covered w/ 6 in of hail. One of the worst storms she's ever seen. Thought skylights and window might break Pix: Channel 4 interviewed her and filmed damage.
EP012	H3,G3, D60, W1,w2, R3,r3, V,S3, C,P,T, Y3,A,a, I,O,Q2	0524245 4367125	Hail size: 1.0 in and smaller Hardness: Bounced off roof, didn't smash Ground coverage: Accum in huge piles where ran off roof. Ground pretty much covered. Duration: 1 hr Wind: Absolutely none, but did hit W.ern side Rain: Very heavy after hail Rain gauge: No Damage: Damaged roof, destroyed garden. Very damaged screens (on W side), not quite as bad as the pool ball guy. Other descriptions: "Never seen anything like it."
EP013	H2,G3, D60, W2,w2, R3,r2, V2,S2, C,P,T2, Y3,A,a, I2,O, Q2	0524890 4366986	Hail size: Some 1.5in (mostly 1.25 in, lots of smaller ones) Hardness: Some kind of soft – aggregate. Not solid ice. Ground coverage: Whole back yard covered, very piled up in places, 8in drifts. Duration: 1 hr Wind: Yes, same from ~W Rain: With hail, lots of rain Rain gauge: No Damage: Loose shingles. Knocked lots of leaves off trees. Damaged ? leaves, mowed honeysuckle. Pit spots on deck uprights, dented lawn. Looked at car, saw dents and chipped plastic.
EP014	H3,G3, D60, W2,w, R3,r2, V,S2, C,P,T2, Y2,A,a, I,O,Q2	0528160 4368013	Hail size: 0.75 in to 1.0 in Hardness: Hard, smashed when hit hard surfaces. Ground coverage: Just about covered. No drifts. Duration: 2:30 pm, continued violently for ~1 hr. Wind: Lots of wind, gusting ~ 35-40 mph Rain: Water with hail at all times Rain gauge: 1.94 in of precip (hail and rain) in 1hr. Damage: Lost some paint. Beat up shingles. Perennial garden 25% damage, trees 10% damage. Other descriptions: Thought was gonna break windows. Very localized – parts of hills covered – white, parts not covered as visible from this location. Highly variable. 1000 ft away garden completely damaged.
EP015	H3,G1, D45,	0530262 4368097	Hail size: 1.0 in and smaller Hardness: Stayed solid

	W2,w3, R3,r1, V2,S2, C,P,T, Y,A,a, I,O,Q2		Ground coverage: Didn't cover ground. Not like snow. Duration: Rain for over an hour, hailing 75% of that time. Wind: Windy (10-20mph) Rain: Rain, then hail came, water in culvert Rain gauge: No Damage: Dented truck, bouncing off hood. Other descriptions: Could see it coming. Heard flash flood warning. Some shingle damage – inspector said just minor. Wind seemed more damaging than hail or rain.
EP016	H3,G1, D13, W2,w3, R3,r,V, S1,C, P,T,Y1, A,a,I, O,Q2	0531997 4368476	Hail size: 0.75 in Hardness: Kept shape, evaporated right away. Ground coverage: Not covered, scattered, melted quickly. Duration: 10-15 min Wind: Strong wind, blowing from SW, rain sideways at times. Rain: Heavy rain, big drops. Rain gauge: Heard 0.5 in Damage: No damage. Garden didn't take too much of a beating. Tomatoes fine. Other descriptions: Hail minor part.
EP017	H,G1, D5,W, w,R2, r,V,S1, C,P,T, Y,A,a, I,O,Q2	0534271 4366606	Hail size: 0.5 in Hardness: unknown Ground coverage: No coverage Duration: Few minutes (5 or so) Wind: Didn't notice Rain: Good rain, but dried up fast. Rain gauge: No Damage: No

Merino, CO Storm 8/24/02

Point	**Code**	**GPS**	Description
M005	H1,G1, D45, W2, w2, R3,r2, V1,S1, C1	0636369 4480731	Hail size: 0.5 in Hardness: Soft, smashed on impact Ground coverage: Not covered Wind: Strong out of S Rain: Heavy (with hail) Damage: None Other descriptions: Rotating lowered cloud base visible out of a north window

			When asked about neighbor's reports, woman said she was essentially at the west edge of the hail area.
M007	H3,G3, D13, W1, w1,R1, r2,V3, S3,T3, A2,Q2	0639695 4432895	Hail size: 0.75 to 1.5 in Hardness: Hard Ground coverage: Covered ground like snow Duration: 10 -15 min Wind: Not strong. Hail fell straight down Rain: Heavy (with hail) 1-3 in Damage: Considerable damage: broken windows in both homes and cars reported. Insurance adjusters found damage to roofs, RV's, air conditioners, etc. People of various ages were trying to get to the church basement (the local tornado shelter); several of them reported bruised skin from hailstone impacts. Other descriptions: Only worse storm experienced by the caretaker was a tornado that struck in the 1975-82 period. Pix: Digital camera pictures of broken house window, punctured rain gutters, and damaged trees in Merino
M009	R3,Q2	0646570 4489822	Hail size: No hail Hardness: No hail Ground coverage: No hail Duration: No hail Wind: From S, SW (back of the house) Rain: Heavy rain only
			Other descriptions: Note: Various intermediate GPS readings were stored while driving between the above points. Many of these were next to various corn fields. The degree of visible corn damage appeared to confirm that the primary hail swath was centered slightly east of Merino).
M013	H3,G1, D10, W2, R2,r2, S1,Y2, Q2	0655577 4444906 1	Hail size: Ping-pong ball Hardness: Hard Ground coverage: Sparse Duration: 10 min Wind: Strong N winds Rain: Some, with hail Damage: Only local damage was to garden plants; individual stone impacts tore leaves, etc, but not enough total stone impacts to destroy plants. No structural damage. Other descriptions: Heavier rain and more hail with second storm later that night.
M014	H3,G3,	0660322	Hail size: Golfball up to 2.5 in

	D20, W1,R1, r2,S3, T3,Y3, O2,Q2	4448438	Hardness: First stones soft, then quickly became hard. Ground coverage: Covered, looked like snow. Duration: 20 min Wind: Not strong, out of N Rain: Relatively little rain with hail Damage: Significant damage: roof to be inspected by insurance company. Attic ventilation fan damaged: outer housing dented down into path of the blades by hail impacts. Much leaf debris; garden destroyed. One window broken on he north side of the house. Other descriptions: Stones had somewhat elliptical shape (i.e., non-spherical). Also appeared that big stones were bumpy aggregates of smaller diameter stones. Hail diameters tapered off with time; ended up being pea sized at the end of the approx 20 minute duration hailfall period. Called worst storm since 1976.
M015	H1,G1, r2,Q2	0673838 4446643	Hail size: 0.5 in Hardness: Soft Ground coverage: Not covered Rain: Rain with hail Damage: None
M016	H3,G2, D20, W2,R3, r2,S3, O2,Q2	0664988 4446901	Hail size: Golf ball Hardness: High density Ground coverage: Almost covered ground Duration: Hail – 20 min, overall storm – 45 min Wind: Pretty windy Rain: Rain accompanied the hail, heaviest rain after the heaviest hail. Rain gauge: Rain gage reading the next AM was 2.5 inches, but this also included the early Sunday AM thunderstorm. Damage: Windows broken on neighbor's houses. Ison's roof to be checked, damage expected. Other descriptions: Stones from the freezer were smooth surfaced oblate spheres. Visual axis ratio roughly .8 Due to the large hailstone sizes, he described this as the worst hailstorm there in "quite a while".
M018	H3,r3, V3,S3, A2,Q2	0663643 4448856	Hail size: Golf ball to 1.75 in Hardness: High density hailstones, observed to bounce off of the ground. Rain: First 15 minutes of storm hail only, then it finally started to rain

			Damage: Hailstone impacts raised welts on the horse's hides Considerable damage: Screens broken; both house and car windows broken. Various running light lenses broken on Otis school bus parked at the house. Other descriptions: Called second worst hailstorm there in 35 years. The worst one was around 1966 / 67 when big, noticeably jagged hailstones fell. Pix: Digital camera picture of a car wind shield with considerable "spider web" cracking

Cheyenne, WY Storm 6/23/03

Point	**Code**	**GPS**	Description
CH001	G3,V2	521725 4542035	Hail size: Just under G-ball sized Ground coverage: Ground covered like snow Damage: Dented vehicles, panicked horses
CH002	G1,S1	528408 4543628	Hail size: Marble Ground coverage: Did not cover ground Damage: No damage
CH003	H1,G1, D20,S2	521845 4544166	Hail size: G-ball and ping pong ball selected Hardness: High density Ground coverage: Did not cover ground Duration: 20 min duration Damage: Damaged house
CH004	G1,V2	520582 4543644	Hail size: Measured 1 in collected stones from freezer. Ground coverage: Sparse ground coverage (one stone per 6 feet). Damage: Some vehicle dents, not calling insurance.
CH005	S3	533127 4551137	Hail size: Ping pong ball; also photographed stones from freezer. Many in 1.5 inch diameter range, some w/ bumpy shapes. Damage: Insurance reports roof total loss.
CH006	T3,V3	529063 4555695	Hail size: 1.25 in wooden ball and red ball (.8 in) selected. Damage: Insurance estimate of $3.7K damage to pickup parked at the site. Significant leaf deposits below trees. Other descriptions: Observer reached site just at the end of the event.
CH007	H1,G3, S2	543658 4562502	Hail size: 1 inch ball selected Hardness: High density

			Ground coverage: Ground covered Damage: Broke vents in trailer roof, some stripped paint on backyard objects.
CH008	G1,V2	544823 4563683	Hail size: 1 inch max dia. Ground coverage: Sporadic ground coverage Damage: Slight vehicle damage at this location. Definite vehicle damage and complete ground coverage at house which he pointed out to the south. (This house turned out to be approx ½ mile N of survey point #7). Other descriptions: Observer was at south house when storm #1 hit. He moved to point 8 before storm 2 hit. Hail diameters were pea to marble in storm 2, and hail ground coverage was eventually achieved. Wheat damage patterns suggested hail severity decreased significantly between Hillsdale (pt 7) and this location (pt 8).
CH009	G3,V3	540638 4556558	Hail size: G-ball selected. Ground coverage: Hail covered ground like snow. Damage: Watched rear car window shatter, also punctured shutters on his trailer. (They appeared to be quite flimsy).

APPENDIX C

Table C.1 Statistical results for all HQP and hail size thresholds.

HQP Thresh	Hail Size (in)	Hits	False Alarms	Misses	Nulls	POD	FAR	CSI	HSS	TSS
0	0.25	85	9	0	0	1.000	0.096	0.904	0.000	0.000
0.1	0.25	73	3	12	6	0.859	0.039	0.830	0.363	0.525
0.2	0.25	70	2	15	7	0.824	0.028	0.805	0.365	0.601
0.3	0.25	69	1	16	8	0.812	0.014	0.802	0.402	0.701
0.4	0.25	66	1	19	8	0.776	0.015	0.767	0.351	0.665
0.5	0.25	59	1	26	8	0.694	0.017	0.686	0.260	0.583
0.6	0.25	51	1	34	8	0.600	0.019	0.593	0.185	0.489
0.7	0.25	36	1	49	8	0.424	0.027	0.419	0.092	0.312
0.8	0.25	21	1	64	8	0.247	0.045	0.244	0.033	0.136
0.9	0.25	11	0	74	9	0.129	0.000	0.129	0.028	0.129
1	0.25	2	0	83	9	0.024	0.000	0.024	0.005	0.024
0	0.5	77	17	0	0	1.000	0.181	0.819	0.000	0.000
0.1	0.5	68	8	9	9	0.883	0.105	0.800	0.403	0.413
0.2	0.5	65	7	12	10	0.844	0.097	0.774	0.388	0.432
0.3	0.5	64	6	13	11	0.831	0.086	0.771	0.412	0.478
0.4	0.5	62	5	15	12	0.805	0.075	0.756	0.416	0.511
0.5	0.5	55	5	22	12	0.714	0.083	0.671	0.302	0.420
0.6	0.5	50	2	27	15	0.649	0.038	0.633	0.338	0.532
0.7	0.5	36	1	41	16	0.468	0.027	0.462	0.213	0.409
0.8	0.5	21	1	56	16	0.273	0.045	0.269	0.095	0.214
0.9	0.5	11	0	66	17	0.143	0.000	0.143	0.057	0.143
1	0.5	2	0	75	17	0.026	0.000	0.026	0.010	0.026
0	0.75	60	34	0	0	1.000	0.362	0.638	0.000	0.000
0.1	0.75	56	20	4	14	0.933	0.263	0.700	0.384	0.345
0.2	0.75	55	17	5	17	0.917	0.236	0.714	0.451	0.417
0.3	0.75	54	16	6	18	0.900	0.229	0.711	0.459	0.429
0.4	0.75	54	13	6	21	0.900	0.194	0.740	0.542	0.518
0.5	0.75	50	10	10	24	0.833	0.167	0.714	0.539	0.539
0.6	0.75	46	6	14	28	0.767	0.115	0.697	0.562	0.590
0.7	0.75	35	2	25	32	0.583	0.054	0.565	0.457	0.525
0.8	0.75	20	2	40	32	0.333	0.091	0.323	0.221	0.275
0.9	0.75	11	0	49	34	0.183	0.000	0.183	0.140	0.183
1	0.75	2	0	58	34	0.033	0.000	0.033	0.024	0.033
0	1	47	47	0	0	1.000	0.500	0.500	0.000	0.000
0.1	1	46	30	1	17	0.979	0.395	0.597	0.340	0.340

0.2	1	45	27	2	20	0.957	0.375	0.608	0.383	0.383
0.3	1	44	26	3	21	0.936	0.371	0.603	0.383	0.383
0.4	1	44	23	3	24	0.936	0.343	0.629	0.447	0.447
0.5	1	41	19	6	28	0.872	0.317	0.621	0.468	0.468
0.6	1	39	13	8	34	0.830	0.250	0.650	0.553	0.553
0.7	1	30	7	17	40	0.638	0.189	0.556	0.489	0.489
0.8	1	17	5	30	42	0.362	0.227	0.327	0.255	0.255
0.9	1	10	1	37	46	0.213	0.091	0.208	0.191	0.191
1	1	2	0	45	47	0.043	0.000	0.043	0.043	0.043
0	1.25	31	63	0	0	1.000	0.670	0.330	0.000	0.000
0.1	1.25	31	45	0	18	1.000	0.592	0.408	0.209	0.286
0.2	1.25	31	41	0	22	1.000	0.569	0.431	0.261	0.349
0.3	1.25	31	39	0	24	1.000	0.557	0.443	0.289	0.381
0.4	1.25	31	36	0	27	1.000	0.537	0.463	0.331	0.429
0.5	1.25	31	29	0	34	1.000	0.483	0.517	0.436	0.540
0.6	1.25	30	22	1	41	0.968	0.423	0.566	0.528	0.619
0.7	1.25	25	12	6	51	0.806	0.324	0.581	0.587	0.616
0.8	1.25	13	9	18	54	0.419	0.409	0.325	0.299	0.277
0.9	1.25	9	2	22	61	0.290	0.182	0.273	0.309	0.259
1	1.25	2	0	29	63	0.065	0.000	0.065	0.085	0.065
0	1.5	26	68	0	0	1.000	0.723	0.277	0.000	0.000
0.1	1.5	26	50	0	18	1.000	0.658	0.342	0.166	0.265
0.2	1.5	26	46	0	22	1.000	0.639	0.361	0.209	0.324
0.3	1.5	26	44	0	24	1.000	0.629	0.371	0.232	0.353
0.4	1.5	26	41	0	27	1.000	0.612	0.388	0.267	0.397
0.5	1.5	26	34	0	34	1.000	0.567	0.433	0.356	0.500
0.6	1.5	26	26	0	42	1.000	0.500	0.500	0.472	0.618
0.7	1.5	21	16	5	52	0.808	0.432	0.500	0.506	0.572
0.8	1.5	12	10	14	58	0.462	0.455	0.333	0.330	0.314
0.9	1.5	9	2	17	66	0.346	0.182	0.321	0.385	0.317
1	1.5	2	0	24	68	0.077	0.000	0.077	0.108	0.077
0	1.75	8	86	0	0	1.000	0.915	0.085	0.000	0.000
0.1	1.75	8	68	0	18	1.000	0.895	0.105	0.043	0.209
0.2	1.75	8	64	0	22	1.000	0.889	0.111	0.055	0.256
0.3	1.75	8	62	0	24	1.000	0.886	0.114	0.062	0.279
0.4	1.75	8	59	0	27	1.000	0.881	0.119	0.072	0.314
0.5	1.75	8	52	0	34	1.000	0.867	0.133	0.100	0.395
0.6	1.75	8	44	0	42	1.000	0.846	0.154	0.140	0.488
0.7	1.75	7	30	1	56	0.875	0.811	0.184	0.199	0.526
0.8	1.75	6	16	2	70	0.750	0.727	0.250	0.314	0.564
0.9	1.75	4	7	4	79	0.500	0.636	0.267	0.358	0.419
1	1.75	2	0	6	86	0.250	0.000	0.250	0.379	0.250
0	2	7	87	0	0	1.000	0.926	0.074	0.000	0.000
0.1	2	7	69	0	18	1.000	0.908	0.092	0.037	0.207
0.2	2	7	65	0	22	1.000	0.903	0.097	0.048	0.253
0.3	2	7	63	0	24	1.000	0.900	0.100	0.054	0.276
0.4	2	7	60	0	27	1.000	0.896	0.104	0.063	0.310
0.5	2	7	53	0	34	1.000	0.883	0.117	0.087	0.391

0.6	2	7	45	0	42	1.000	0.865	0.135	0.122	0.483
0.7	2	6	31	1	56	0.857	0.838	0.158	0.169	0.501
0.8	2	5	17	2	70	0.714	0.773	0.208	0.261	0.519
0.9	2	4	7	3	80	0.571	0.636	0.286	0.389	0.491
1	2	2	0	5	87	0.286	0.000	0.286	0.425	0.286

Table C.2 Statistical results for all H_{dr} and hail size thresholds.

Hdr Thresh	Hail Size (in)	Hits	False Alarms	Misses	Nulls	POD	FAR	CSI	HSS	TSS
0	0.25	80	4	5	5	0.941	0.048	0.899	0.473	0.497
1	0.25	79	3	6	6	0.929	0.037	0.898	0.519	0.596
2	0.25	79	3	6	6	0.929	0.037	0.898	0.519	0.596
3	0.25	78	3	7	6	0.918	0.037	0.886	0.487	0.584
4	0.25	77	3	8	6	0.906	0.038	0.875	0.459	0.573
5	0.25	76	3	9	6	0.894	0.038	0.864	0.432	0.561
6	0.25	74	3	11	6	0.871	0.039	0.841	0.384	0.537
7	0.25	74	3	11	6	0.871	0.039	0.841	0.384	0.537
8	0.25	74	3	11	6	0.871	0.039	0.841	0.384	0.537
9	0.25	74	3	11	6	0.871	0.039	0.841	0.384	0.537
10	0.25	74	3	11	6	0.871	0.039	0.841	0.384	0.537
11	0.25	72	2	13	7	0.847	0.027	0.828	0.404	0.625
12	0.25	72	2	13	7	0.847	0.027	0.828	0.404	0.625
13	0.25	71	2	14	7	0.835	0.027	0.816	0.384	0.613
14	0.25	70	2	15	7	0.824	0.028	0.805	0.365	0.601
15	0.25	68	2	17	7	0.800	0.029	0.782	0.331	0.578
16	0.25	67	2	18	7	0.788	0.029	0.770	0.315	0.566
17	0.25	65	2	20	7	0.765	0.030	0.747	0.286	0.542
18	0.25	65	2	20	7	0.765	0.030	0.747	0.286	0.542
19	0.25	65	2	20	7	0.765	0.030	0.747	0.286	0.542
20	0.25	63	2	22	7	0.741	0.031	0.724	0.260	0.519
21	0.25	62	1	23	8	0.729	0.016	0.721	0.295	0.618
22	0.25	58	1	27	8	0.682	0.017	0.674	0.249	0.571
23	0.25	55	1	30	8	0.647	0.018	0.640	0.220	0.536
24	0.25	53	1	32	8	0.624	0.019	0.616	0.202	0.512
25	0.25	51	1	34	8	0.600	0.019	0.593	0.185	0.489
26	0.25	48	1	37	8	0.565	0.020	0.558	0.163	0.454
27	0.25	43	1	42	8	0.506	0.023	0.500	0.130	0.395
28	0.25	40	1	45	8	0.471	0.024	0.465	0.113	0.359
29	0.25	37	0	48	9	0.435	0.000	0.435	0.129	0.435
30	0.25	35	0	50	9	0.412	0.000	0.412	0.118	0.412
31	0.25	33	0	52	9	0.388	0.000	0.388	0.108	0.388
32	0.25	32	0	53	9	0.376	0.000	0.376	0.104	0.376
33	0.25	26	0	59	9	0.306	0.000	0.306	0.078	0.306
34	0.25	26	0	59	9	0.306	0.000	0.306	0.078	0.306
35	0.25	25	0	60	9	0.294	0.000	0.294	0.074	0.294

0	0.5	74	10	3	7	0.961	0.119	0.851	0.444	0.373
1	0.5	73	9	4	8	0.948	0.110	0.849	0.473	0.419
2	0.5	73	9	4	8	0.948	0.110	0.849	0.473	0.419
3	0.5	72	9	5	8	0.935	0.111	0.837	0.447	0.406
4	0.5	71	9	6	8	0.922	0.113	0.826	0.422	0.393
5	0.5	70	9	7	8	0.909	0.114	0.814	0.398	0.380
6	0.5	68	9	9	8	0.883	0.117	0.791	0.354	0.354
7	0.5	68	9	9	8	0.883	0.117	0.791	0.354	0.354
8	0.5	68	9	9	8	0.883	0.117	0.791	0.354	0.354
9	0.5	68	9	9	8	0.883	0.117	0.791	0.354	0.354
10	0.5	68	9	9	8	0.883	0.117	0.791	0.354	0.354
11	0.5	66	8	11	9	0.857	0.108	0.776	0.362	0.387
12	0.5	66	8	11	9	0.857	0.108	0.776	0.362	0.387
13	0.5	65	8	12	9	0.844	0.110	0.765	0.342	0.374
14	0.5	64	8	13	9	0.831	0.111	0.753	0.324	0.361
15	0.5	62	8	15	9	0.805	0.114	0.729	0.288	0.335
16	0.5	61	8	16	9	0.792	0.116	0.718	0.272	0.322
17	0.5	60	7	17	10	0.779	0.104	0.714	0.299	0.367
18	0.5	60	7	17	10	0.779	0.104	0.714	0.299	0.367
19	0.5	60	7	17	10	0.779	0.104	0.714	0.299	0.367
20	0.5	59	6	18	11	0.766	0.092	0.711	0.324	0.413
21	0.5	58	5	19	12	0.753	0.079	0.707	0.348	0.459
22	0.5	54	5	23	12	0.701	0.085	0.659	0.288	0.407
23	0.5	51	5	26	12	0.662	0.089	0.622	0.249	0.368
24	0.5	49	5	28	12	0.636	0.093	0.598	0.224	0.342
25	0.5	47	5	30	12	0.610	0.096	0.573	0.201	0.316
26	0.5	46	3	31	14	0.597	0.061	0.575	0.256	0.421
27	0.5	42	2	35	15	0.545	0.045	0.532	0.244	0.428
28	0.5	39	2	38	15	0.506	0.049	0.494	0.213	0.389
29	0.5	37	0	40	17	0.481	0.000	0.481	0.251	0.481
30	0.5	35	0	42	17	0.455	0.000	0.455	0.232	0.455
31	0.5	33	0	44	17	0.429	0.000	0.429	0.213	0.429
32	0.5	32	0	45	17	0.416	0.000	0.416	0.205	0.416
33	0.5	26	0	51	17	0.338	0.000	0.338	0.156	0.338
34	0.5	26	0	51	17	0.338	0.000	0.338	0.156	0.338
35	0.5	25	0	52	17	0.325	0.000	0.325	0.148	0.325
0	0.75	59	25	1	9	0.983	0.298	0.694	0.293	0.248
1	0.75	59	23	1	11	0.983	0.280	0.711	0.357	0.307
2	0.75	59	23	1	11	0.983	0.280	0.711	0.357	0.307
3	0.75	59	22	1	12	0.983	0.272	0.720	0.388	0.336
4	0.75	58	22	2	12	0.967	0.275	0.707	0.366	0.320
5	0.75	57	22	3	12	0.950	0.278	0.695	0.345	0.303
6	0.75	56	21	4	13	0.933	0.273	0.691	0.354	0.316
7	0.75	56	21	4	13	0.933	0.273	0.691	0.354	0.316
8	0.75	56	21	4	13	0.933	0.273	0.691	0.354	0.316
9	0.75	56	21	4	13	0.933	0.273	0.691	0.354	0.316

10	0.75	56	21	4	13	0.933	0.273	0.691	0.354	0.316
11	0.75	55	19	5	15	0.917	0.257	0.696	0.393	0.358
12	0.75	55	19	5	15	0.917	0.257	0.696	0.393	0.358
13	0.75	55	18	5	16	0.917	0.247	0.705	0.422	0.387
14	0.75	54	18	6	16	0.900	0.250	0.692	0.401	0.371
15	0.75	53	17	7	17	0.883	0.243	0.688	0.409	0.383
16	0.75	53	16	7	18	0.883	0.232	0.697	0.438	0.413
17	0.75	53	14	7	20	0.883	0.209	0.716	0.494	0.472
18	0.75	53	14	7	20	0.883	0.209	0.716	0.494	0.472
19	0.75	53	14	7	20	0.883	0.209	0.716	0.494	0.472
20	0.75	52	13	8	21	0.867	0.200	0.712	0.500	0.484
21	0.75	52	11	8	23	0.867	0.175	0.732	0.554	0.543
22	0.75	50	9	10	25	0.833	0.153	0.725	0.565	0.569
23	0.75	47	9	13	25	0.783	0.161	0.681	0.506	0.519
24	0.75	46	8	14	26	0.767	0.148	0.676	0.512	0.531
25	0.75	45	7	15	27	0.750	0.135	0.672	0.518	0.544
26	0.75	44	5	16	29	0.733	0.102	0.677	0.548	0.586
27	0.75	41	3	19	31	0.683	0.068	0.651	0.540	0.595
28	0.75	38	3	22	31	0.633	0.073	0.603	0.486	0.545
29	0.75	36	1	24	33	0.600	0.027	0.590	0.498	0.571
30	0.75	35	0	25	34	0.583	0.000	0.583	0.503	0.583
31	0.75	33	0	27	34	0.550	0.000	0.550	0.469	0.550
32	0.75	32	0	28	34	0.533	0.000	0.533	0.453	0.533
33	0.75	26	0	34	34	0.433	0.000	0.433	0.356	0.433
34	0.75	26	0	34	34	0.433	0.000	0.433	0.356	0.433
35	0.75	25	0	35	34	0.417	0.000	0.417	0.341	0.417
0	1	47	37	0	10	1.000	0.440	0.560	0.213	0.213
1	1	47	35	0	12	1.000	0.427	0.573	0.255	0.255
2	1	47	35	0	12	1.000	0.427	0.573	0.255	0.255
3	1	47	34	0	13	1.000	0.420	0.580	0.277	0.277
4	1	47	33	0	14	1.000	0.413	0.588	0.298	0.298
5	1	47	32	0	15	1.000	0.405	0.595	0.319	0.319
6	1	46	31	1	16	0.979	0.403	0.590	0.319	0.319
7	1	46	31	1	16	0.979	0.403	0.590	0.319	0.319
8	1	46	31	1	16	0.979	0.403	0.590	0.319	0.319
9	1	46	31	1	16	0.979	0.403	0.590	0.319	0.319
10	1	46	31	1	16	0.979	0.403	0.590	0.319	0.319
11	1	45	29	2	18	0.957	0.392	0.592	0.340	0.340
12	1	45	29	2	18	0.957	0.392	0.592	0.340	0.340
13	1	45	28	2	19	0.957	0.384	0.600	0.362	0.362
14	1	44	28	3	19	0.936	0.389	0.587	0.340	0.340
15	1	43	27	4	20	0.915	0.386	0.581	0.340	0.340
16	1	43	26	4	21	0.915	0.377	0.589	0.362	0.362
17	1	43	24	4	23	0.915	0.358	0.606	0.404	0.404
18	1	43	24	4	23	0.915	0.358	0.606	0.404	0.404
19	1	43	24	4	23	0.915	0.358	0.606	0.404	0.404

20	1	43	22	4	25	0.915	0.338	0.623	0.447	0.447
21	1	43	20	4	27	0.915	0.317	0.642	0.489	0.489
22	1	41	18	6	29	0.872	0.305	0.631	0.489	0.489
23	1	39	17	8	30	0.830	0.304	0.609	0.468	0.468
24	1	38	16	9	31	0.809	0.296	0.603	0.468	0.468
25	1	37	15	10	32	0.787	0.288	0.597	0.468	0.468
26	1	36	13	11	34	0.766	0.265	0.600	0.489	0.489
27	1	34	10	13	37	0.723	0.227	0.596	0.511	0.511
28	1	32	9	15	38	0.681	0.220	0.571	0.489	0.489
29	1	31	6	16	41	0.660	0.162	0.585	0.532	0.532
30	1	30	5	17	42	0.638	0.143	0.577	0.532	0.532
31	1	29	4	18	43	0.617	0.121	0.569	0.532	0.532
32	1	28	4	19	43	0.596	0.125	0.549	0.511	0.511
33	1	25	1	22	46	0.532	0.038	0.521	0.511	0.511
34	1	25	1	22	46	0.532	0.038	0.521	0.511	0.511
35	1	24	1	23	46	0.511	0.040	0.500	0.489	0.489
0	1.25	31	53	0	10	1.000	0.631	0.369	0.111	0.159
1	1.25	31	51	0	12	1.000	0.622	0.378	0.134	0.190
2	1.25	31	51	0	12	1.000	0.622	0.378	0.134	0.190
3	1.25	31	50	0	13	1.000	0.617	0.383	0.146	0.206
4	1.25	31	49	0	14	1.000	0.613	0.388	0.159	0.222
5	1.25	31	48	0	15	1.000	0.608	0.392	0.171	0.238
6	1.25	31	46	0	17	1.000	0.597	0.403	0.196	0.270
7	1.25	31	46	0	17	1.000	0.597	0.403	0.196	0.270
8	1.25	31	46	0	17	1.000	0.597	0.403	0.196	0.270
9	1.25	31	46	0	17	1.000	0.597	0.403	0.196	0.270
10	1.25	31	46	0	17	1.000	0.597	0.403	0.196	0.270
11	1.25	31	43	0	20	1.000	0.581	0.419	0.235	0.317
12	1.25	31	43	0	20	1.000	0.581	0.419	0.235	0.317
13	1.25	31	42	0	21	1.000	0.575	0.425	0.248	0.333
14	1.25	31	41	0	22	1.000	0.569	0.431	0.261	0.349
15	1.25	30	40	1	23	0.968	0.571	0.423	0.252	0.333
16	1.25	30	39	1	24	0.968	0.565	0.429	0.266	0.349
17	1.25	30	37	1	26	0.968	0.552	0.441	0.294	0.380
18	1.25	30	37	1	26	0.968	0.552	0.441	0.294	0.380
19	1.25	30	37	1	26	0.968	0.552	0.441	0.294	0.380
20	1.25	30	35	1	28	0.968	0.538	0.455	0.322	0.412
21	1.25	30	33	1	30	0.968	0.524	0.469	0.352	0.444
22	1.25	30	29	1	34	0.968	0.492	0.500	0.413	0.507
23	1.25	30	26	1	37	0.968	0.464	0.526	0.461	0.555
24	1.25	29	25	2	38	0.935	0.463	0.518	0.453	0.539
25	1.25	28	24	3	39	0.903	0.462	0.509	0.446	0.522
26	1.25	27	22	4	41	0.871	0.449	0.509	0.455	0.522
27	1.25	25	19	6	44	0.806	0.432	0.500	0.456	0.505
28	1.25	24	17	7	46	0.774	0.415	0.500	0.466	0.504
29	1.25	23	14	8	49	0.742	0.378	0.511	0.495	0.520

30	1.25	23	12	8	51	0.742	0.343	0.535	0.534	0.551
31	1.25	22	11	9	52	0.710	0.333	0.524	0.526	0.535
32	1.25	22	10	9	53	0.710	0.313	0.537	0.546	0.551
33	1.25	19	7	12	56	0.613	0.269	0.500	0.523	0.502
34	1.25	19	7	12	56	0.613	0.269	0.500	0.523	0.502
35	1.25	18	7	13	56	0.581	0.280	0.474	0.494	0.470
0	1.5	26	58	0	10	1.000	0.690	0.310	0.087	0.147
1	1.5	26	56	0	12	1.000	0.683	0.317	0.106	0.176
2	1.5	26	56	0	12	1.000	0.683	0.317	0.106	0.176
3	1.5	26	55	0	13	1.000	0.679	0.321	0.116	0.191
4	1.5	26	54	0	14	1.000	0.675	0.325	0.125	0.206
5	1.5	26	53	0	15	1.000	0.671	0.329	0.135	0.221
6	1.5	26	51	0	17	1.000	0.662	0.338	0.156	0.250
7	1.5	26	51	0	17	1.000	0.662	0.338	0.156	0.250
8	1.5	26	51	0	17	1.000	0.662	0.338	0.156	0.250
9	1.5	26	51	0	17	1.000	0.662	0.338	0.156	0.250
10	1.5	26	51	0	17	1.000	0.662	0.338	0.156	0.250
11	1.5	26	48	0	20	1.000	0.649	0.351	0.187	0.294
12	1.5	26	48	0	20	1.000	0.649	0.351	0.187	0.294
13	1.5	26	47	0	21	1.000	0.644	0.356	0.198	0.309
14	1.5	26	46	0	22	1.000	0.639	0.361	0.209	0.324
15	1.5	25	45	1	23	0.962	0.643	0.352	0.197	0.300
16	1.5	25	44	1	24	0.962	0.638	0.357	0.208	0.314
17	1.5	25	42	1	26	0.962	0.627	0.368	0.231	0.344
18	1.5	25	42	1	26	0.962	0.627	0.368	0.231	0.344
19	1.5	25	42	1	26	0.962	0.627	0.368	0.231	0.344
20	1.5	25	40	1	28	0.962	0.615	0.379	0.255	0.373
21	1.5	25	38	1	30	0.962	0.603	0.391	0.280	0.403
22	1.5	25	34	1	34	0.962	0.576	0.417	0.332	0.462
23	1.5	25	31	1	37	0.962	0.554	0.439	0.373	0.506
24	1.5	24	30	2	38	0.923	0.556	0.429	0.362	0.482
25	1.5	24	28	2	40	0.923	0.538	0.444	0.391	0.511
26	1.5	23	26	3	42	0.885	0.531	0.442	0.394	0.502
27	1.5	21	23	5	45	0.808	0.523	0.429	0.387	0.469
28	1.5	20	21	6	47	0.769	0.512	0.426	0.391	0.460
29	1.5	20	17	6	51	0.769	0.459	0.465	0.459	0.519
30	1.5	20	15	6	53	0.769	0.429	0.488	0.496	0.549
31	1.5	20	13	6	55	0.769	0.394	0.513	0.534	0.578
32	1.5	20	12	6	56	0.769	0.375	0.526	0.553	0.593
33	1.5	17	9	9	59	0.654	0.346	0.486	0.521	0.521
34	1.5	17	9	9	59	0.654	0.346	0.486	0.521	0.521
35	1.5	16	9	10	59	0.615	0.360	0.457	0.489	0.483
0	1.75	8	76	0	10	1.000	0.905	0.095	0.022	0.116
1	1.75	8	74	0	12	1.000	0.902	0.098	0.027	0.140
2	1.75	8	74	0	12	1.000	0.902	0.098	0.027	0.140
3	1.75	8	73	0	13	1.000	0.901	0.099	0.029	0.151

4	1.75	8	72	0	14	1.000	0.900	0.100	0.032	0.163
5	1.75	8	71	0	15	1.000	0.899	0.101	0.035	0.174
6	1.75	8	69	0	17	1.000	0.896	0.104	0.040	0.198
7	1.75	8	69	0	17	1.000	0.896	0.104	0.040	0.198
8	1.75	8	69	0	17	1.000	0.896	0.104	0.040	0.198
9	1.75	8	69	0	17	1.000	0.896	0.104	0.040	0.198
10	1.75	8	69	0	17	1.000	0.896	0.104	0.040	0.198
11	1.75	8	66	0	20	1.000	0.892	0.108	0.049	0.233
12	1.75	8	66	0	20	1.000	0.892	0.108	0.049	0.233
13	1.75	8	65	0	21	1.000	0.890	0.110	0.052	0.244
14	1.75	8	64	0	22	1.000	0.889	0.111	0.055	0.256
15	1.75	8	62	0	24	1.000	0.886	0.114	0.062	0.279
16	1.75	8	61	0	25	1.000	0.884	0.116	0.065	0.291
17	1.75	8	59	0	27	1.000	0.881	0.119	0.072	0.314
18	1.75	8	59	0	27	1.000	0.881	0.119	0.072	0.314
19	1.75	8	59	0	27	1.000	0.881	0.119	0.072	0.314
20	1.75	8	57	0	29	1.000	0.877	0.123	0.080	0.337
21	1.75	8	55	0	31	1.000	0.873	0.127	0.088	0.360
22	1.75	8	51	0	35	1.000	0.864	0.136	0.105	0.407
23	1.75	8	48	0	38	1.000	0.857	0.143	0.119	0.442
24	1.75	8	46	0	40	1.000	0.852	0.148	0.129	0.465
25	1.75	8	44	0	42	1.000	0.846	0.154	0.140	0.488
26	1.75	8	41	0	45	1.000	0.837	0.163	0.157	0.523
27	1.75	8	36	0	50	1.000	0.818	0.182	0.191	0.581
28	1.75	8	33	0	53	1.000	0.805	0.195	0.215	0.616
29	1.75	8	29	0	57	1.000	0.784	0.216	0.251	0.663
30	1.75	8	27	0	59	1.000	0.771	0.229	0.271	0.686
31	1.75	8	25	0	61	1.000	0.758	0.242	0.293	0.709
32	1.75	8	24	0	62	1.000	0.750	0.250	0.305	0.721
33	1.75	7	19	1	67	0.875	0.731	0.259	0.324	0.654
34	1.75	7	19	1	67	0.875	0.731	0.259	0.324	0.654
35	1.75	6	19	2	67	0.750	0.760	0.222	0.269	0.529
0	2	7	77	0	10	1.000	0.917	0.083	0.019	0.115
1	2	7	75	0	12	1.000	0.915	0.085	0.023	0.138
2	2	7	75	0	12	1.000	0.915	0.085	0.023	0.138
3	2	7	74	0	13	1.000	0.914	0.086	0.025	0.149
4	2	7	73	0	14	1.000	0.913	0.088	0.028	0.161
5	2	7	72	0	15	1.000	0.911	0.089	0.030	0.172
6	2	7	70	0	17	1.000	0.909	0.091	0.035	0.195
7	2	7	70	0	17	1.000	0.909	0.091	0.035	0.195
8	2	7	70	0	17	1.000	0.909	0.091	0.035	0.195
9	2	7	70	0	17	1.000	0.909	0.091	0.035	0.195
10	2	7	70	0	17	1.000	0.909	0.091	0.035	0.195
11	2	7	67	0	20	1.000	0.905	0.095	0.043	0.230
12	2	7	67	0	20	1.000	0.905	0.095	0.043	0.230
13	2	7	66	0	21	1.000	0.904	0.096	0.045	0.241

14	2	7	65	0	22	1.000	0.903	0.097	0.048	0.253
15	2	7	63	0	24	1.000	0.900	0.100	0.054	0.276
16	2	7	62	0	25	1.000	0.899	0.101	0.057	0.287
17	2	7	60	0	27	1.000	0.896	0.104	0.063	0.310
18	2	7	60	0	27	1.000	0.896	0.104	0.063	0.310
19	2	7	60	0	27	1.000	0.896	0.104	0.063	0.310
20	2	7	58	0	29	1.000	0.892	0.108	0.069	0.333
21	2	7	56	0	31	1.000	0.889	0.111	0.076	0.356
22	2	7	52	0	35	1.000	0.881	0.119	0.091	0.402
23	2	7	49	0	38	1.000	0.875	0.125	0.104	0.437
24	2	7	47	0	40	1.000	0.870	0.130	0.112	0.460
25	2	7	45	0	42	1.000	0.865	0.135	0.122	0.483
26	2	7	42	0	45	1.000	0.857	0.143	0.138	0.517
27	2	7	37	0	50	1.000	0.841	0.159	0.168	0.575
28	2	7	34	0	53	1.000	0.829	0.171	0.188	0.609
29	2	7	30	0	57	1.000	0.811	0.189	0.221	0.655
30	2	7	28	0	59	1.000	0.800	0.200	0.239	0.678
31	2	7	26	0	61	1.000	0.788	0.212	0.259	0.701
32	2	7	25	0	62	1.000	0.781	0.219	0.270	0.713
33	2	6	20	1	67	0.857	0.769	0.222	0.279	0.627
34	2	6	20	1	67	0.857	0.769	0.222	0.279	0.627
35	2	5	20	2	67	0.714	0.800	0.185	0.222	0.484

Table C.3 Statistical results for all HQP and H_{dr} with respect to damage

HQP/H_{dr} Thresh	Hits	False Alarms	Misses	Nulls	POD	FAR	CSI	HSS	TSS
0	50	36	0	0	1	0.419	0.581	0.000	0.000
0.1	50	21	0	15	1	0.296	0.704	0.454	0.417
0.2	49	19	1	17	0.98	0.279	0.710	0.486	0.452
0.3	49	18	1	18	0.98	0.269	0.721	0.514	0.480
0.4	49	15	1	21	0.98	0.234	0.754	0.596	0.563
0.5	46	11	4	25	0.92	0.193	0.754	0.632	0.614
0.6	45	8	5	28	0.9	0.151	0.776	0.686	0.678
0.7	36	5	14	31	0.72	0.122	0.655	0.561	0.581
0.8	23	3	27	33	0.46	0.115	0.434	0.345	0.377
0.9	13	1	37	35	0.26	0.071	0.255	0.204	0.232
1	4	1	46	35	0.08	0.200	0.078	0.044	0.052
20	47	14	3	22	0.94	0.230	0.734	0.576	0.551
21	47	12	3	24	0.94	0.203	0.758	0.629	0.607
22	46	10	4	26	0.92	0.179	0.767	0.658	0.642
23	44	9	6	27	0.88	0.170	0.746	0.637	0.630
24	43	9	7	27	0.86	0.173	0.729	0.615	0.610
25	42	8	8	28	0.84	0.160	0.724	0.618	0.618

26	41	7	9	29	0.82	0.146	0.719	0.621	0.626
27	39	5	11	31	0.78	0.114	0.709	0.626	0.641
28	38	4	12	32	0.76	0.095	0.704	0.629	0.649
29	37	2	13	34	0.74	0.051	0.712	0.656	0.684
30	36	2	14	34	0.72	0.053	0.692	0.635	0.664
31	34	2	16	34	0.68	0.056	0.654	0.592	0.624
32	33	1	17	35	0.66	0.029	0.647	0.595	0.632
33	29	0	21	36	0.58	0.000	0.580	0.536	0.580
34	29	0	21	36	0.58	0.000	0.580	0.536	0.580
35	27	0	23	36	0.54	0.000	0.540	0.496	0.540

Graphs showing skill score values for both HQP and H_{dr} for several hail size thresholds.

a)

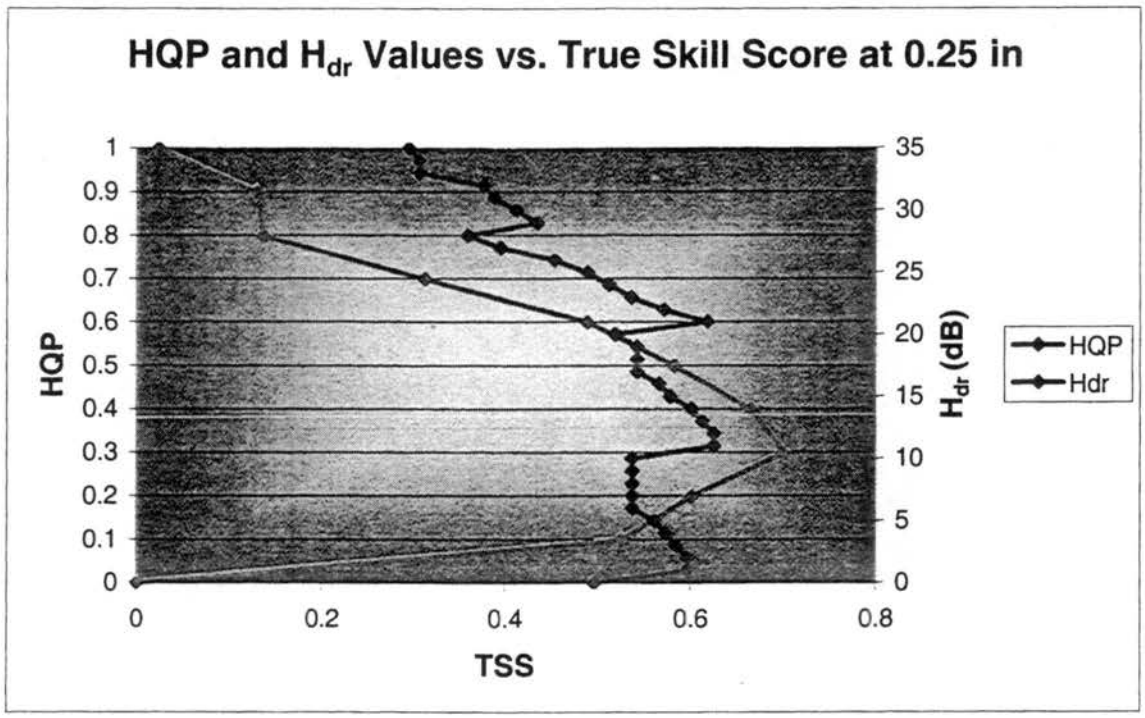

b)

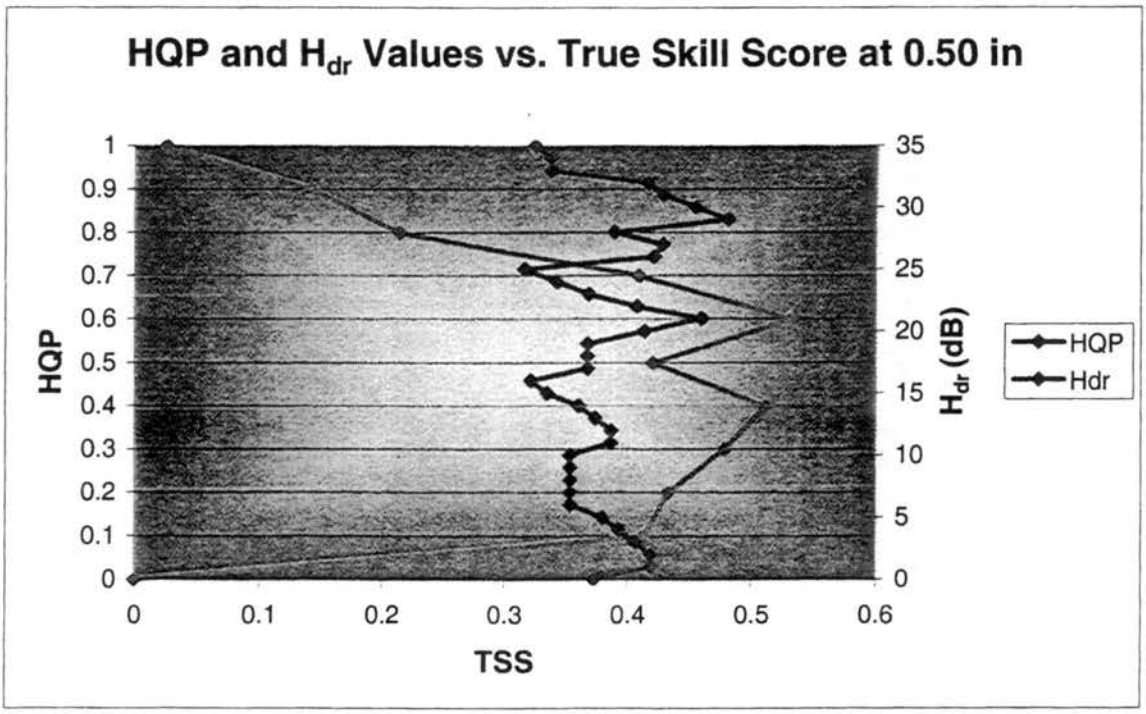

Figure C.1: True Skill Score (TSS) values for each threshold of HQP from 0.0-1.0 and each threshold of H_{dr} from 0-35 at hail size thresholds of greater than or equal to a) 0.25 in, b) 0.50 in, c) 0.75 in, d) 1.00 in, e) 1.25 in, f) 1.50 in, g) 1.75 in, and h) 2.00 in.

c)

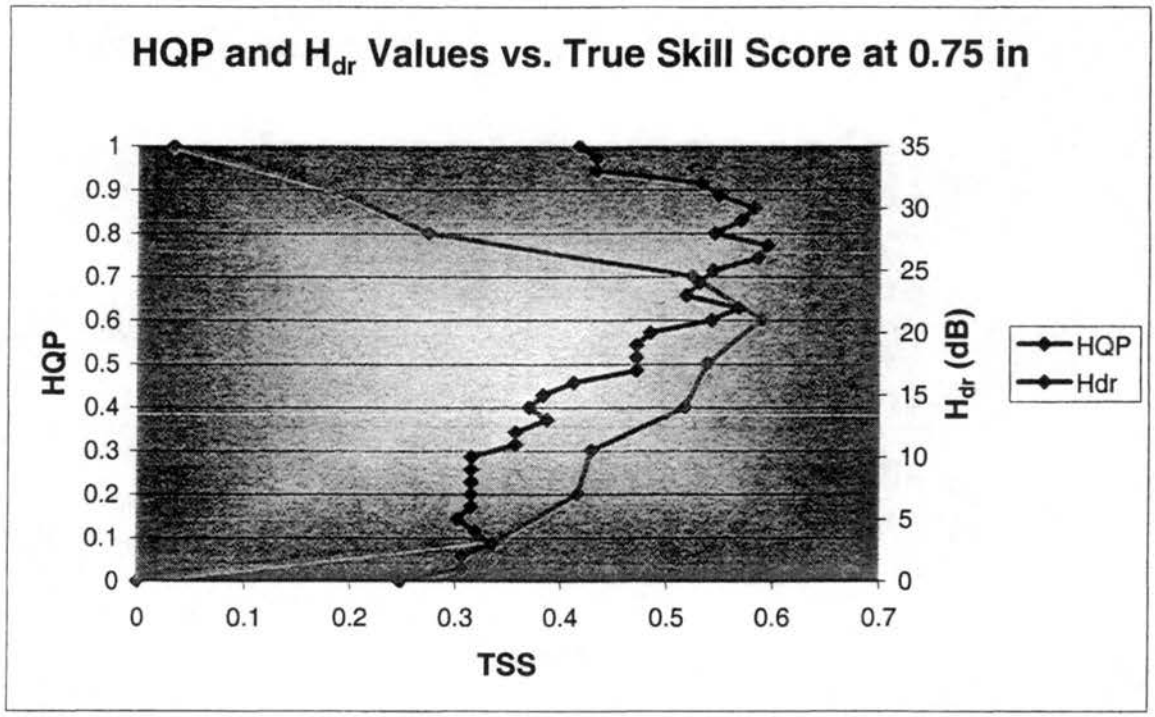

d)

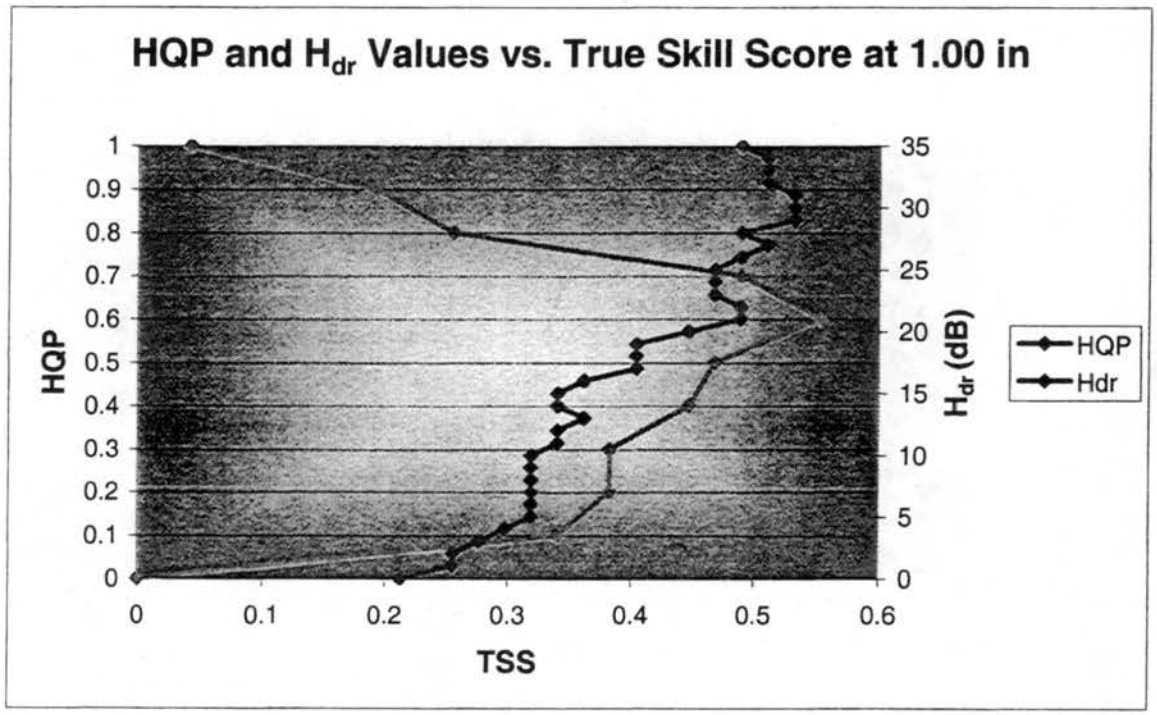

Figure C.1: (Cont.)

e)

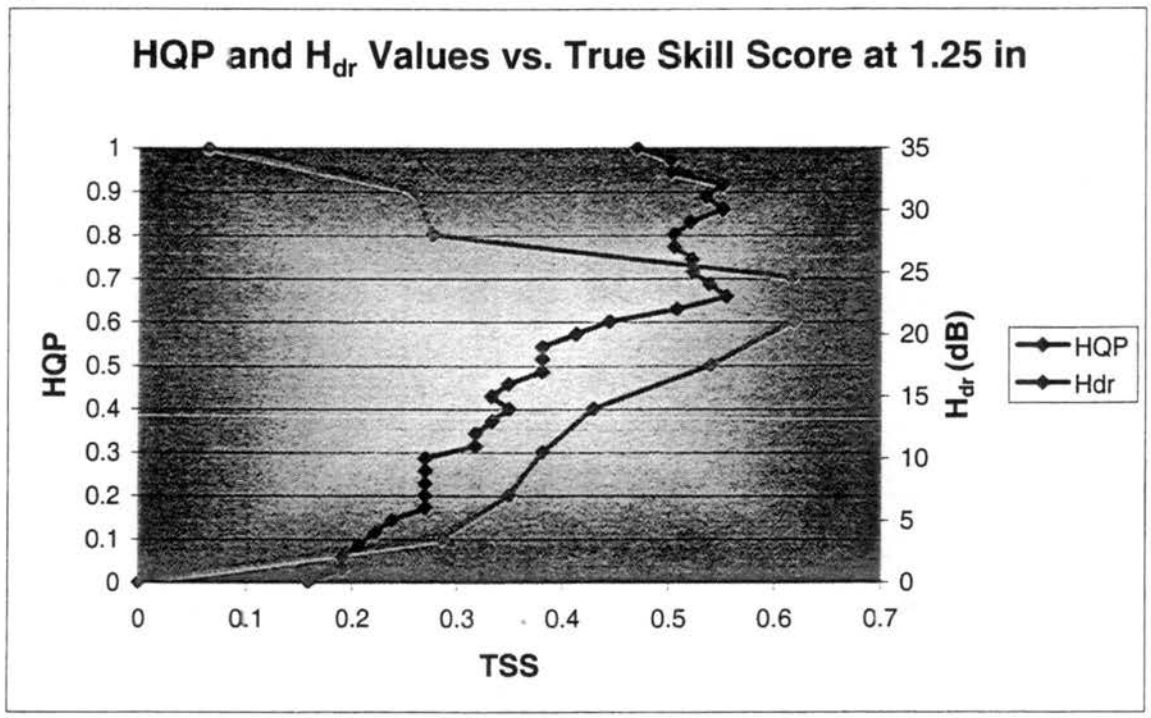

f)

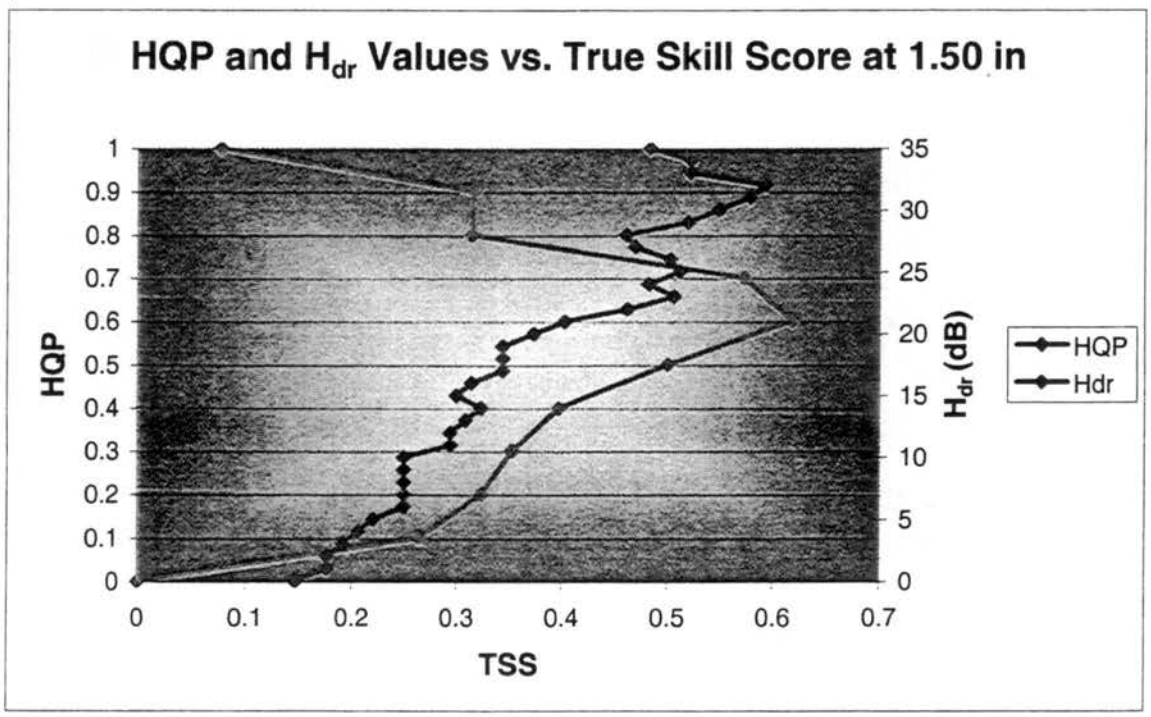

Figure C.1: (Cont.)

g)

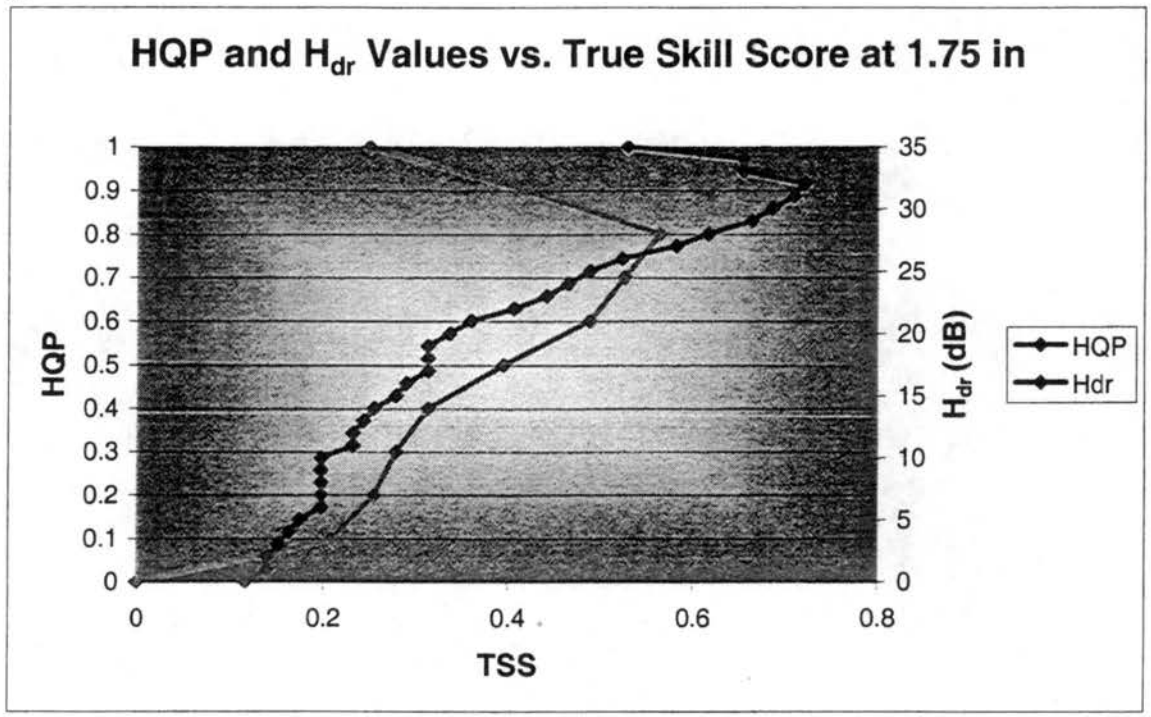

h)

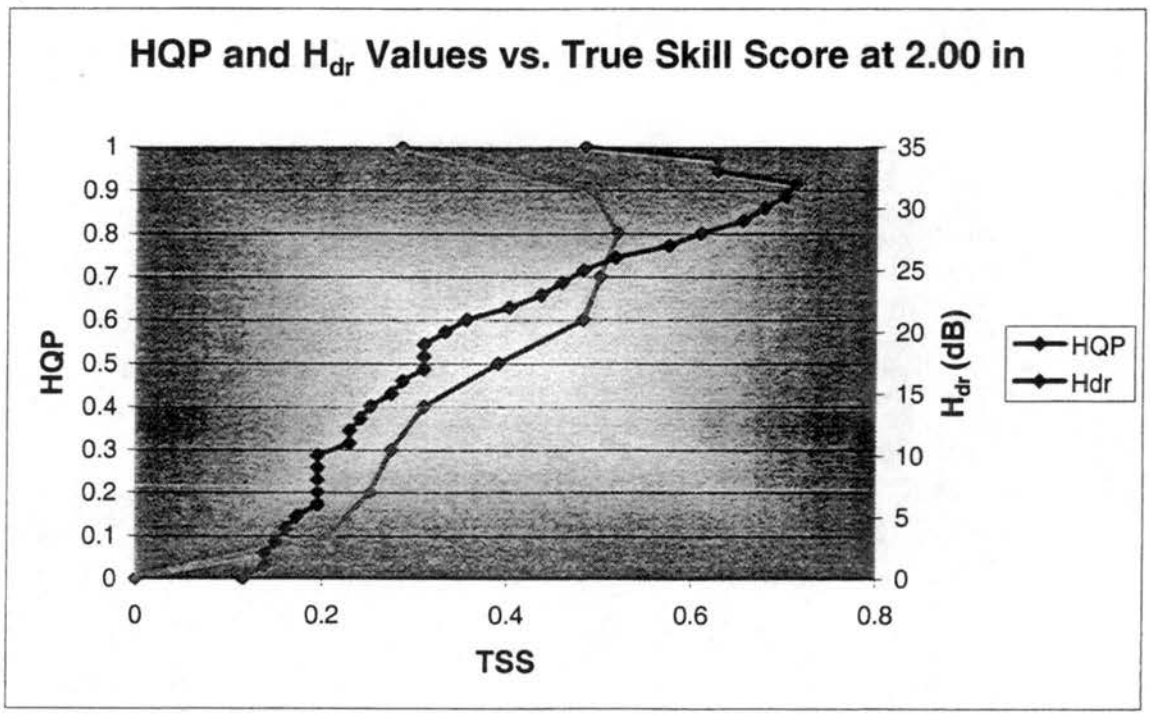

Figure C.1: (Cont.)

a)

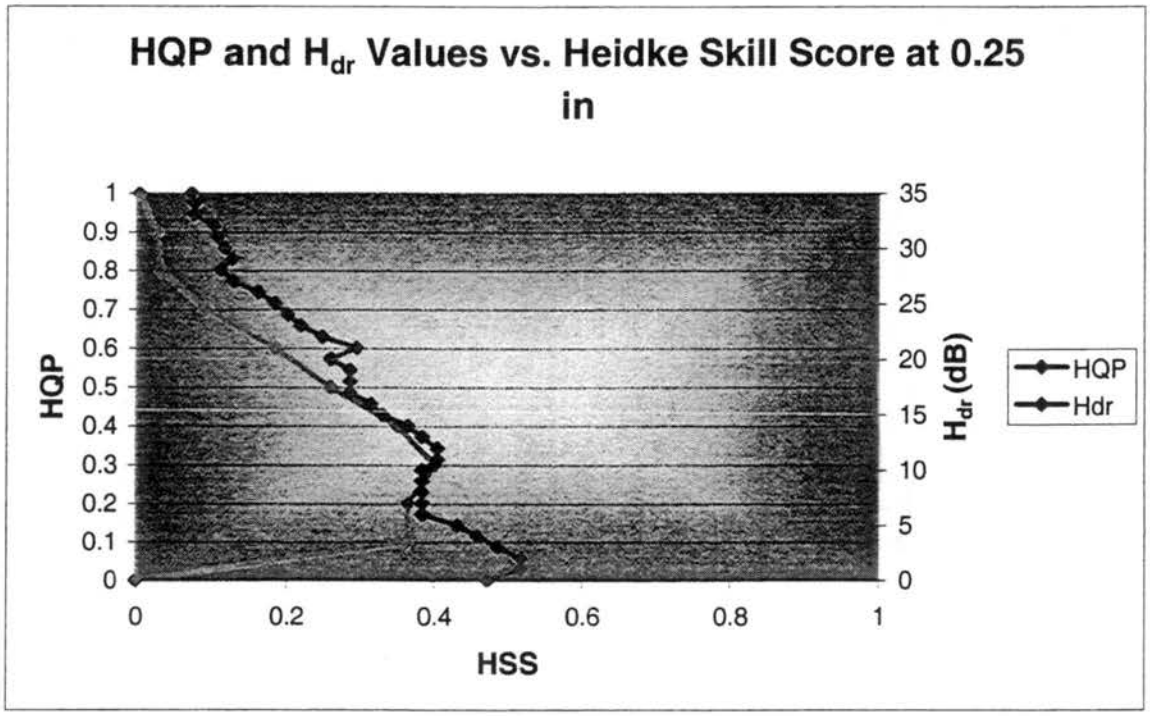

b)

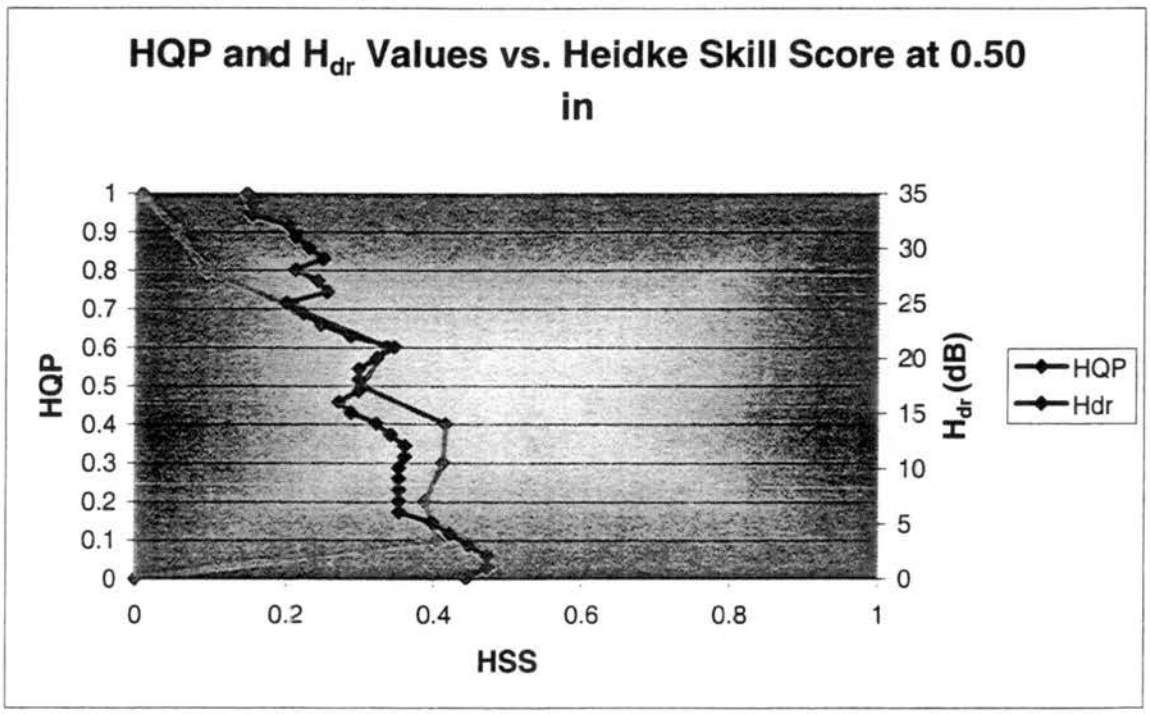

Figure C.2: Heidke Skill Score (HSS) values for each threshold of HQP from 0.0-1.0 and each threshold of H_{dr} from 0-35 at hail size thresholds of greater than or equal to a) 0.25 in, b) 0.50 in, c) 0.75 in, d) 1.00 in, e) 1.25 in, f) 1.50 in, g) 1.75 in, and h) 2.00 in.

c)

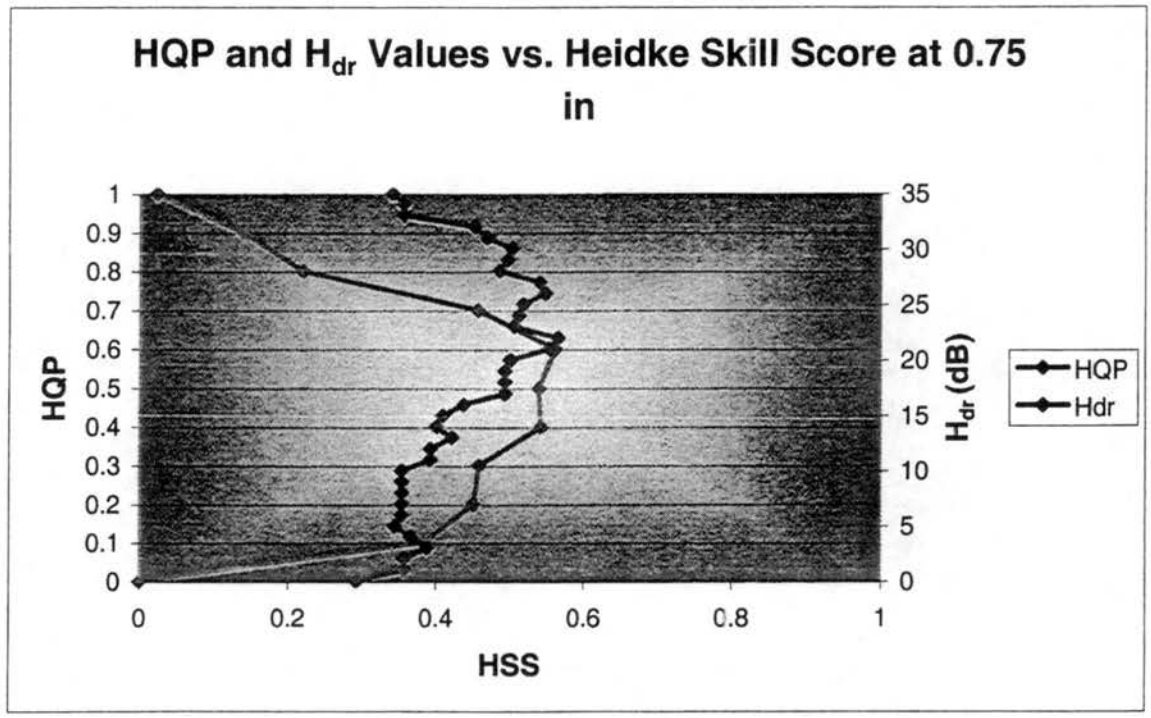

d)

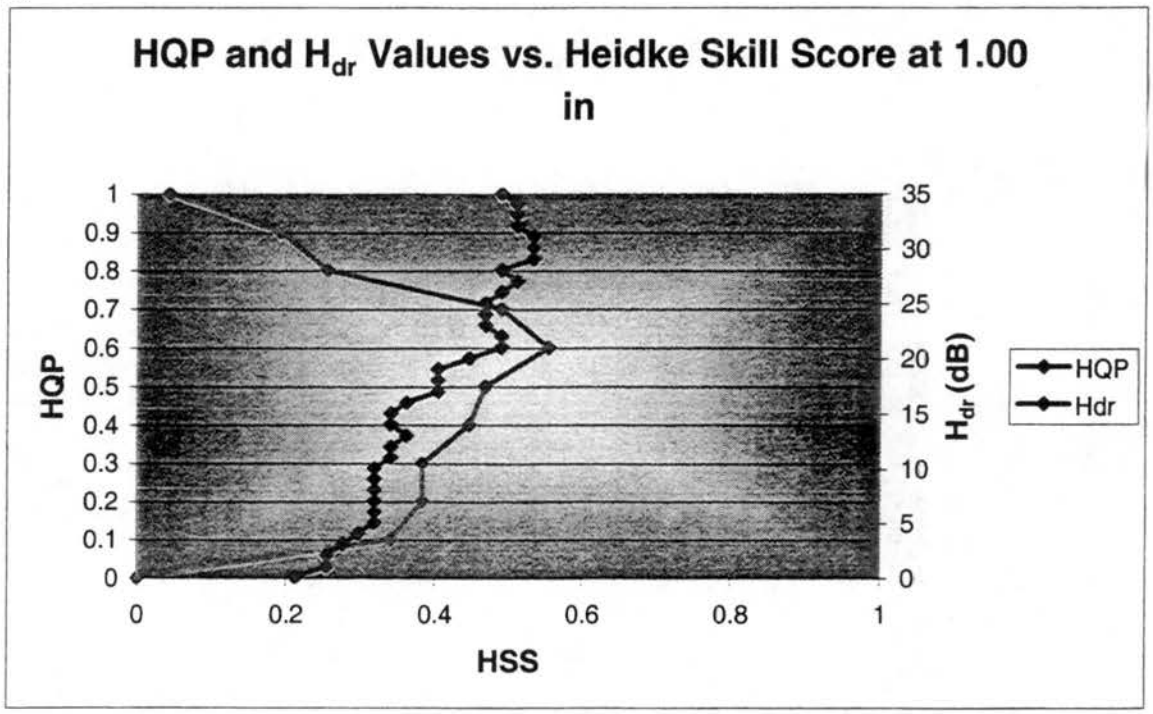

Figure C.2: (Cont.)

e)

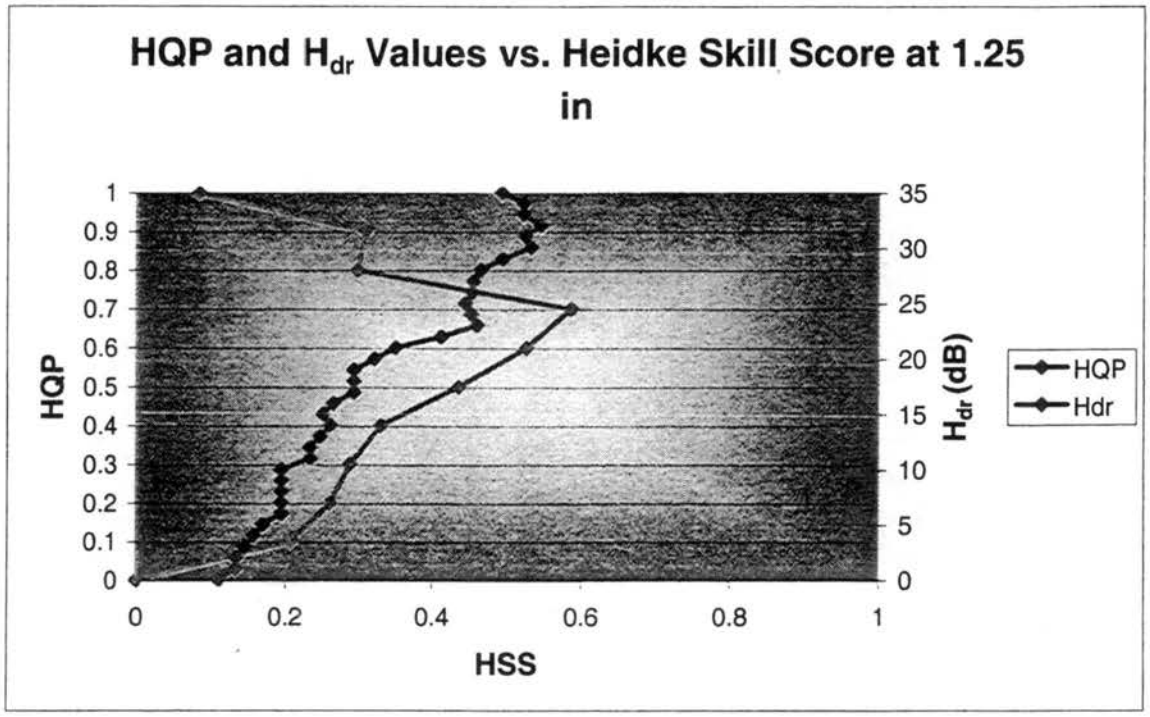

f)

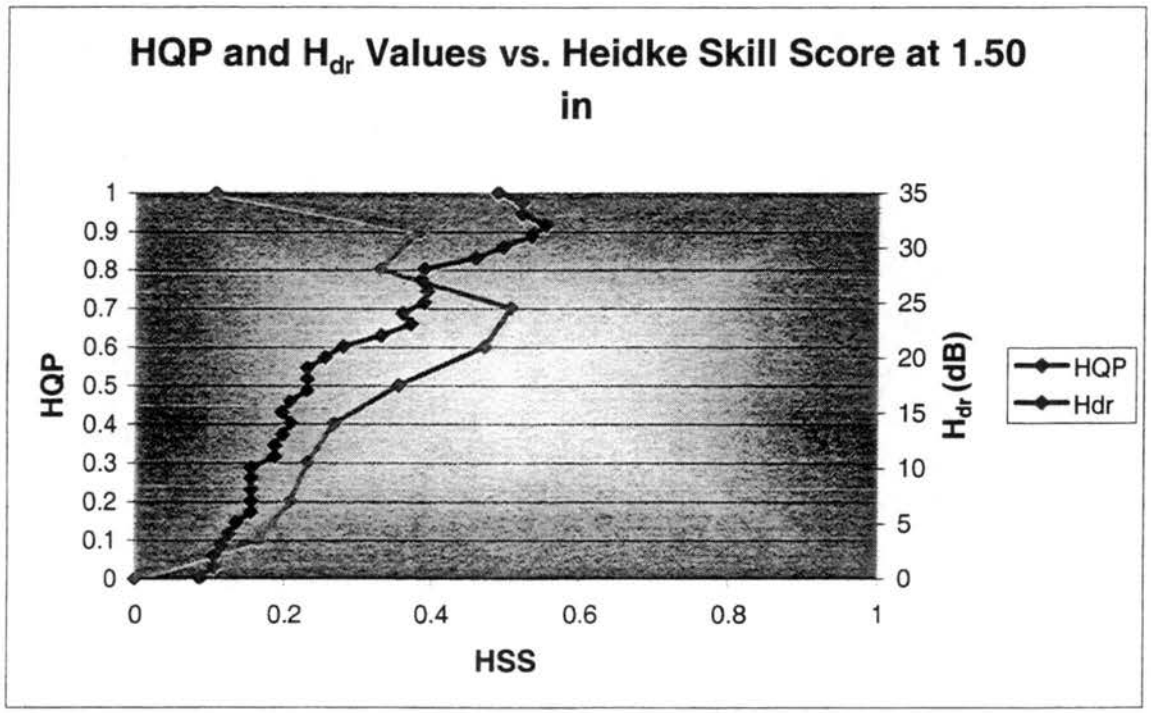

Figure C.2: (Cont.)

g)

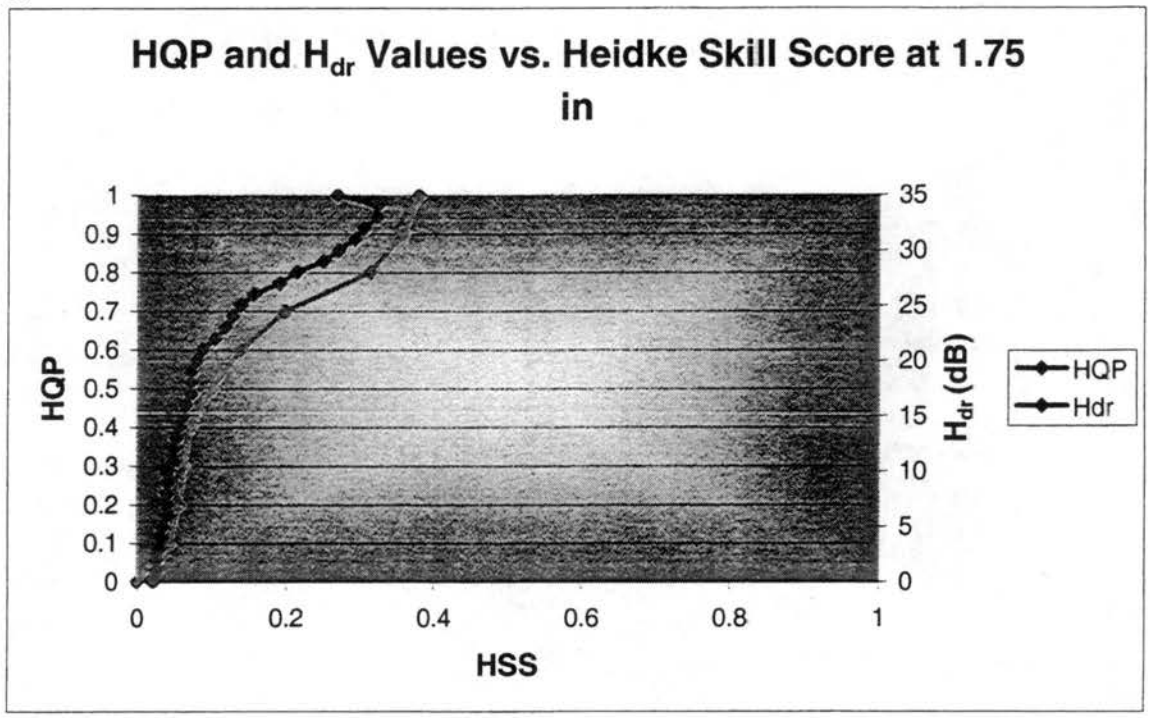

h)

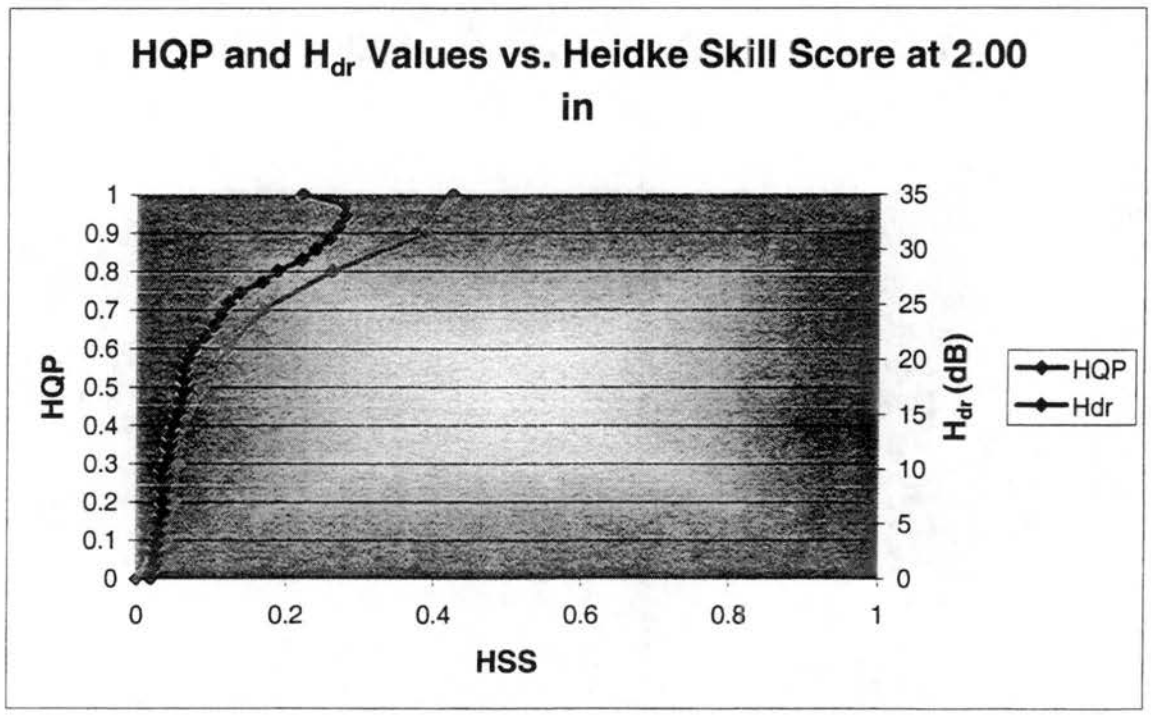

Figure C.2: (Cont.)